



GRADO EN INGENIERÍA EN TECNOLOGÍAS
INDUSTRIALES

TRABAJO FIN DE GRADO

**EFFECTS OF OVER-EXTRUSION ON POROSITY,
MECHANICAL PROPERTIES AND PRINTING QUALITY
OF ADDITIVELY MANUFACTURED PEKK AND CF-PEKK
PARTS. FUTURE ORIENTATION OF FUSED FILAMENT
FABRICATION**

Autor: Jimena Martínez Díaz

Director: Mehran Tehrani

Co-Director: Timothy Yap

Madrid

Junio de 2022

Declaro, bajo mi responsabilidad, que el Proyecto presentado con el título
Effects of over-extrusion on porosity, mechanical properties and printing quality of
additively manufactured PEKK and CF-PEKK parts. Future orientation of fused filament
fabrication

en la ETS de Ingeniería - ICAI de la Universidad Pontificia Comillas en el
curso académico 2021/22 es de mi autoría, original e inédito y
no ha sido presentado con anterioridad a otros efectos.

El Proyecto no es plagio de otro, ni total ni parcialmente y la información que ha sido
tomada de otros documentos está debidamente referenciada.

Fdo.: Jimena Martínez Díaz

Fecha: 08 / 06 / 2022



Autorizada la entrega del proyecto

EL DIRECTOR DEL PROYECTO

Fdo.: Merhan Terhani

Fecha: 08 / 06 / 2022





GRADO EN INGENIERÍA EN TECNOLOGÍAS
INDUSTRIALES

TRABAJO FIN DE GRADO

**EFFECTS OF OVER-EXTRUSION ON POROSITY,
MECHANICAL PROPERTIES AND PRINTING QUALITY
OF ADDITIVELY MANUFACTURED PEKK AND CF-PEKK
PARTS. FUTURE ORIENTATION OF FUSED FILAMENT
FABRICATION**

Autor: Jimena Martínez Díaz

Director: Mehran Tehrani

Co-Director: Timothy Yap

Madrid

Junio de 2022

EFFECTOS DE LA SOBRE-EXTRUSIÓN SOBRE LA POROSIDAD, LAS PROPIEDADES MECÁNICAS Y LA CALIDAD DE IMPRESIÓN DE PIEZAS DE PEKK Y CF-PEKK OBTENIDAS POR FABRICACIÓN ADITIVA. ORIENTACIÓN FUTURA DEL MODELADO POR DEPOSICIÓN FUNDIDA

Autor: Martínez Díaz, Jimena

Director: Terhani, Merhan.

Entidad Colaboradora: Walker Department of Mechanical Engineering at the University of Texas at Austin.

RESUMEN DEL PROYECTO

Este estudio investiga la sobre-extrusión como solución para reducir el alto nivel de anisotropía mecánica de piezas de PEKK y CF-PEKK obtenidas mediante el modelado por deposición fundida (FDM). En el caso del PEKK un aumento del 5% en el multiplicador de extrusión (ME) no es suficiente para apreciar una mejora en las propiedades mecánicas, mientras que en el caso del CF-PEKK la misma sobre-extrusión resulta en una mejora del 32,6% de la resistencia a la tracción. Además, el incremento en el ME no empeora la calidad de la impresión.

Palabras clave: Modelado por deposición fundida; Multiplicador de extrusión; Anisotropía; PEKK; CF-PEKK

1. Introducción

El FDM es la tecnología más común dentro de la fabricación aditiva. Se distingue por los bajos costes de producción, la facilidad para obtener piezas con formas complejas y el amplio abanico de materiales compatibles. Hasta la fecha, la mayoría de los estudios sobre el FDM se han centrado en polímeros de baja temperatura de fusión, como el ABS y el PLA, debido a la comodidad de impresión y al bajo coste de fabricación [1]. No obstante, las propiedades mecánicas de estos materiales no son suficientes para muchas aplicaciones industriales. Recientemente, el desarrollo de impresoras 3D de alta temperatura ha permitido la incorporación de polímeros con propiedades termomecánicas relativamente altas y de sus correspondientes materiales compuestos. Entre ellos se encuentran el PEKK y el PEKK reforzado con fibras de carbono (CF-PEKK). El PEKK es un termoplástico de alto rendimiento que pertenece a la familia de la poliariletercetona (PAEK) con excelentes propiedades mecánicas. Destaca su alta resistencia a la tracción y su módulo de elasticidad comparable al del aluminio, así como su resistencia a elevadas temperaturas. La adición de fibras de carbono (FC) a la matriz de PEKK mejora las ya excelentes propiedades mecánicas que ofrece el polímero por sí mismo. Por todo ello, existe un creciente interés en ambos materiales para aplicaciones de alta exigencia.

A pesar de las ventajas mencionadas, las piezas modeladas por deposición fundida presentan deficiencias intrínsecas, que han limitado mayormente las aplicaciones de esta tecnología a la creación de prototipos [2-4]. Las concentraciones de tensiones que se forman en los poros interiores, junto con la débil adhesión entre capas debido a la falta de presiones externas aparte de la gravedad, dan lugar a piezas anisótropas. La anisotropía mecánica depende de dos variables fundamentales, el material y la orientación de la pieza impresa. En concreto, si la dirección de la trayectoria seguida por

la boquilla al depositar el material es siempre la misma, las piezas tendrán propiedades ortotrópicas. Estudios basados en los dos materiales más comunes del FDM, el ABS [3] y el PLA [4], han reportado que la resistencia a la tracción de piezas fabricadas en la dirección z (verticalmente) es hasta un 60% inferior a la resistencia de la misma pieza fabricada en las direcciones x e y.

El objetivo de este estudio es investigar la sobre-extrusión como potencial solución para reducir el grado de anisotropía de piezas fabricadas de PEKK y CF-PEKK. El multiplicador de extrusión (ME) es un parámetro de impresión que determina el flujo del filamento a través de la boquilla. Un aumento del ME resulta en una reducción del número de poros, así como en una disminución de su tamaño [7]. Hasta la fecha, sólo hay un estudio acerca del impacto de la sobre-extrusión en las propiedades mecánicas y la calidad de impresión de piezas modeladas por deposición fundida [8]. Un aumento del 20% en el ME dio lugar a una mejora en el rendimiento mecánico del ABS. Este efecto fue especialmente notable en la resistencia a la tracción de los cupones impresos a lo largo de la dirección z, que aumentó en un 50% con respecto al ME estándar. Además, el estudio concluyó que un aumento en el ME no afecta negativamente la calidad de impresión. Los resultados de los dos estudios citados se basan en polímeros de baja temperatura de fusión (ABS y PLA). Sin embargo, no existe ningún estudio destinado a conocer los efectos de la sobre-extrusión sobre la anisotropía mecánica de polímeros de alto rendimiento ni de materiales compuestos y de ahí, el interés de este proyecto.

2. Metodología

El primer paso en el planteamiento del estudio fue crear un diseño asistido por ordenador (modelo CAD) que incluyera las piezas mostradas en la Figura 1 (b), (c), (d) y (e): seis cupones de tipo IV (según la norma ASTM D638-14) para los ensayos de tracción, una pieza para estudiar la porosidad de la sección transversal y dos piezas con características difíciles de recrear para evaluar la calidad de impresión (un cubo de calibración y una pieza estándar desarrollada por Autodesk y Kickstarter). En segundo lugar, en línea con las aplicaciones reales y antes de iniciar el estudio, se imprimió un prototipo del modelo con PLA para comprobar que este cumplía con las expectativas. Una vez realizada esta verificación, fue necesario determinar la configuración óptima de impresión para cada uno de los materiales analizados. Con el fin de evitar cualquier desperdicio de material, la búsqueda de los parámetros óptimos se llevó a cabo únicamente con una pieza de metrología adicional, mostrada en la Figura 1 (a), el 3DBenchy. A continuación, el modelo se imprimió dos veces, manteniendo todos los parámetros constantes excepto el ME. Un estudio preliminar mostró que un aumento del 5% en el ME es suficiente para reducir considerablemente la porosidad interior tanto del PEKK como del CF-PEKK. Además, al ser materiales de alto rendimiento con un alto punto de fusión, resultaría muy complicado aumentar más el ME sin que se produjesen fallos de impresión. Por todo ello, en este trabajo se compara la calidad, las propiedades mecánicas y la porosidad del modelo impreso con un ME de 1 y de 1,05.

Tras la impresión de las piezas, estas fueron sometidas a un post-tratamiento de recocido para aumentar el grado de cristianización y, de esa forma, mejorar sus propiedades termo-mecánicas. Estudios previos han determinado que el recocido permite homogeneizar y aumentar la cristalinidad de piezas impresas con PEKK y CF-PEKK en 26 pp y 16 pp, respectivamente [9]. Este tratamiento térmico requiere elevar la temperatura por encima de la temperatura de cristalización de ambos materiales (156°C en el caso del PEKK y 160°C en el caso del CF-PEKK), lo que puede tener un impacto negativo en las características complejas de las piezas de metrología, como los puentes

y los voladizos. Para evitar cambios dimensionales y estructurales, las piezas se sumergieron en sal en polvo durante el recocido. Por último, los cupones se sometieron a ensayos de tracción utilizando un sistema de prueba universal (MTS Criterion™ Modelo 43) con una célula de carga de 1 kN, las muestras de sección transversal se examinaron mediante tomografía micro computada (máquina MicroXCT 400 Zeiss), y las características de interés de las piezas de metrología se cotejaron con las esperadas.

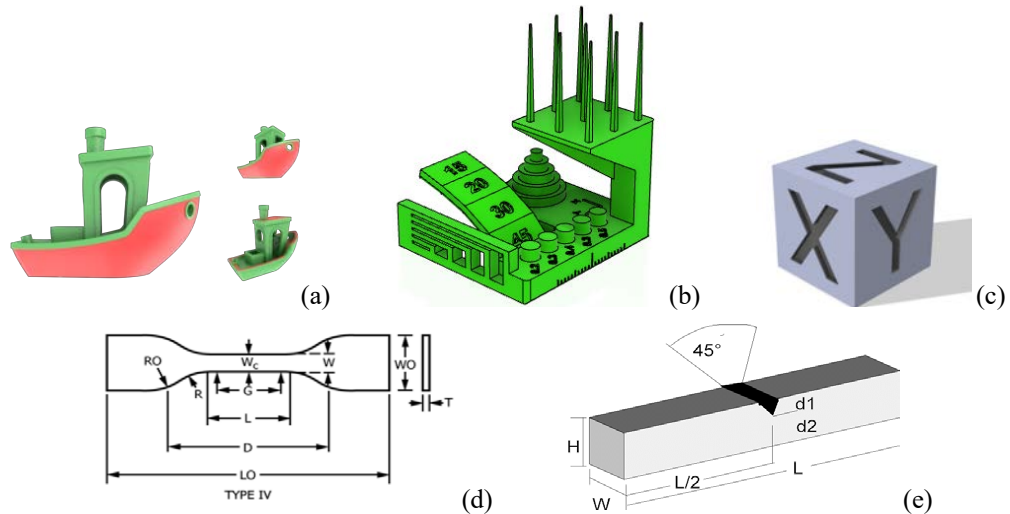


Figura 1. (a) 3DBenchy; (b) pieza estándar desarrollada por Autodesk and Kickstarter; (c) cubo de calibración; (d) cupones de tracción de tipo IV según la norma ASTM D638-14; y (e) muestra de sección transversal.

3. Resultados

La figura 2 (a) muestra los resultados del análisis de porosidad. En el caso del PEKK, un aumento del 5% en el ME resulta en una disminución de la porosidad de 0,53 pp. Teniendo en cuenta que la porosidad interna del PEKK para un ME estándar es relativamente baja (0,76% en comparación con la del CF-PEKK), esta técnica resulta muy eficaz para eliminar prácticamente todos los poros internos. Además, un aumento del 5% en el ME dio lugar a una reducción de la porosidad interna del CF-PEKK de 1,63 pp, de 22,09% a 20,46%. La porosidad del CF-PEKK es mucho mayor en comparación con la del PEKK debido a la presencia de poros dentro de los propios filamentos.

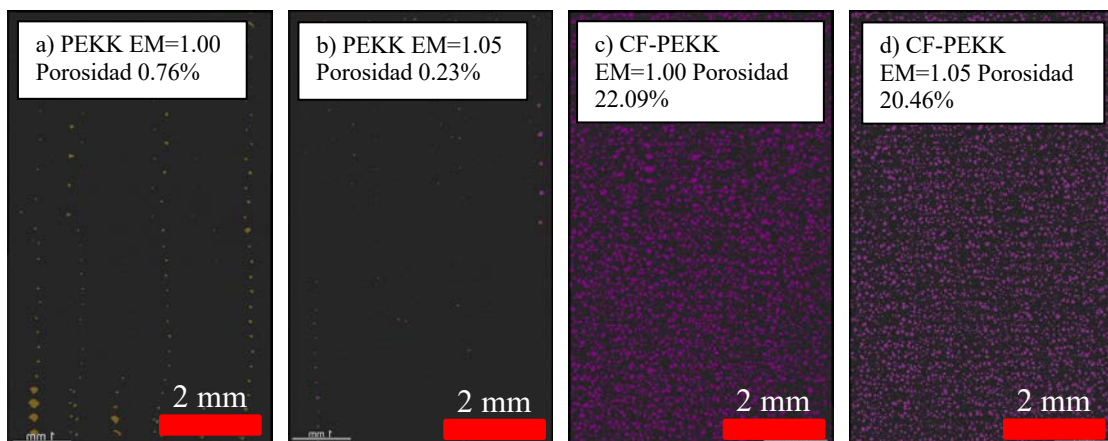


Figura 2. Porosidad interior del PEKK con un ME de (a) 1,00 y (b) 1,05; y del CF-PEKK con un ME de (c) 1,00 y (d) 1,05

El aumento del ME no resultó en una mejora significativa de las propiedades mecánicas del PEKK. La resistencia a la tracción, la elongación de rotura y el módulo de Young para ambos ME fueron muy similares, con intervalos de confianza solapados, a un nivel de confianza del 95%. En el caso del CF-PEKK, un aumento del 5% en el ME dio lugar a una mejora del 32,6% de la resistencia a la tracción. Por el contrario, el módulo de Young y el alargamiento de rotura no cambiaron significativamente dado el margen de error.

Hasta la fecha, no existen estudios acerca del proceso de recocido con sal para el PEKK y el CF-PEKK. Por lo tanto, la evaluación de la calidad de impresión se llevó a cabo antes y después del tratamiento para conocer mejor su efecto en las piezas impresas. Todas las puntuaciones permanecieron inalteradas, es decir, no se detectaron cambios estructurales ni dimensionales tras el tratamiento, lo que permitió verificar la eficacia del mismo. Además, los resultados del análisis sugerían dos conclusiones: (1) ni el PEKK ni el CF-PEKK ofrecen una buena calidad de impresión debido a las altas temperaturas de procesamiento; y (2) un aumento del 5% en el ME no tiene un impacto negativo en la calidad de la impresión.

4. Conclusiones

Este estudio investiga la sobre-extrusión como posible solución para disminuir el gran grado de anisotropía de piezas de PEKK y CF-PEKK fabricadas mediante el FDM. Los resultados sugieren que la mejora del rendimiento mecánico es función de la reducción de la porosidad y, por tanto, depende del material. En el caso del PEKK, un aumento del 5% en el ME da lugar a una reducción de la porosidad de 0,53 pp, pero no se detecta ninguna mejora en las propiedades mecánicas. En el caso del CF-PEKK, la misma sobre-extrusión resulta en una reducción de la porosidad interna más de tres veces mayor. A pesar de que la porosidad final (20,46%) sigue siendo muy elevada debido a la presencia de poros en los filamentos, la reducción alcanzada (1.63 pp) da lugar a una mejora del rendimiento mecánico. Este efecto es especialmente notable en la resistencia a la tracción, que aumenta en un 32,6%. El aumento del 5% en el ME no es suficiente para apreciar una mejora significativa ni del módulo de Young ni del alargamiento a rotura, lo que indica que la resistencia a la tracción es la propiedad más afectada por la sobre-extrusión.

Este estudio también demuestra que una ligera sobre-extrusión no afecta negativamente la calidad de impresión del PEKK ni del CF-PEKK. En ambos casos, las piezas impresas no ofrecen una buena calidad debido a las altas temperaturas de procesamiento. Además, el recocido con sal es un tratamiento eficaz para aumentar el grado de cristalización del PEKK y del CF-PEKK, evitando cambios estructurales y dimensionales.

5. Referencias

- [1] G. Bräuer, K. Sachsenhofer, R.W. Lang, Material and process engineering aspects to improve the quality of the bonding layer in a laser-assisted fused filament fabrication process, *Additive Manufacturing* 46 (2021) 102105.
- [2] X. Gao, S. Qi, X. Kuang, Y. Su, J. Li, D. Wang, Fused filament fabrication of polymer materials: A review of interlayer bond, *Additive Manufacturing* 37 (2021) 101658.
- [3] J. Allum, A. Moetazedian, A. Gleadall, V.V. Silberschmidt, Interlayer bonding has bulk-material strength in extrusion additive manufacturing: New understanding of anisotropy, *Additive Manufacturing* 34 (2020) 101297.

- [4] N.P. Levenhagen, M.D. Dadmun, Improving Interlayer Adhesion in 3D Printing with Surface Segregating Additives: Improving the Isotropy of Acrylonitrile–Butadiene–Styrene Parts, *ACS Applied Polymer Materials* 1(4) (2019) 876-884.
- [5] J.F. Rodriguez, J.P. Thomas, J.E. Renaud, Maximizing the Strength of Fused-Deposition ABS Plastic Parts, 1999.
- [6] X. Gao, D. Zhang, S. Qi, X. Wen, Y. Su, Mechanical properties of 3D parts fabricated by fused deposition modeling: Effect of various fillers in polylactide, *Journal of Applied Polymer Science* 136(31) (2019) 47824.
- [7] E. Gordeev, A. Galushko, V. Ananikov, Improvement of quality of 3D printed objects by elimination of microscopic structural defects in fused deposition modeling, *PLOS ONE* 13 (2018) e0198370.
- [8] P.K. J. Ghorbani, Y. Shen, M. Tehrani, Reducing Mechanical Anisotropy in Fused Filament Fabrication Additive Manufacturing via Over-Extrusion, (under review).
- [9] T. Yap, N. Heathman, T. Phillips, J. Beaman, M. Tehrani, Fused Filament Fabrication and Selective Laser Sintering of PAEK Polymers and their Composites, (under review)

EFFECTS OF OVER-EXTRUSION ON POROSITY, MECHANICAL PROPERTIES AND PRINTING QUALITY OF ADDITIVELY MANUFACTURED PEKK AND CF-PEKK PARTS. FUTURE ORIENTATION OF FUSED FILAMENT FABRICATION

Author: Martínez Díaz, Jimena.

Supervisor: Terhani, Merhan.

Collaborating Entity: Walker Department of Mechanical Engineering at the University of Texas at Austin.

ABSTRACT

This study investigates over-extrusion as a solution to reduce the high level of mechanical anisotropy of PEKK and CF-PEKK parts manufactured via fused filament fabrication. In the case of PEKK, a 5% increase in extrusion multiplier (EM) is not enough to appreciate an improvement in mechanical properties, whereas for CF-PEKK the same over-extrusion results in a 32.6% enhancement of the tensile strength. Also, the increase in EM does not worsen print quality.

Keywords: Fused filament fabrication; Extrusion multiplier; Anisotropy; PEKK; CF-PEKK

1. Introduction

Fused filament fabrication (FFF) is a very promising additive manufacturing (AM) technology that offers many advantages including lower production costs, ease of manufacturing complex parts and abundant compatible feedstock. So far, most FFF studies have focused on low melting temperature polymers such as acrylonitrile butadiene styrene (ABS) and polylactic acid (PLA) due to printing convenience and low manufacturing cost [1]. Nevertheless, mechanical properties of these materials are insufficient for many industrial applications. The development of high-temperature FFF 3D printers has allowed the incorporation of polymers with relatively high thermomechanical properties and their composites. Among them are polyetherketoneketone (PEKK) and PEKK reinforced with chopped carbon fibers (CF-PEKK). PEKK is a high-performance thermoplastic that belongs to the polyaryletherketone (PAEK) family with excellent mechanical properties, namely their high tensile strength and modulus comparable to aluminum, and their resistance to elevated temperatures. Moreover, the addition of carbon fibers (CF) to the PEKK matrix improves the already excellent properties offered by the polymer alone and hence there is growing interest for future high-demanding applications.

Despite the aforementioned advantages, intrinsic deficiencies of FFF printed parts have prevented this technology from competing with other AM processes and have mostly limited its applications to rapid prototyping [2-4]. Stress concentrations formed at voids, together with weak interlayer adhesion due to the lack of external pressures apart from gravity, leads to anisotropic parts with mechanical properties off the longitudinal direction worse than expected. Mechanical anisotropy is primarily a function of two variables, material and printing orientation. In particular, if all rasters (also known as beads or roads) are printed in the same direction, the parts will have orthotropic properties. Studies based on ABS [5] and PLA [6] have reported that the tensile strength

of FFF parts built in the z-direction is lower by 45% and 60%, respectively, compared to the same part's strength built in the x- and y-directions.

This paper aims to investigate over-extrusion as a potential solution to address the large degree of anisotropy of PEKK and CF-PEKK printed parts. The extrusion multiplier (EM) is a printing parameter that determines the flowrate of filament through the nozzle. An increase in the EM results in a reduction of the number of pores as well as in a decrease of the pores' diameter [7]. To date, there is only one paper focused on the impact of over-extrusion on the mechanical properties and features of interest (dimensional accuracy, flow control, negative features and overhangs, excluding surface roughness) of FFF parts [8]. Increasing the EM by 20% resulted in improved mechanical properties of ABS printed items. This effect was especially noticeable in the tensile strength of coupons along the z-direction, which increased by 50% with respect to the standard EM (1). In addition, the study concluded that a higher EM does not negatively affect printability. The results of the two cited studies are based on parts printed with low melting polymers (ABS and PLA) using desktop printers. However, to the best of the reader's knowledge, there is no study aimed to understand the effects of over-extrusion on high-performance polymers or on composites.

2. Methodology

The first step in the study's approach was to create a CAD model including the parts shown in Figure 1 (b), (c), (d), and (e): six ASTM D638-14 type IV tensile coupons, one cross-section sample, and two metrology parts to assess printability (a calibration cube and a common standard piece developed by Autodesk and Kickstarter). Secondly, in line with real applications and prior to starting the research, a prototype of the CAD file was created with PLA in order to check that the model was indeed the desired one. Once this verification was successfully completed, it was necessary to determine the optimal parameters for each of the materials analyzed. To avoid wasting material, the search for the optimal parameters was carried out only with an additional metrology part shown in Figure 1 (a), the 3DBenchy. Then, the CAD model was printed twice, keeping all the input settings constant and changing the EM. A preliminary FFF study performed with PEKK and CF-PEKK using the same printer showed that increasing the EM by 5% is enough to considerably reduce the void content. In addition, as both materials have a high melting point, it would be very difficult to further increase the EM without any printing failure. Therefore, this paper compares the quality, mechanical properties and porosity of the model printed with an EM of 1 and EM of 1.05

After printing the parts, these were subjected to an annealing post-treatment in order to improve their thermomechanical properties. Annealing allows to homogenize and increase the crystallinity of PEKK and CF-PEKK parts by 26 pp and 16 pp, respectively [9]. This thermal treatment requires raising the temperature above the thermoplastic crystallization temperature, which can have a negative impact on complex features of printed parts, such as bridges and overhangs. To avoid dimensional and structural changes, parts were submerged in very fine salt powder during annealing. Finally, all test coupons were subjected to a tensile test using an MTS Criterion™ Model 43 universal test system with a 1 kN load cell, cross-section samples were examined using micro computed tomography (MicroXCT 400 Zeiss machine), and the features of interest of the metrology parts were checked against the expected ones.

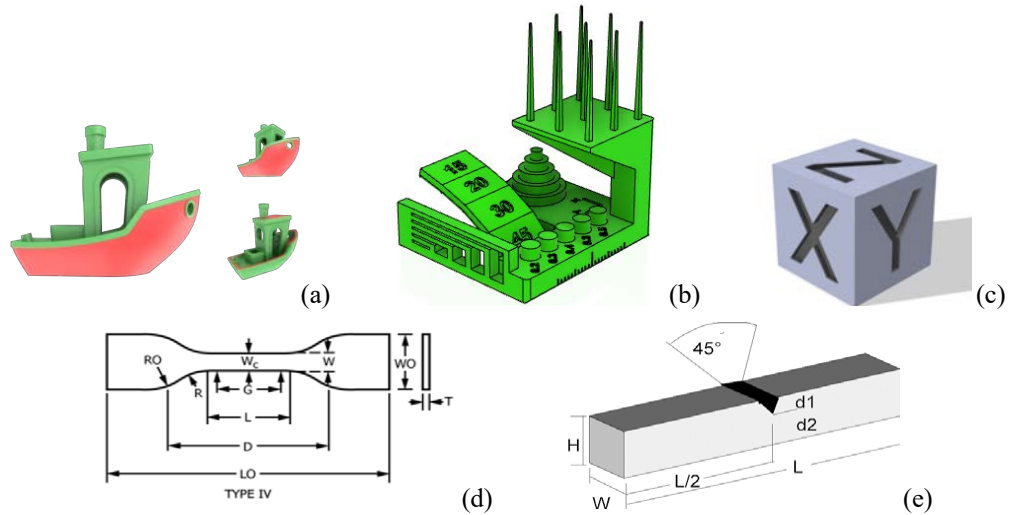


Figure 1. (a) 3DBenchy; (b) Common standard piece developed by Autodesk and Kickstarter; (c) calibration cube; (d) Type IV tensile coupons; and (e) cross-section sample.

3. Results

Figure 2 (a) shows the results from the porosity analysis. In the case of PEKK, 5% increase in the EM results in 0.53 pp decrease in porosity. Considering that the internal porosity of PEKK for a standard EM is relatively low (0.76% as compared to that of CF-PEKK), this approach is very effective to practically eliminate the internal pores. In addition, 5% increase in the EM resulted in a reduction of CF-PEKK internal porosity of 1.63 pp, from 22.09% to 20.46%. The porosity of CF-PEKK is much higher compared to that of PEKK due to the presence of intra-bead voids in the raw filaments. It is questionable whether over-extrusion can help to decrease this type of pores.

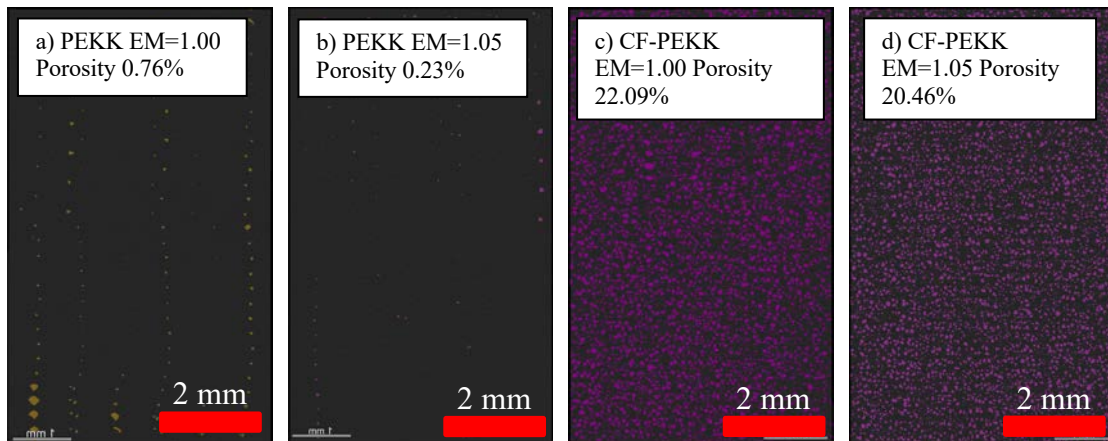


Figure 2. Interior porosity of PEKK parts printed at an EM of (a) 1.00 and (b) 1.05; and CF-PEKK parts printed at an EM of (c) 1.00 and (d) 1.05

Increasing the EM by 5% did not result in a significant improvement of PEKK mechanical properties. The mean tensile strength, strain to failure (STF) and Young's modulus for the two EMs were very similar, with overlapping confidence intervals at a 95% confidence level. In the case of CF-PEKK, a 5% increase in the EM resulted in 32.6% improvement of the tensile strength. By contrast, the Young's modulus and the STF did not change significantly, given the margin of error at a 95% confidence level.

To date, there are no studies on the annealing process with salt for PEKK and CF-PEKK. Therefore, the printability assessment was carried out before and after the process to get a better understanding of its impact on the quality and functionality of the parts. All scores remained unchanged, that is, neither structural nor dimensional changes were detected. This verified the effectiveness of the thermal treatment. The printability results suggest: (1) neither PEKK nor CF-PEKK offer a good printability due to the high processing temperatures; and (2) a 5% increase in the EM does not have a negative impact on the print quality (all the scores remained almost the same for both EMs).

4. Conclusions

This study investigates over-extrusion as a potential solution to decrease the large degree of anisotropy of PEKK and CF-PEKK parts manufactured via FFF. The results suggest that the improvement of the mechanical performance is a function of the porosity reduction and thus, it depends on the material. For PEKK, a 5% increase in the EM results in a 0.53 pp porosity reduction and no improvement in mechanical properties is detected. For CF-PEKK, a 1.63 pp reduction in internal porosity is achievable. The final porosity with the higher EM (20.46%) is still very high due to the presence of intra-bead voids in the raw filaments, but it results in an improvement of the mechanical properties, especially noticeable in the ultimate tensile strength that increases by 32.6%. The 5% increase in the EM is not enough to appreciably enhance the Young's modulus and the STF, that is, the tensile strength is the most affected property by over-extrusion.

This study also demonstrates that a slight over-extrusion does not have a negative impact on the printability of PEKK and CF-PEKK. In both cases, printed parts do not offer a good quality due to the high processing temperatures. In addition, annealing PEKK and CF-PEKK parts packed in salt is an effective approach for increasing the degree of crystallization, while preventing structural and dimensional changes.

5. References

- [1] G. Bräuer, K. Sachsenhofer, R.W. Lang, Material and process engineering aspects to improve the quality of the bonding layer in a laser-assisted fused filament fabrication process, *Additive Manufacturing* 46 (2021) 102105.
- [2] X. Gao, S. Qi, X. Kuang, Y. Su, J. Li, D. Wang, Fused filament fabrication of polymer materials: A review of interlayer bond, *Additive Manufacturing* 37 (2021) 101658.
- [3] J. Allum, A. Moetazedian, A. Gleadall, V.V. Silberschmidt, Interlayer bonding has bulk-material strength in extrusion additive manufacturing: New understanding of anisotropy, *Additive Manufacturing* 34 (2020) 101297.
- [4] N.P. Levenhagen, M.D. Dadmun, Improving Interlayer Adhesion in 3D Printing with Surface Segregating Additives: Improving the Isotropy of Acrylonitrile–Butadiene–Styrene Parts, *ACS Applied Polymer Materials* 1(4) (2019) 876-884.
- [5] J.F. Rodriguez, J.P. Thomas, J.E. Renaud, Maximizing the Strength of Fused-Deposition ABS Plastic Parts, 1999.
- [6] X. Gao, D. Zhang, S. Qi, X. Wen, Y. Su, Mechanical properties of 3D parts fabricated by fused deposition modeling: Effect of various fillers in polylactide, *Journal of Applied Polymer Science* 136(31) (2019) 47824.
- [7] E. Gordeev, A. Galushko, V. Ananikov, Improvement of quality of 3D printed objects by elimination of microscopic structural defects in fused deposition modeling, *PLOS ONE* 13 (2018) e0198370.
- [8] P.K. J. Ghorbani, Y. Shen, M. Tehrani, Reducing Mechanical Anisotropy in Fused Filament Fabrication Additive Manufacturing via Over-Extrusion, (under review).
- [9] T. Yap, N. Heathman, T. Phillips, J. Beaman, M. Tehrani, Fused Filament Fabrication and Selective Laser Sintering of PAEK Polymers and their Composites, (under review).

Index

Chapter 1. Introduction.....	7
Chapter 2. State of the art	12
Chapter 3. Materials.....	16
3.1 PLA.....	16
3.2 PEKK	17
3.3 CF-PEKK.....	20
Chapter 4. Methodology.....	22
4.1 Design of the CAD model.....	23
4.2 Prototype of the model	27
4.3 Real model.....	32
4.4 Annealing post-treatment with salt	40
Chapter 5. Effects of over-extrusion on porosity and mechanical properties.....	44
5.1 Objective	44
5.2 Porosity analysis and results	44
5.3 Mechanical performance analysis and results.....	49
5.4 Relationship between porosity and mechanical performance	59
Chapter 6. Effects of over-extrusion on printability	61
6.1 Objective	61
6.2 Assessment of the common standard piece developed by Autodesk and Kickstarter..	61
6.3 Assessment of the calibration cube	66
Chapter 7. Future orientation of FFF	71
Chapter 8. Conclusions.....	77

<i>Chapter 9. References</i>	<i>79</i>
<i>ANNEX I</i>	<i>82</i>
<i>ANNEX II</i>	<i>86</i>
<i>ANNEX III</i>	<i>91</i>

Index of figures

Figure 1. Schematic description of FFF [5].....	8
Figure 2. Illustration of the main characteristics of FFF, (a) layers: real vs. theoretical extrusion profile and; (b) infill: internal structure for different infill percentages [6].....	9
Figure 3. Effect of the extrusion multiplier (EM) on the internal structure of FFF parts, perpendicular to the X (top three figures) and Z (bottom three figures) directions, respectively. (a and d: EM=1, b and e: EM=1.1, c and f: EM=1.2). [15].....	10
Figure 4. Strength versus load-to-fiber angle for unidirectional FD-ABS specimens [23].....	13
Figure 5. Effect of extrusion multiplier on tensile strength, modulus, and failure strain of FFF ABS coupons along the X and Z directions [15].....	15
Figure 6. Pyramid showing the different performance levels of materials used for FFF technology [34]	17
Figure 7. Comparison between PEEK and PEKK in terms of characteristics, price and producers [34]	18
Figure 8. (a) Print orientations and raster patterns for ASTM type I samples tested in the cited study; and (b) representative stress-strain curves of ESD PEKK in the Edge, Flat, and Vertical print orientations with a 45° perpendicular raster infill [39]	20
Figure 9. Ultimate tensile strengths, Young's modulus, and failure strains for tested specimens manufactured via SLS and FFF [25]	21
Figure 10. 3DBenchy [40].....	23
Figure 11. Metrology part developed by Autodesk and Kickstarter [41].....	24
Figure 12. Calibration cube [42]	25
Figure 13. ASTM D638-14 standard, type IV tensile coupons	26
Figure 14. Cross-section sample [43].....	26
Figure 15. Chimney of the 3Dbenchy	28
Figure 16. 3DBenchy printed with PLA optimal parameters.....	30
Figure 17. PLA calibration cube	30
Figure 18. PLA tensile coupons	31
Figure 19. PLA cross-section sample.....	31
Figure 20. PLA metrology part	31
Figure 21. First 3DBenchy printed with PEKK, following the parameters listed in Table 16.....	34
Figure 22. 3DBenchy printed with the PEKK, following the optimal printing parameters (Table 3)	34
Figure 23. Evolution of the 3DBenchy printed with PEKK.....	34

Figure 24. Infill comparison for different coupons thickness: in the three images the left coupon corresponds to a thickness of 4.1 mm and the right one corresponds to a thickness of 2.9 mm.....	36
Figure 25. Final slicing of the tensile coupons with a single raft, common for all the coupons	37
Figure 26. First 3DBenchy printed with CF-PEKK	38
Figure 27. 3DBenchy printed with Kimya filaments following the optimal parameters, listed in Table 5	40
Figure 28. Step-by-step configuration of the annealing process	42
Figure 29. Schematic of the annealing process	42
Figure 30. (a) PEKK color before (right) and after (left) annealing and (b) CF-PEKK color before(right) and after (left) annealing.....	43
Figure 31. Cross-section samples of PEKK (right) and CF-PEKK (left) printed at the two EMs	44
Figure 32. 2D views of the entire porosity of: PEKK at an EM of (a) 1 and (b) 1.05; and CF-PEKK at an EM of (c) 1 and (d) 1.05	45
Figure 33. 3D views of the entire porosity of: PEKK at an EM of (a) 1 and (b) 1.05; and CF-PEKK at an EM of (c) 1 and (d) 1.05	46
Figure 34. Raster gaps in the cross-sample	47
Figure 35. Interior porosity of PEKK printed at (a) EM=1 and (b) EM=1.05; and CF-PEKK at (c) EM=1 and (d) EM=1.05	47
Figure 36. Porosity in (a) PEKK and (b) CF-PEKK raw filaments	48
Figure 37. CF-PEKK coupon, held by the jaws of the tensile machine, with the extensometer placed in the gauge section	50
Figure 38. PEKK tensile coupons once annealed.....	50
Figure 39. Stress-strain curve of PEKK tested specimens printed at an EM of 1.00	51
Figure 40. Stress-strain curve of PEKK tested specimens printed at an EM of 1.05	52
Figure 41. Comparison of the mechanical properties of PEKK printed at an EM of 1.00 and 1.05	52
Figure 42. (a) CF-PEKK coupon as came from the annealing treatment (b) same coupons once the salt was removed and the surface was sanded down.....	53
Figure 43. Stress-strain curve of CF-PEKK tested specimens printed at an EM of 1.00.....	54
Figure 44 Stress-strain curve of CF-PEKK tested specimens printed at an EM of 1.05.....	54
Figure 45. Comparison of the mechanical properties of CF-PEKK printed at an EM of 1.00 and 1.05..	55
Figure 46. Stress concentrations in tensile coupons: (a) Coupon directly printed using a CAD model with the shape and size required by the standard (b) Coupon machined from a blank to the to the standard shape and size	56

Figure 47. Comparison of the mechanical properties of PEKK and CF-PEKK printed at an EM of 1.00 and 1.05	58
Figure 48. PEKK common standard piece developed by Autodesk and Kickstarter after annealing printed at an Extrusion multiplier of: (a) 1 and (b) 1.05.....	62
Figure 49. CF- PEKK common standard piece developed by Autodesk and Kickstarter after annealing printed at an Extrusion multiplier of: (a) 1 and (b) 1.05.....	64
Figure 50. Geometry features of CF-PEKK metrology part: (a) material dimensions, (b) overhangs, (c) pins, (d) fine flow control; and (e) bridging.....	66
Figure 51. Warping experienced by the CF-PEKK calibration cube during annealing	68
Figure 52. PEKK calibration cube printed at EM=1.00 (a) and (b); and at EM=1.05 (c) and (d)	69
Figure 53. CF-PEKK calibration cube printed at EM=1.00 (a) and (b); and at EM=1.05 (c) and (d)	70
Figure 54. U.S. 3D printing filaments market share, by application, 2019 (%) [57]	71
Figure 55. Global 3D Printing market share, by usage in 2021[59].....	72
Figure 56. Global 3D printing filament market size 2016-2027 (USD Million) [57]	73
Figure 57. Future directions to drive the development of FFF technology	76
Figure 58. Pre-print simulation of the 3dBenchy made with Simplify3D	82
Figure 59. Pre-print simulation of the metrology part made with Simplify3D	82
Figure 60. Pre-print simulation of the calibration cube made with Simplify3D	82
Figure 61. Pre-print simulation of ASTM D638-14 type IV specimen made with Simplify3D	83
Figure 62. Pre-print simulation and raster pattern of the cross-section sample made with Simplify3D..	83
Figure 63. Original Prusa i3 MK3	83
Figure 64. CAD FILE created for the PLA bridging study	84
Figure 65. AON3D m2 printer [63].....	84
Figure 66. PEKK common standard piece developed by Autodesk and Kickstarter before annealing printed at an Extrusion multiplier of: (a) 1 and (b) 1.05.....	84
Figure 67. CF- PEKK common standard piece developed by Autodesk and Kickstarter before annealing printed at an Extrusion multiplier of: (a) 1 and (b) 1.05.....	85

Index of tables

Table 1. Results of the bridging analysis.....	29
Table 2. Optimal printing parameters for PLA.....	32
Table 3. Optimal printing parameters for PEKK.....	35
Table 4. Results of the retraction study carried out on CF-PEKK	38
Table 5. Optimal printing parameters for CF-PEKK	39
Table 6. Anisotropy of z-printed parts as a function of the EM for PEKK and CF-PEKK	57
Table 7. Confidence intervals for the ultimate tensile strength and the strain to failure of CF-PEKK at the two EM	59
Table 8. Relationship between the reduction of internal porosity and the % improvement of the mechanical properties	60
Table 9. Assessment score for PEKK at the two different extrusion multipliers.....	62
Table 10. Assessment score for PLA	63
Table 11. Assessment score for CF-PEKK printed at different extrusion multipliers	65
Table 12. Calibration cube dimension accuracy assessment for both EMs before and after annealing...	67
Table 13. Dimension of type IV ASTM D638-14 tensile coupons.....	86
Table 14. Initial printing parameters for PLA	86
Table 15. Physical, mechanical and thermal properties of PEKK provided by 3DXTech [44].....	87
Table 16. Initial printing parameters for PEKK	87
Table 17. Physical, mechanical and thermal properties of CF-PEKK provided by Kimya [51].....	88
Table 18. Reported mechanical properties for each of the PEKK coupons, sample mean and standard deviation.	89
Table 19. Reported mechanical properties for each of the CF- PEKK coupons, sample mean and standard deviation.	90

Chapter 1. INTRODUCTION

Additive manufacturing (AM), also known as 3D printing, is a fast-growing technology with a special focus on rapid prototyping. Although this application represents more than half of all its applications [1], the usage of AM to fabricate end use parts is growing substantially. The advantages offered by this promising technology include reduced production costs, increased complexity, custom materials, generative design, reduced waste and distributed manufacture (Digital designs can be shared with manufacturing centers easily and quickly, avoiding transportation costs) [2].

According to (ASTM) F2792-12a, AM processes can be classified into seven groups: (1) material extrusion; (2) vat photopolymerization; (3) binder jetting; (4) sheet lamination; (5) directed energy deposition; (6) material jetting; and (7) powder bed fusion [3]. All these categories share the basic principle of manufacturing, components are created by adding material in a layer-by-layer fashion. One of the key aspects to this technology is the need to use a slicing software to convert the computer-aided design (CAD) model into a G-code file. This file guides the hardware of the printer when adding new layers of material to obtain the desired part.

This paper focuses on fused filament fabrication (FFF), one of the most widely used AM processes. FFF belongs to the material extrusion family and stands out for its cost effectiveness and printing flexibility. The printing process, shown in Figure 1, is as follows. The material is loaded into the machine in a filament-based form. When the nozzle has reached the target temperature, the material is melted and deposited layer-by-layer, following the instructions given by the software. Completing a layer could be likened to coloring a figure, the nozzle extrudes material in a structured way until the area in the slice is filled. Once the layer is finished the extrusion head moves up and starts creating the next layer. This cycle is repeated as many times as necessary to finish the object [4].

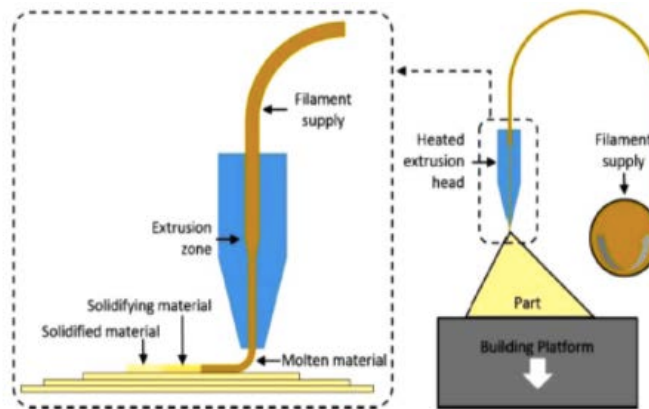


Figure 1. Schematic description of FFF [5]

FFF has three main characteristics: layers, supports and infill [6]. The surface quality of the object is mainly determined by the layers. It is essential that layers bond to one another in order to achieve a solid and cohesive part. When printing a new layer, the nozzle presses down the previous one, slightly re-melting the contact surface and bonding both layers together. As a result, the cross-section of the layers are oblongs rather than circles. This effect is shown in Figure 2 (a). Additionally, the layer height plays an important role in the surface finish. The thicker the layer, the shorter the manufacturing time, but the higher the roughness. The second key feature of this technology is supports. The melted material must be deposited on a solid surface and thus, printing complex geometries with angles greater than 45° requires the use of support structures. Problems arise when removing these supports. The areas of the part in direct contact are generally very affected and have undesirable surface finishes, which leads to the need of surface improvement with post manufacturing processes. Finally, infill is the third factor to be considered when printing FFF parts. The infill percentage defines the internal structure, as shown in Figure 2 (b) and thus, has a great impact on mechanical performance, cost and production time. If strength is not required, the infill percentage may be decreased in order to make parts cost effectively and quickly. Designers can also adjust other printing parameters such as the temperature of the chamber, the nozzle and the building platform, the build speed, the extrusion rate, etc. Although these inputs are generally set by the operator, some of them can be modified to study their impact on the performance and quality of printed parts.

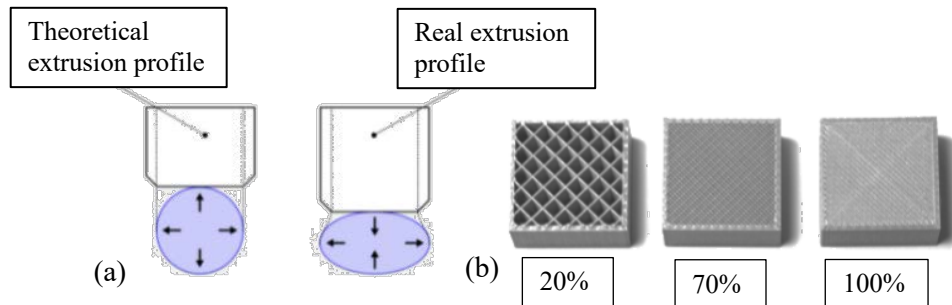


Figure 2. Illustration of the main characteristics of FFF, (a) layers: real vs. theoretical extrusion profile and; (b) infill: internal structure for different infill percentages [6]

Benefits and limitations of this printing process are critical for understanding its applications. The main advantages of FFF compared to other AM technologies are lower production costs, simplicity and versatility. The equipment required is cheap and easy to operate. Another benefit is that FFF can be applied on many materials, ranging from simple thermoplastic polymers to polymer matrix composites (PMC) reinforced with carbon fibers (CF) or glass fibers. The material choice, which depends on the desired mechanical properties and accuracy of the part, determines the printing difficulty. Generally, the higher the performance of the polymer, the more difficult it is to manufacture. Polylactide (PLA) and acrylonitrile butadiene styrene (ABS) should be highlighted as the most common materials for this AM process.

Despite the aforementioned advantages offered by this technology, intrinsic deficiencies of FFF printed parts constitutes a barrier to high-demanding practical applications [7]. Low dimensional accuracy and resolution, high porosity, poor inter-layer adhesion, mechanical anisotropy and the need to apply post-processing treatments to the printed parts [8-10], have slowed down the transition from rapid prototyping to printing end use parts. As explained in detail in Chapter 2. all the solutions that have been devised to date involve either the introduction of new steps in the printing process [11-13] or the combination of different materials [14]. One potential solution to address the large degree of anisotropy of printed parts could be to increase the filament feed rate. The extrusion multiplier (EM), also known as flow rate, determines the quantity of filament per slice time that comes out from the nozzle. Preliminary studies have shown there is a relationship between the degree of over-

extrusion and the structure, mechanical properties, and printing quality of FFF parts [15]. As shown in Figure 3, increasing the filament feed rate is an effective approach to reducing the void content. However, while over-extrusion could improve interlayer strength and reduce mechanical anisotropy, it might also lead to a loss of printability of AM features of interest. Printability is one of the main advantages offered by FFF and thus, there is a need to determine to what extent the EM could be increased, without losing print quality.

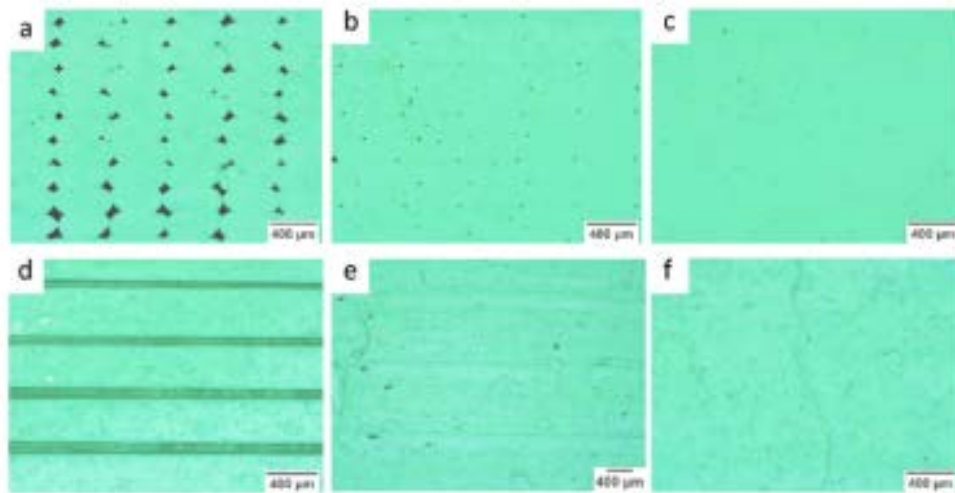


Figure 3. Effect of the extrusion multiplier (EM) on the internal structure of FFF parts, perpendicular to the X (top three figures) and Z (bottom three figures) directions, respectively. (a and d: EM=1, b and e: EM=1.1, c and f: EM=1.2). [15]

In addition, this paper is focused on a high-performance thermoplastic, Polyetheretherketone (PEKK), and its composite (CF-PEKK). Traditional materials used to manufacture parts via FFF, such as PLA and ABS, offer insufficient mechanical properties for many high industrial applications. The interest in this manufacturing technique has led to material evolution which, in turn, has required improvements in the process [16]. The development of high-temperature FFF 3D printers has allowed the incorporation of polymers with relatively high thermomechanical properties, such as Polyaryletherketone (PAEK) family members, and their composites. A composite is defined as a material formed artificially from two independent components, which provide the best of their properties. These materials offer high strength, high stiffness, good shear strength and low density and therefore, they have become the main substitutes of traditional neat materials. There are many classifications of composites according to the matrix, the type of fibers, the

manufacturing process, and so on. This study is focused on CF-PEKK, a composite material with a thermoplastic matrix (PEKK) reinforced with chopped carbon fibers (CF). The addition of CF to the PEKK matrix improves the already excellent properties offered by the polymer alone and hence there is growing interest for future high-demanding applications.

Chapter 2. STATE OF THE ART

The aim of this chapter is to explain the importance of the study based on the current status of FFF. The lack of comprehensive design guidelines, coupled with the printing weaknesses mentioned in the introduction, has prevented this technology from competing with other AM processes and has mostly limited its applications to rapid prototyping [17]. In order to provide a deeper insight of the situation, this chapter discusses the causes of FFF limitations and the solutions found to date. In addition, EM is introduced as a potential solution to address some of the intrinsic deficiencies associated with this manufacturing technology.

The layer-by-layer fashion of AM processes results in parts with a high degree of porosity. Pores, also known as voids, can be classified into five categories depending on their mechanism of formation: raster gap voids, partial neck growth voids, sub-perimeter voids, intra-bead voids and infill voids [7]; among them, only infill voids and raster gap voids are controllable. An increased porosity is desirable for applications where weight is more important than mechanical performance; the reverse is true for applications relying on the mechanical performance of the printed part. Feedstock material and processing parameters have a significant impact on the porosity of 3D printed parts. Many studies have shown that increasing the extrusion temperature is an effective approach to reducing porosity [18, 19]. Other printing parameters that have been found to be relevant in void formation are bed temperature [20, 21], printing speed [22], layer height [21], infill; and position on the z-axis [22]. Moreover, the addition of plasticizers to raw filaments has proven to be a good technique to reduce the degree of porosity. Despite these results, there have not been comprehensive studies on the effect of printing parameters and materials on the presence and formation of these pores [7] and hence, there is a need to understand it more in depth.

Another important deficiency of FFF technology is low inter-layer bonding. During deposition, large temperature gradients and the lack of external pressures apart from gravity result in poor bonding between layers [8]. Stress concentrations formed at voids, together

with weak interlayer adhesion leads to anisotropic parts with mechanical properties off the longitudinal direction worse than expected.

Mechanical anisotropy is primarily a function of two variables, feedstock and printing orientation. In particular, if all rasters (also known as beads or roads) are printed in the same direction, the parts will have orthotropic properties and consequently their mechanical performance will be anisotropic. Studies have shown that the tensile strength of FFF parts built in the z-direction (perpendicular to the build plate) is significantly lower compared to the same part's strength built in the x- and y-directions. Among them are the papers written by J.F. Rodriguez et al. [23] and X. Gao et al. [24] on the anisotropy of the two most common materials in FFF, ABS and PLA. Rodriguez et al. found the optimal parameter settings for ABS with the aim of maximizing transverse strength. As can be seen in Figure 4, the highest transverse strength was reported to be 13.4 MPa, a value that is lesser by 45% with respect to the longitudinal strength (24.4 MPa). For its part, Gao et al. studied the mechanical properties of neat PLA, PLA/talc and PLA/CF for different raster angles. Neat PLA specimens with a 90° printing orientation showed the highest level of anisotropy, which was found to be 60%. Another important conclusion of this study is that the mechanical property most affected by raster angles and therefore, the one that presents the highest anisotropy, is the tensile strength.

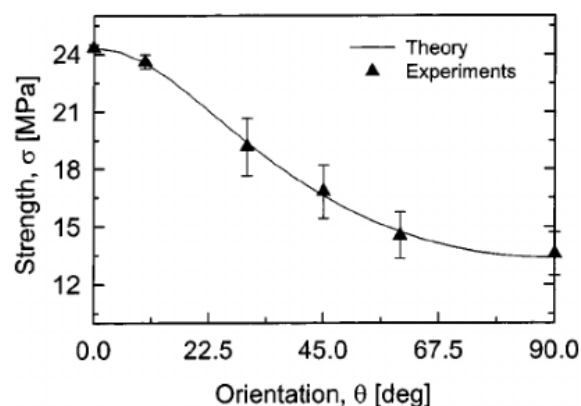


Figure 4. Strength versus load-to-fiber angle for unidirectional FD-ABS specimens [23]

Although in-plane anisotropy can be improved with the combination of different raster angles (0°/45°/-45°/90°), this technique is not an effective approach for reducing the

anisotropy of parts printed in the z-direction [25]. In an attempt to improve out-of-plane performance, several research projects have been conducted from various perspectives. In-situ heating, blending different thermoplastics and incorporating additives to the raw filaments are different approaches that have proven to be quite effective to decrease anisotropy. In-situ heating is a very simple technique that consists in increasing the temperature of the last printed layer, just prior to adding a new one, by using infrared radiation (IR). Studies have demonstrated that this procedure improves adhesion between layers contributing to a better z-strength [11-13]. Secondly, the combination of various thermoplastics with nano-additives has proved to reduce anisotropy by up to 50% [14]. Nevertheless, all these solutions imply either the incorporation of new steps in the printing process or the modification of raw materials and thus, the search for alternative approaches such as over-extrusion.

As explained in the introduction, the EM is a printing parameter that determines the flow rate of filament through the nozzle. An increase in the amount of extruded material per slice time results in a reduction of the number of pores as well as in a decrease of the pores' diameter [26]. According to the cited study, the use of a higher extrusion multiplier is helpful unless it deteriorates the outer surface of the printed part. Moreover, the paper concludes that the optimal EM depends on the type of feedstock material and the gear design used in the printer. To date, there is only one paper focused on the impact of over-extrusion on the mechanical properties and features of interest (dimensional accuracy, flow control, negative features and overhangs, excluding surface roughness) of FFF parts [15]. Increasing the EM by 20% resulted in improved mechanical properties of ABS printed items. As shown in Figure 5, this effect was especially noticeable in the tensile strength of coupons along the z-direction. The tensile strength reported with an EM of 1.2 was 50% higher than that reported with an EM of 1 and consequently, relatively isotropic tensile properties could be achieved. In addition, the study concluded that over-extrusion does not negatively affect printability, which is a very important finding. The results of the two mentioned studies are based on parts printed with low melting polymers (ABS and PLA) using desktop printers. However, to the best of the reader's knowledge, there is no study aimed to understand the effects of over-extrusion on high-performance polymers or on composites. As will be developed in the

next chapter, both super polymers and composites are in the spotlight, which enhances the interest in this study.

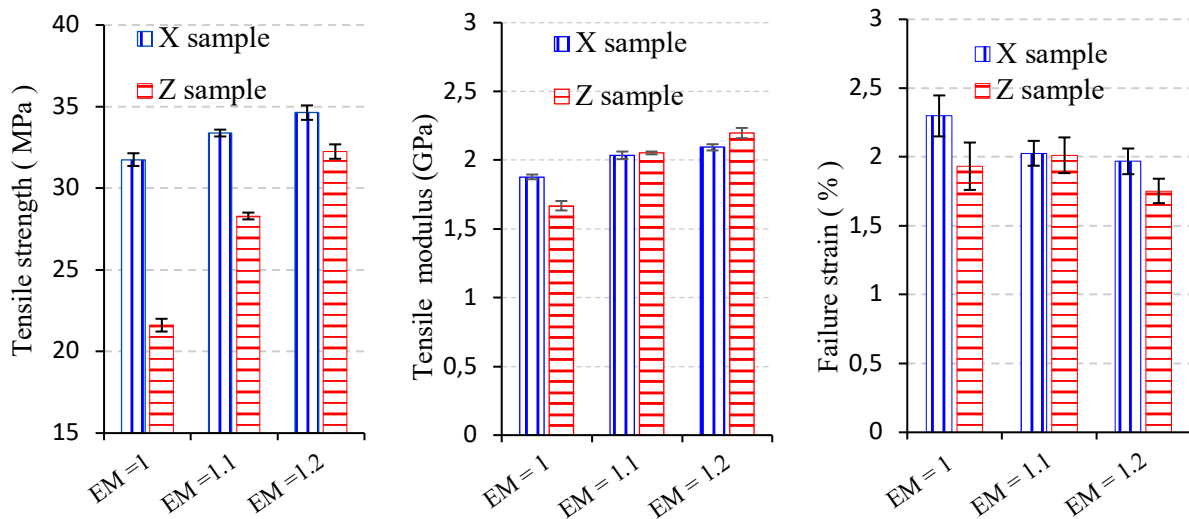


Figure 5. Effect of extrusion multiplier on tensile strength, modulus, and failure strain of FFF ABS coupons along the X and Z directions [15]

Chapter 3. MATERIALS

This chapter introduces the materials used for the study: PLA, PEKK and PEKK reinforced with chopped carbon fibers (CF-PEKK). It includes a description of the properties, limitations and applications of the chosen materials to give a better understanding of their importance in the realm of 3D printing. Although the initial idea was to repeat the research in PEEK and CF-PEEK, the lack of time coupled with some printing difficulties led to the decision to abandon these materials.

3.1 PLA

PLA is a biodegradable polymer typically made from natural resources such as sugar cane or corn, yucca or cassava starch [27]. The structural unit of PLA is a lactide, the cyclic diester of the lactic acid [28]. It has a low melting point (between 170°C and 180°C), which makes it ideal for manufacturing processes such as FFF. The benefits of this material include ease of use, low cost compared to high-performance thermoplastics, great printing flexibility (in terms of 3D printers that can be used) and decomposition by the action of living organisms [29]. Among the applications of PLA parts manufactured via FFF, rapid prototyping and packaging are the most representative ones. In addition, PLA is a promising material for biomedical applications. To date, it has been used for tissue engineering, drug fabrication, orthopedic devices and dental implantology [30].

Despite the numerous advantages offered by this thermoplastic, its mechanical properties are insufficient for many high-demanding industrial applications. A typical value for the tensile strength of PLA is 56 MPa. Considering that this value is about 6 times lower than the tensile strength of aluminum (~300 MPa), it can be deduced that the mechanical properties of PLA represent a barrier for many applications.

Currently, there are many studies on 3D printing with PLA [11, 24, 31, 32]. Although this thermoplastic is not the focus of interest of the study, a prototype of model was developed with this material. The purpose of creating this prototype was to verify that the virtual model met the expectations without wasting the other materials, which are more

difficult to print and much more expensive. The price of PLA filaments is around \$32 per spool, a significantly low price compared to the \$395 that costs a spool of PEKK filament.

3.2 PEKK

So far, most FFF studies have focused on low melting temperature polymers such as acrylonitrile butadiene styrene (ABS) and polylactic acid (PLA) due to printing convenience and low manufacturing cost [33]. As mentioned in the previous section, mechanical properties of these materials are insufficient for many industrial applications. The strong potential of FFF technology has led to the search for new compatible materials, with better mechanical properties. Among them are polyetheretherketone (PEEK), Polyetherketone (PEK) and PEKK, three semi-crystalline thermoplastics that belong to the (PAEK) family. As shown in Figure 6, they are considered the best polymers compatible with FFF technology in terms of mechanical performance.

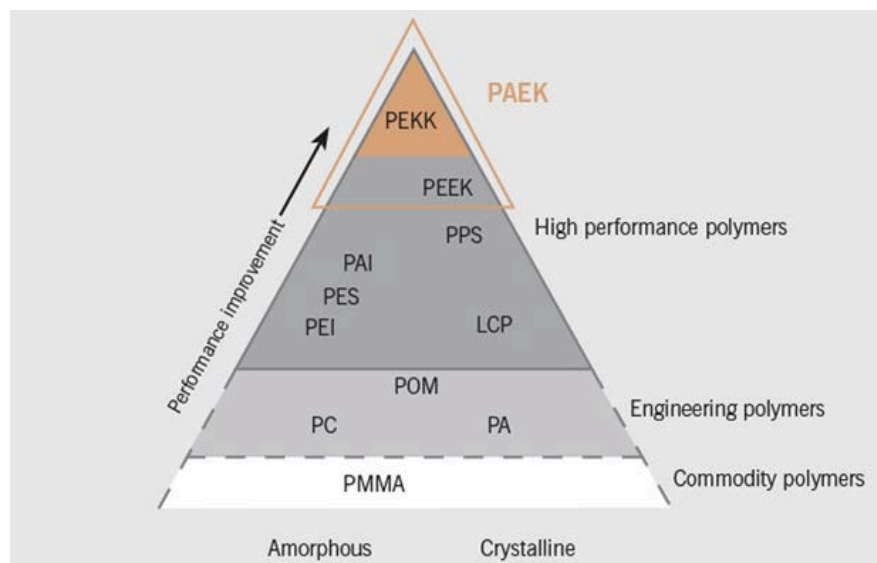


Figure 6. Pyramid showing the different performance levels of materials used for FFF technology [34]

During the last years, the interest in polymers belonging to the PAEK family was focused on PEEK. This super polymer stands out for its superior thermal degradation resistance and its high weight-to-strength ratio. It has a high melting temperature (340°C) and a high crystallization temperature (144°C), which is a great challenge when it comes to 3D printing [35, 36]. Moreover, this thermoplastic has a high rate of crystallization and therefore, it

requires a continuous monitoring of the extrusion temperature and the cooling steps. It is very difficult for the last layer to maintain an amorphous structure before the next layer is added, resulting in serious adhesion problems. For this reason, PEKK, which also offers excellent thermomechanical properties but has a lower crystallization rate, has become a strong candidate as an alternative to PEEK. The main difference between these thermoplastics is that they have an inverse molecular structure. Whereas PEEK has one ketone and two ethers, PEKK has one ether and two ketones. Ketones are stiffer than ether linkages [37, 38], which implies that PEKK has a higher melting temperature (360°C-380°C), a higher glass transition temperature (156°C) and a slower crystallization rate. The cooling process has a lower impact on the properties of the final part and consequently, it is easier to print [34]. Nevertheless, it is to be noted that this polymer requires post processing [25]. Once the printed part is finished, it must undergo an annealing process to increase the crystallinity and thus, improve the final properties.

<h1>PEEK</h1>	<h1>PEKK</h1>
<p style="text-align: center;">Characteristics</p> <ul style="list-style-type: none"> • Lower glass transition temperature • Good ratio weight/resistance • Higher extrusion temperature (almost 400°C) • Main applications: transport, aeronautics, medical • Compatible technologies: FDM 	<p style="text-align: center;">Characteristics</p> <ul style="list-style-type: none"> • High dielectric strength • Easier to 3D print • Doesn't release toxic smoke • Lower extrusion temperature (340 - 360°C) • Main applications: transport, aeronautics, oil&gas • Compatible technologies: FDM / SLS
<p style="text-align: center;">Price</p> <p style="text-align: center;">\$300-350*</p> <p style="text-align: right; font-size: small;">*per 500g spool</p>	<p style="text-align: center;">Price</p> <p style="text-align: center;">\$350-400*</p> <p style="text-align: right; font-size: small;">*per 500g spool</p>
<p style="text-align: center;">Producers/Manufacturers</p> <ul style="list-style-type: none"> <li style="width: 50%;">• Victrex <li style="width: 50%;">• 3D4Makers <li style="width: 50%;">• Evonik <li style="width: 50%;">• 3DXTech <li style="width: 50%;">• Solvay <li style="width: 50%;">• W2 Polymer 	<p style="text-align: center;">Producers/Manufacturers</p> <ul style="list-style-type: none"> <li style="width: 50%;">• Arkema <li style="width: 50%;">• Kimya <li style="width: 50%;">• Lehvoss <li style="width: 50%;">• 3D4Makers <li style="width: 50%;">• Oxford Performance Materials <li style="width: 50%;">• 3DXTech

Figure 7. Comparison between PEEK and PEKK in terms of characteristics, price and producers [34]

The lack of time did not allow to carry out the study on both PEEK and PEKK. Therefore, it was necessary to weigh the pros and cons of each of them and make a decision. Figure 7 shows a more detailed comparison between both thermoplastics. The low number of studies

carried out with PEKK, together with the greater ease of printing via FFF, led to the choice to prioritize it over PEEK.

As stated, little research has been done with PEKK in the realm of 3D printing and hence, there is a lack of literature in this field. B.W. Kaplun et al. investigated the influence of print orientation and raster patterns on the mechanical properties of this material [39]. He carried out tensile tests with coupons printed in three directions (edge, vertical and flat as shown in Figure 8 (a)), for different raster patterns. Once the tensile strength, Young's modulus and strain to failure were computed for the different configurations, he was able to compare them and draw different conclusions. As illustrated in Figure 8 (b), he demonstrated that the mechanical performance of vertically printed samples is much worse compared to that of edge and flat oriented samples. The anisotropy is especially remarkable in vertical parts printed with a 0° parallel raster, where the difference in strength reached 59.6%. As explained in the next chapter, this paper is focused on tensile coupons printed in the z-direction (vertical) with 0° parallel rasters. The mechanical properties reported in this study for the same configuration are 2.457 GPa for the Young's Modulus, 41 MPa for the ultimate tensile strength and 1.6% for the strain to failure. Secondly, B.W. Kaplun et al. concluded that altering the infill pattern is detrimental to mechanical properties in comparison to those shown by edge printed samples with 45° perpendicular raster. In other words, he proved that the optimal printing orientation for PEKK is 45° perpendicular configuration.

In addition, it is worth mentioning the study carried out by T. Yap et al.[25], aimed to investigate the effects of selective laser sintering (SLS) and FFF on the PAEK family of polymers and their composites. This paper reports the anisotropic mechanical behavior of PEKK parts manufactured via FFF (see Figure 9). Moreover, the analysis of the crystallization degree led to the conclusion that PEKK parts must undergo an annealing post-treatment in order to increase their crystallinity and improve their thermomechanical properties. Thanks to this thermal treatment the degree of crystallinity could be increased from 4% (as printed) to 30% (once annealed).

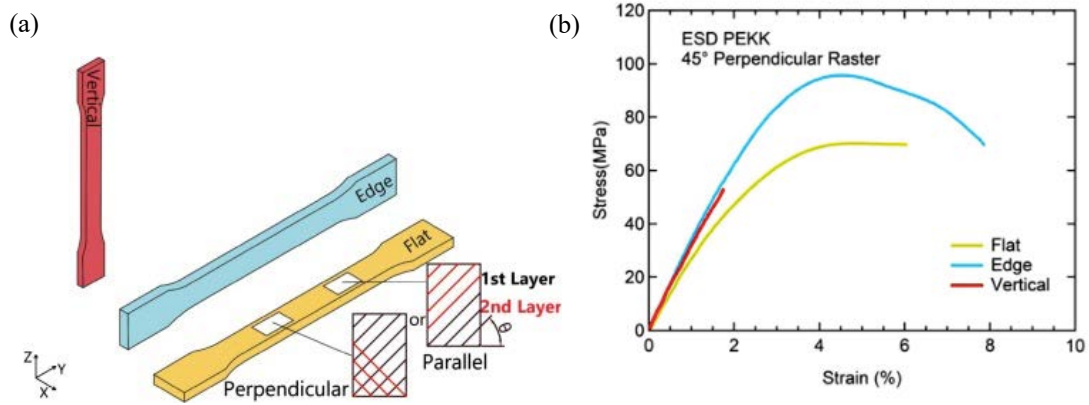


Figure 8. (a) Print orientations and raster patterns for ASTM type I samples tested in the cited study; and (b) representative stress-strain curves of ESD PEKK in the Edge, Flat, and Vertical print orientations with a 45° perpendicular raster infill [39]

3.3 CF-PEKK

CF-PEKK is among the best high-performance composites that exist in the world. The addition of CF improves the already excellent properties offered by PEKK. This reinforcement increases the strength by almost 10% (from 105 MPa to 115 MPa) and enhances the longitudinal Young's modulus by almost 200% (from 3.2 GPa to 9.56 GPa) [25]. Other advantages offered by this composite include superior chemical resistance, low coefficient of thermal expansion and almost zero moisture absorption. Currently, the future projections for this composite are very encouraging in industries that require materials with superior mechanical, chemical and thermal properties.

The merging of AM, a groundbreaking technology, and composites, the materials of the future, is a very attractive and promising idea. As in the case of PEKK and PEEK, CF-PEKK properties are similar to those of CF-PEEK except for the degree of crystallization. CF-PEKK has a lower degree of crystallization, around 7% compared to the 27% of CF-PEEK, and consequently, it is a more amorphous material. This is an advantage when printing because the shrinking effect is limited to 0.01% (CF-PEEK has a shrinking effect of about 2%) [25]. Nonetheless, most FFF studies have focused on CF-PEEK, instead of CF-PEKK, and hence, there is growing interest in exploring 3D printing with this composite.

It is relevant to note the study carried out by T. Yap et al. [25], previously mentioned in PEKK literature. The ultimate tensile strength, Young's Modulus and strain to failure of CF-PEKK samples printed in the x-direction were reported to be 110 MPa, 7.2 GPa and 2.75%, respectively. These excellent properties contrast with those obtained for the test specimens printed in the z-direction: 30 MPa for the ultimate tensile strength, 2 GPa for the Young's modulus and 0.5% strain to failure. This anisotropic behavior is illustrated in Figure 9. In addition, a high percentage of void content ($\sim 18.3\%$) was observed in CF-PEKK samples manufactured via FFF, mainly caused by the presence of tiny holes in the raw filaments. Lastly, X-ray tomography on gauge sections of broken z-direction coupons revealed that chopped CF tend to align in print-x direction.

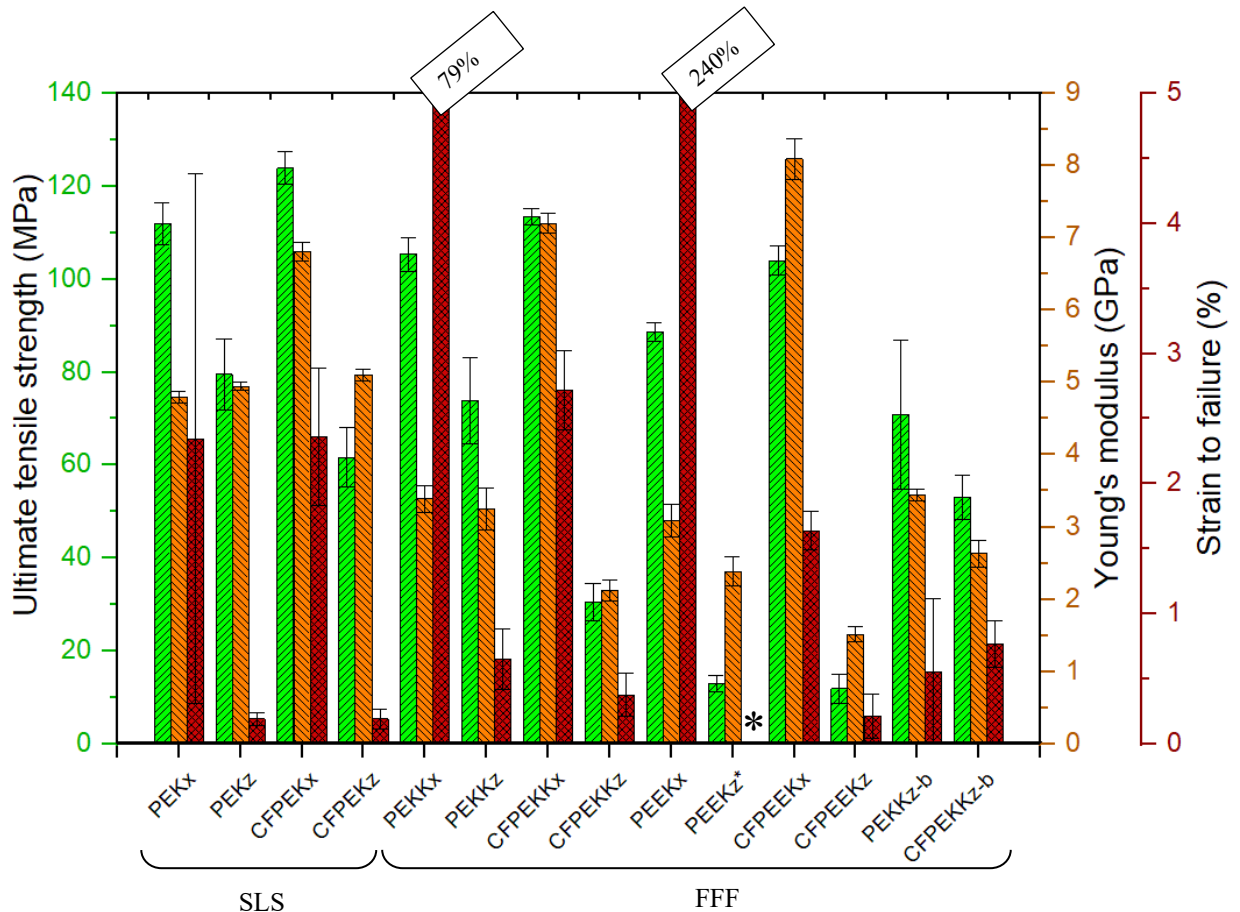


Figure 9. Ultimate tensile strengths, Young's modulus, and failure strains for tested specimens manufactured via SLS and FFF [25]

Chapter 4. METHODOLOGY

The aim of this chapter is to elaborate on the methodology followed for the purpose of analyzing the effects of over-extrusion on the mechanical properties, structure and quality of PEKK and CF-PEKK. The first step in the study's approach was to create a CAD model including six ASTM Type IV tensile coupons, one cross-section sample, and two metrology parts to assess printability (a calibration cube and a common standard piece developed by Autodesk and Kickstarter). Secondly, in line with real applications and prior to starting the research, a prototype of the CAD file was created with PLA in order to check that the model was indeed the desired one. Once this verification was successfully completed, it was necessary to determine the optimal parameters for each of the materials analyzed. To avoid wasting material, the search for the optimal parameters was carried out only with an additional metrology part, the 3DBenchy. Then, the CAD model was printed twice, keeping all the input settings constant and changing the extrusion multiplier. A preliminary FFF study performed with PEKK and CF-PEKK using the same printer showed that increasing the EM by 5% is enough to considerably reduce the void content. In addition, as both materials have a high melting point, it would be very difficult to further increase the EM without any printing failure. Therefore, this paper compares the quality, mechanical properties and porosity of the model printed with an EM of 1 and EM of 1.05

After printing the parts, they underwent an annealing post-treatment with salt, explained in section 4.3.3. Finally, all test coupons were subjected to a tensile test, cross-section samples were examined using micro computed tomography, and the features of interest of the metrology parts were checked against the expected ones. Each of the steps followed to obtain the parts to be tested (design of the CAD file; creation of the prototype; printing process with PEKK and CF-PEKK; and annealing post-treatment) will be explained in detail in a subsection of this chapter in chronological order.

4.1 DESIGN OF THE CAD MODEL

This subsection presents the parts of the CAD file, including a brief description of each part as well as its role in the study.

4.1.1 3DBenchy

3DBenchy, also known as Benchy Boat, is a virtual model design to test the printing quality of any 3D printer with multiple materials. As shown in Figure 10, it has special characteristics, difficult to recreate, and very specific dimensions whose analysis can yield conclusions about resolution and printability. For this study, 3DBenchy was used as a reference to find the optimal parameters with each of the materials. In other words, several prints, all of them with the standard EM (1), were carried out until the print quality achieved with those input settings was good enough. These parameters, except for the filament feed rate, remained invariable in the successive model prints in order to study the effect of over-extrusion. Figure 58 in ANNEX I shows the aspect of the sliced 3DBenchy with Simplify3D, the slicing software used with the high-temperature 3D printer.

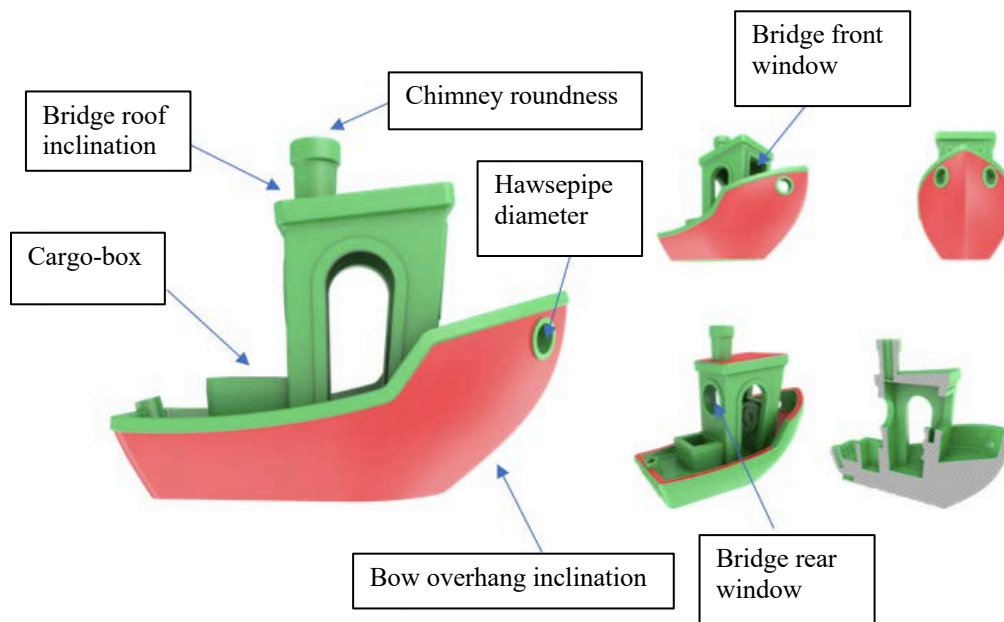


Figure 10. 3DBenchy [40]

4.1.2 Common standard piece developed by Autodesk and Kickstarter

Figure 11 shows one of the parts that was used to evaluate the effects of over-extrusion on AM features of interest. Unlike 3DBenchy, this part was printed once the optimal parameters were found to assess whether increasing the filament feed rate by 5% has a negative impact on the print quality of PEKK and CF-PEKK. The design has challenging features, including bridges, overhangs, flow control, negative feature resolution and dimension accuracy, to check the quality and precision of the manufactured part. Kickstart and Autodesk, the developers of this metrology part, have created an assessment protocol to ensure that the conclusions drawn are as objective as possible [41]. The scoring criteria is explained in section 6.2, along with the analysis of the results. Lastly, the simplify 3D simulation of this part is shown in Figure 59 (see ANNEX I)

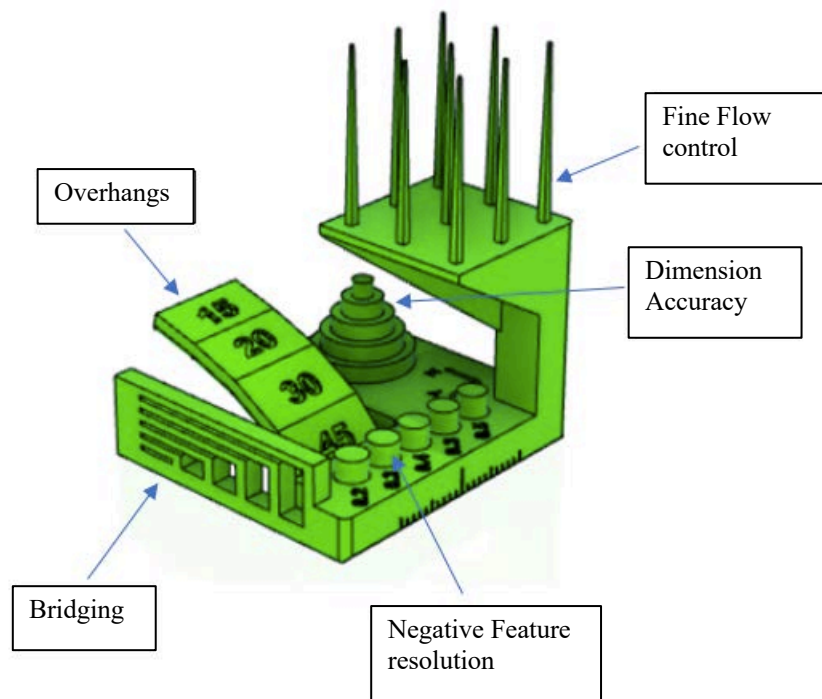


Figure 11. Metrology part developed by Autodesk and Kickstarter [41]

4.1.3 Calibration cube

The calibration cube is a very common tool, used to examine the accuracy and precision of 3D printers. As shown in Figure 12, it is a simple cube with the letters X, Y and Z engraved on three of the faces. Thanks to this part it is possible to identify problems such as ringing and shrinkage, and refine the printer's tolerances. In the case of this study, this figure was useful to evaluate the potential change in dimensions caused not only by over-extrusion, but also by the annealing post-treatment. The slicing of the part made with Simplify3D is shown in Figure 60 (See ANNEX I).



Figure 12. Calibration cube [42]

4.1.4 Tensile coupons

According to ASTM D638-14 standard, type IV tensile coupons are to be used to determine the mechanical properties of thermoplastic materials. In case of anisotropic parts, the norm recommends testing at least five specimens parallel with and five normal to the principle axis of anisotropy. Nevertheless, mechanical properties of the parts printed parallel to the build platform have already been determined and verified [25], so this study focuses only on the specimens built in the (z-) direction. As explained in Chapter 2, preliminary studies have shown that parts printed in the (x-) and (y-) directions meet the expected mechanical properties and consequently, the focus of interest is the influence of over-extrusion on the out-of-plane performance. By comparing the mechanical properties of parts manufactured parallel to the (x-) or (y-) axis and specimens printed normal to the XY plane (z-direction), it is possible to determine the degree of anisotropy and check whether over-extrusion is an effective solution to this problem. Figure 13 shows the shape of tensile

specimen that was tested, Table 13 (see ANNEX II) contains the exact dimensions of the part, and Figure 61 (see ANNEX I) represents the sliced part with Simplify3D.

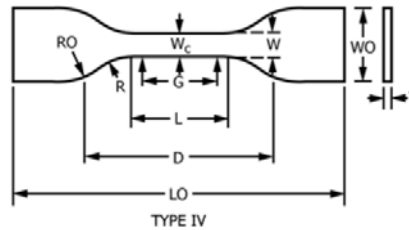


Figure 13. ASTM D638-14 standard, type IV tensile coupons

4.1.5 Cross section sample

The presence of voids inside printed parts is another limitation that could be reduced via over-extrusion. In order to analyze the evolution of the internal structure as the extrusion multiplier is increased, cross section samples with a V-notch were printed. The aspect and dimensions of the part are shown in Figure 14. It is important to note that, to determine the percentage of porosity, all the rasters had to have the same printing orientation, 0° . This specification was defined in the slicing of the virtual model, shown in Figure 62 (see ANNEX I).

The initial idea was to break the samples and analyze the fractured surface with a microscope and hence the presence of the V-notch to facilitate brittle fracture. Nevertheless, micro computed tomography (Micro-CT) was finally used to achieve greater precision and, therefore, it was not necessary to break the samples. The device chosen for the inspection was a MicroXCT 400 Zeiss machine. Thanks to the accuracy of the system, explained in detail in Chapter 5. it was possible to determine the fraction of voids and study their morphology.

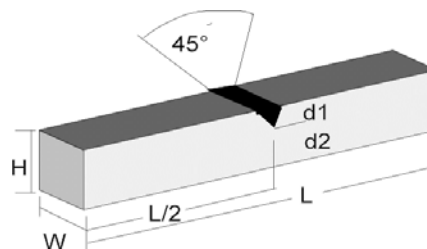


Figure 14. Cross-section sample [43]

4.2 PROTOTYPE OF THE MODEL

This section is focused on the physical prototype of the model created with PLA. Prototyping is very useful for any new design since it can save time and material if the virtual model is not the desired one.

4.2.1 Printer and slicing software

The PLA prototype was manufactured with a printer that belongs to Prusa, a leading company in 3D printing created by Josef Prusa in 2012. There are many models of 3D printers, but the prototype was printed with the original Prusa, named Original Prusa i3 MK3, shown in Figure 63 (see ANNEX I). Firstly, it is important to note that this printer has a build volume of 25x25x21 cm, which makes it ideal for numerous locations (Desktop printer). The printing procedure follows the general pattern of all FFF processes. The conversion from the virtual model to the tangible part begins with the generation of the G-code, a programming language responsible for giving orders to the hardware. Prusa has its own program, PrusaSlicer, with three levels of increasing complexity that differ in the printing parameters that can be modified. Each level has three configurations: the printing configuration with parameters such as speed, infill, layers and perimeters, support material, and so on; the filament configuration where the properties of the filament, the extrusion temperature or the cooling process can be modified; and lastly, the printer configuration with variables that include the limits of the printer, the characteristics of the nozzle, calibration of the axes, etc.

Original Prusa is very easy to operate and is compatible with a wide range of thermoplastics. However, the nozzle can reach a maximum temperature of 300 °C, which poses a major limitation in its application for high-performance polymers such as PEKK. In addition, it lacks a closed chamber capable of maintaining the temperature during the manufacturing process. This is one of the requirements for thermoplastic materials with a high melting temperature, whose final properties depend largely on the degree of crystallization.

4.2.2 Printing process

The first step prior to creating the prototype of the model was to determine the optimal printing parameters using 3DBenchy. To this effect, the default settings configured in PrusaSlicer for PLA were chosen as the starting point (see Table 14 in ANNEX II). The results obtained with this configuration suggested aspects to improve, including bridges and smaller diameters. The analysis of the small details such as the chimney indicated that the nozzle temperature was too high. The higher the extrusion temperature, the greater the deformation that the printed layers experience when more material is added. As shown in Figure 15, this affects the viscosity of the material, making it difficult for the layers to remain in the place deposited by the nozzle. However, it is very important to find the right balance between good quality and good layer bonding. If the extrusion temperature is too low, the filaments do not blend properly at the interface. The lack of bonding between layers leads to worse than expected mechanical properties and favors brittle fracture, the most critical fracture for any application [31]. On this basis, the optimum nozzle temperature for PLA was found to be 200°C for the first layer and 205 °C for the successive layers.



Figure 15. Chimney of the 3DBenchy

In addition, two other factors that could be improved were the bridges and the 40° overhang in the front part of the boat. Bridges and overhangs are two of the most challenging aspects of FFF manufacturing process that can be assessed with the 3DBenchy model. From an overhang point of view, the boat printed with the first configuration gave the feeling of layers being too close together, at some point overlapping. One possible solution to address this problem is to decrease the extrusion temperature and increase the layer height, without this becoming excessive. An excessive layer height can lead to a considerable loss of quality. The new layer height, set to 0.1 mm, together with the previously mentioned decrease in the

nozzle temperature, turned out to work very well. The study of the bridges was more complex. In order to understand the effect of the bridging flow rate and the printing speed on bridges, a new CAD file was created. The model was based on a 50 mm long bridge that was replicated six times, and the printing was configured so that each of the replicas had a different speed and bridging flow rate. Figure 64 (see ANNEX I) shows an image of the virtual model in PrusaSlicer.







	[10 – 20]	[20 – 30]
Speed (mm/s) / Flow rate		
0.7		
0.5		
0.3		

Table 1. Results of the bridging analysis

The results of the analysis are shown in Table 1. As can be deduced from the images, the optimal bridging parameters turned out to be 0.7 for the bridging flow rate and a range between 10 and 20 mm/s for the printing speed. On the one hand, if the printing speed is too low, the material is suspended in the air for an excessively period of time and part of the filament ends up drooping. On the other hand, if the printing speed is very high, the filament does not have enough time to adhere to the prior layers and this can cause a big mess [31].

In addition, the bridging flow rate is recommended to be relatively less than one, the standard value. The lower its value, the lower the amount of material that the nozzle expels while making the bridge. However, if the value is too low, the new layers will not have any surface to adhere to and the bridge will have the appearance of fine, randomly placed filaments rather than a compact surface.



Figure 16. 3DBenchy printed with PLA optimal parameters

Thanks to all the studies mentioned above, it was possible to find the optimal printing parameters for PLA with Original Prusa. These values are listed in Table 2. The next step was to print the entire CAD file with this material, in order to verify that it was indeed the desired model for the future study. Figure 17, Figure 18, Figure 19, Figure 20 show the different parts of the model. None of them gave problems so the procedure was repeated with PEKK and its CF composite.

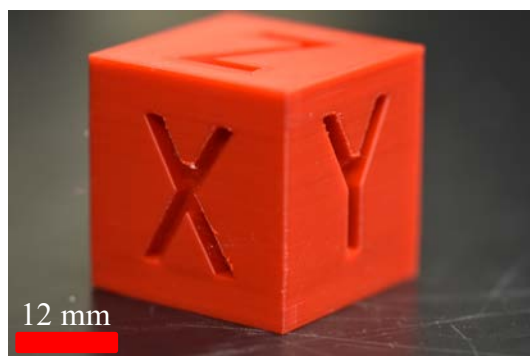


Figure 17. PLA calibration cube



Figure 18. PLA tensile coupons

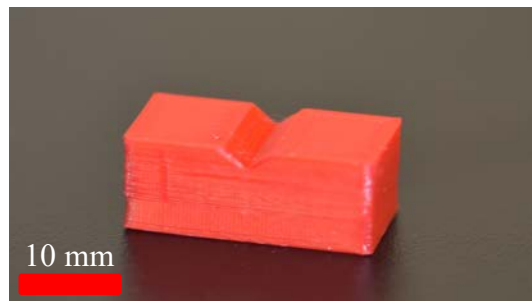


Figure 19. PLA cross-section sample

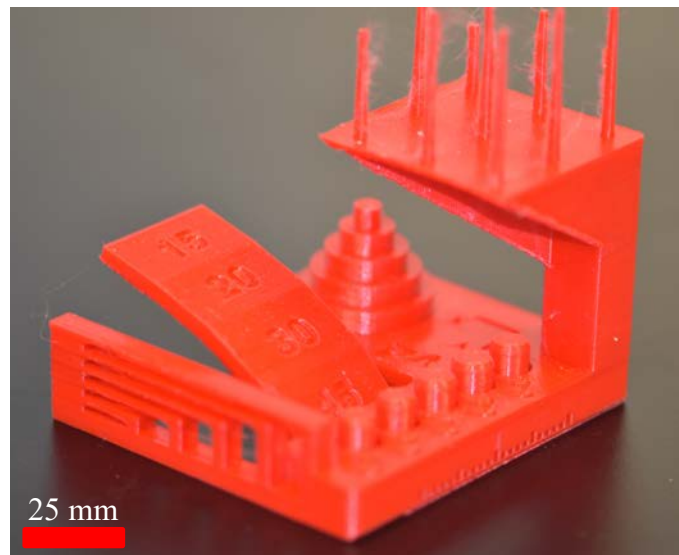


Figure 20. PLA metrology part

Printing parameter	Default value
Nozzle Temperature for the first layer	205 °C
Nozzle Temperature	200 °C
Bed Temperature	60 °C
Layer Height	0.1 mm
Speed for printing movements	10 mm/s – 20 mm/s
Infill	15 %
Bridging flow rate	0.7

Table 2. Optimal printing parameters for PLA

4.3 REAL MODEL

This section explains the printing process followed to obtain the different parts of the model with PEKK and CF-PEKK, the materials of interest of the study. It includes a description of the printer and software used, the procedure followed to obtain the optimal printing parameters for each material, the problems encountered and the changes that had to be made to the initial model.

4.3.1 Printer and slicing software

AON3D, founded in 2015 in Montreal, is a company dedicated to the development of hardware and software for AM processes. This study was carried out with their flagship product, AON3D m2, shown in Figure 65 (see ANNEX I). AON3D m2 is a high temperature 3D printer, compatible with abundant feedstock. Currently, it is one of the few printers on the market that allows printing parts made from PEEK, PEEK and their composites. The extruder temperature can be raised up to 500°C, the chamber is capable of reaching 120°C and the maximum bed temperature is 170°C.

In accordance with the manufacturer recommendations, Simplify3D was chosen as the slicing software to convert 3D digital models into print files. This program enables users to

control all printing parameters, and allows to simulate the entire printing process from the first to the last layer. Thanks to this advantage, operators can check whether the extruder follows the desired path and, otherwise, change it without wasting material.

4.3.2 Printing the model with PEKK

For this study, ThermaX PEKK-C from 3DXTech was used [44]. The physical, mechanical and thermal properties of this filaments can be found in Table 15 of ANNEX II. PEKK is very sensitive to moisture and thus, filaments had to be dried in a convection oven at a temperature of 120°C for at least 4 hours, prior to printing. According to the recommendations given by the material manufacturer and the material guidelines provided by the printer vendor, the parameters listed in Table 16 (see ANNEX II) were chosen as the starting point in the search for the optimal settings.

Figure 21 shows the 3DBenchy obtained with simplify3D default parameters. The color of the material suggested that the thermoplastic had not achieved a high degree of crystallization. However, as explained in section 3.2, parts printed with PEKK should undergo an annealing post-processing treatment and thus, the non-uniform crystallization was not a concern at that moment. Moreover, two aspects to improve were detected. Firstly, stringing was an issue due to high processing temperature [45]. This problem was improved by decreasing the extrusion temperature and increasing the retraction distance and retraction speed. Secondly, neither the chimney nor the hole in the back of the boat were properly printed. This issue was due to the fact that the cross-section of both features is very small and the nozzle was not capable of printing them with a better accuracy. More specifically, the chimney problem could be attributed to a lack of cooling between layers and thus, the best solution was to increase the fan speed for small layers. The only option offered by Simplify3D is to increase the fan speed for layers that take less than a certain amount of time to be completed.

Once the aspects to improve were detected and the potential solutions were found, new printings of the boat were carried out. The parameters of interest: extruder temperature, retraction distance, retraction speed and cooling settings, were modified until the printing was good enough. In this case, it was necessary to print just two additional boats apart from

the first one to find a set of parameters that provided reasonably good quality for PEKK. Figure 22 shows the final results, with the optimal printing parameters, listed in Table 3. As can be appreciated in Figure 23, thanks to the changes made, the stringing problem was reduced and both the hole at the back and the chimney were significantly improved.

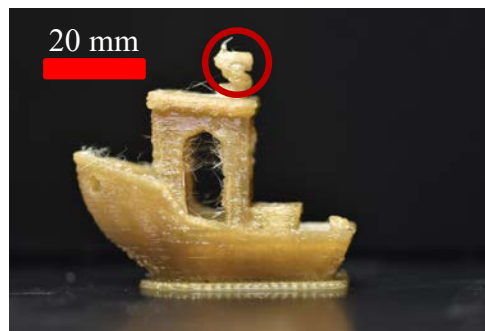


Figure 21. First 3DBenchy printed with PEKK, following the parameters listed in Table 16

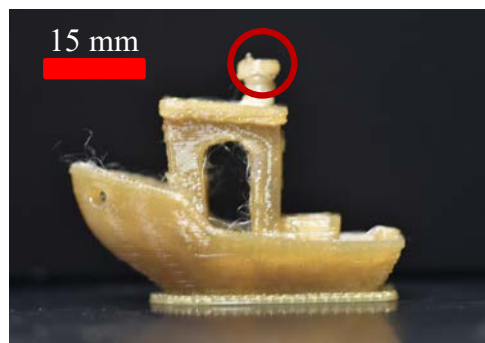


Figure 22. 3DBenchy printed with the PEKK, following the optimal printing parameters (Table 3)



Figure 23. Evolution of the 3DBenchy printed with PEKK

PRINTING PARAMETERS	FINAL VALUES
Nozzle diameter (mm)	0.60
Extruder	1.00
Retraction distance (mm)	0.80
Retraction speed (mm/s)	50
Nozzle Temperature (°C)	360
Bed Temperature (°C)	140
Heated chamber (°C)	120
Layer Height (mm)	0.25
Printing speed (mm/s)	20

Table 3. Optimal printing parameters for PEKK

The next step was to print all the parts in CAD file with the parameters found with 3DBenchy, just varying the extrusion multiplier. Despite having printed a PLA prototype to avoid wasting PEKK and its CF composite, the use of different printers and slicing software led to changes in the result of the first print of interest (the first CAD file print with PEKK) with respect to the prototype. Firstly, two areas with different texture and color could be distinguished in the coupons. This problem was due to the fact that the height of the coupons was greater compared to the height of the rest of the pieces in the file. As a result, the time to complete the first layers was much longer compared to the last layers, allowing them to cool down before the nozzle redeposited new material. From a certain height the nozzle only had to paint the coupons and thus, the deposited material barely had time to cool down before a new layer was added. Although this effect was also present in PLA coupons, it was hardly noticeable due to the low melting point of this material compared to that of high-performance thermoplastics such as PEKK. The only solution to obtain homogeneous coupons was to print them separately.

Also, there was a problem related to the infill of the gage section. Although the infill percentage was set to 100%, the gage section did not present a complete infill. This issue stemmed from the thickness of the coupons and the way there were sliced. The diameter of the deposited material is slightly larger than the nozzle diameter (0.6 mm) and the initial thickness of the gage section was 4.1 mm. Figure 24 shows an infill comparison between two coupons with different thicknesses. The left one has a thickness of 4.1 mm and, as can be appreciated in the last image, the inner part of the section was empty, because this area was not wide enough to add more material, given the nozzle diameter. The solution to this problem was to reduce the thickness of the coupons, always within the allowed range by the ASTM standard norm, until a complete infill was achieved. The final slicing of the coupons, with a thickness of 2.9 mm, is represented by the right coupon in Figure 24.

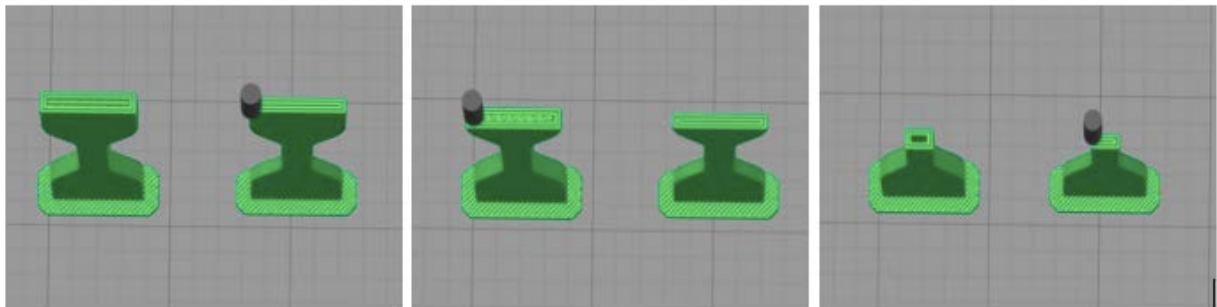


Figure 24. Infill comparison for different coupons thickness: in the three images the left coupon corresponds to a thickness of 4.1 mm and the right one corresponds to a thickness of 2.9 mm

Lastly, the change in thickness had a negative effect on the adherence of coupons to the print platform. The bonding surface between the coupons and the platform was too small compared to their height and, consequently, some of the coupons took off when printing the upper layers. This caused the printing to topple. Increasing the size of the individual rafts was not effective, the contact area was still too small, and the only solution was to create a single, big raft. In this way, it is possible to maximize the size of the first layer and therefore, avoid losing the print due to a lack of adherence to the build platform. In other words, the optimal solution was to create a better bonding surface. The final result is shown in Figure 25.

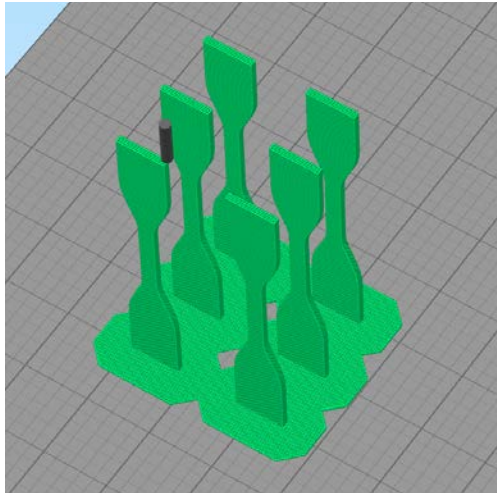


Figure 25. Final slicing of the tensile coupons with a single raft, common for all the coupons

4.3.3 Printing the model with CF-PEKK

Following the same procedure as with PEKK, the first step was to determine the optimal printing parameters. The only difference between PEKK and CF-PEKK is that the latter has carbon fibers that reinforce the thermoplastic. Therefore, it has a higher melting point and requires a higher extrusion temperature. According to the manufacturer, the nozzle temperature must be between 360 °C and 390 °C. The first 3DBenchy, shown in Figure 26, was printed at the highest extrusion temperature keeping the rest of the parameters invariable with respect to PEKK. This printing suggested some aspects to improve. The presence of carbon fibers makes the filament stiffer, which can be deduced from the absence of stringing and the differentiation between layers. The retraction parameters used for PEKK were too high, leading to a discontinuous flow with gaps (missing material) on the printed part, and the noticeable distinction between layers led to a rough surface finish. To find the optimal retraction parameters without losing much material and time, a new study was carried out. The idea was to print six parts that were the exact same model, but with different retraction distances and speeds. The chosen prototype was the base of a coupon up to a height of 10 mm. The results suggested 50 mm/s as the best retraction speed and 0.6 mm as the best retraction distance for CF-PEKK filaments. In addition, the layer height was reduced from 0.25 mm to 0.2 mm to reduce surface roughness. Then, various 3DBenchy models were

printed at lower extrusion temperatures until the complex geometric features were good enough. The final result was achieved with the printing settings listed in Table 4.



Figure 26. First 3DBenchy printed with CF-PEKK



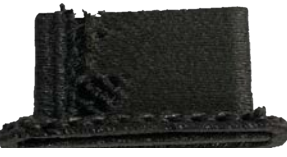



	Retraction speed (mm/s) / Retraction distance (mm)	
	30	50
0.60		
0.80		
1.00		

Table 4. Results of the retraction study carried out on CF-PEKK

PRINTING PARAMETERS	FINAL VALUES
Nozzle diameter (mm)	0.60
Extrusion multiplier	1.00
Retraction distance (mm)	0.40
Retraction speed (mm/s)	50
Nozzle Temperature (°C)	380
Bed Temperature (°C)	140
Heated chamber (°C)	120
Layer Height (mm)	0.20
Printing speed (mm/s)	20

Table 5. Optimal printing parameters for CF-PEKK

During the parametrization process, serious clogging problems arose. Every time the spool had to be removed from the printer to dry the filaments, the nozzle clogged. Clogging is an issue that has always been present in 3D printing. However, this case was different. While with other materials clogs could easily be removed by raising the nozzle temperature above the material's melting temperature and manually pushing the filament, for CF-PEKK this was not possible. Regardless of the nozzle temperature and the forced applied to the filament to expel it, it seemed to have stuck to the walls of the nozzle, damaging it. All the solutions aimed to unclog the nozzle were unsuccessful, which led to the question of whether it was worth continuing printing with this filament. In order to make a decision, it was necessary to balance the interest in this material and the cost of replacing the nozzle every time the filament had to be dried. On the one hand, given the number of printings to be made and considering that the aim of the study is to draw conclusions that can be applied further on to future printings, it was not profitable nor rational to buy so many new nozzles to finish the research. On the other hand, the interest in the material motivated the search for alternative solutions such as the use of filaments with the same characteristics, but provided by other suppliers. Following to the recommendations of AON3D, CF-PEKK filaments

supplied by Kimya were used. The specific properties of Kimya filaments can be found in Table 17 (see ANNEX II). Fortunately, with these filaments the clogging problems were neither as frequent nor as severe as before and therefore, the study on CF-PEKK could be finished with Kimya filaments. It should be noted that despite the change, the filaments also had to be dried for at least 4 hours at 120°C to eliminate the moisture.

Considering the change in CF-PEKK filaments supplier, a new 3DBenchy was printed to check that the optimal parameters found were still optimal. As can be deduced from Figure 27 these parameters (listed in Table 5) gave an excellent result also for the new filaments and, as a consequence, they were followed to print the rest of the parts in the CAD file. All the improvements that had to be made with PEKK due to the slicing software change with respect to the prototype, were also applied to CF-PEKK. The coupons were printed separately from the rest of the parts of the CAD file and the thickness of these specimens was reduced from 4.1 mm to 2.9 mm.



Figure 27. 3DBenchy printed with Kimya filaments following the optimal parameters, listed in Table 5

4.4 ANNEALING POST-TREATMENT WITH SALT

This section focuses on the annealing post-treatment applied to all printed parts with the aim of achieving the best results. Annealing allows to homogenize and increase the crystallinity of certain additive manufactured parts and thus, improve their mechanical, thermal and chemical resistance properties [46]. It is worth emphasizing that this treatment is not effective for all materials. For instance, annealing is not able to decrease the porosity

nor to improve interlayer adhesion in PEEK printed parts [47]. This is not the case of the materials of interest in this study. Thanks to annealing, it is possible to increase the degree of crystallinity of PEKK and CF-PEKK by 26 pp and 16 pp, respectively [25]. Theoretically, when PEKK printed parts are subjected to a post-crystallization treatment, the maximum use temperature increases from 150°C to 260°C.

Nevertheless, there are disadvantages associated with annealing. During this thermal treatment, parts are placed on the oven at a temperature of 160°C for 30 minutes and, after this time, the temperature must be raised to 200°C until the parts turn into a uniform tan color (the timing of the second step depends on the capability of the oven and on both the size and surface of the part) [44]. These changes in temperatures favor warping. Going further, raising the temperature above the thermoplastic crystallization temperature (156°C for PEKK) can have a negative impact on complex features of printed parts, such as bridges and hangovers. If any key feature of the piece melts and loses its structure, it is very likely that the part will collapse and lose its functionality. The potential solution found to avoid this issue was submerging the parts in very fine salt powder during the annealing process. In this way, the pieces would be compressed and thus, it would not be possible for them to undergo structural changes. The reason why salt was used to pack all the parts is because it is inert, non-toxic, biodegradable and has a high melting point. Moreover, salt had to be very fine because the surface finish and dimension accuracy are directly dependent on the grain size. The finer, the better [48]. This post-processing treatment is very innovative. To the best author's knowledge, the use of this technique in PEKK and CF-PEKK has not been reported to date.

Apart from the salt and the oven, it was necessary to use a stainless container, two aluminum plates and a thermocouple. As shown in Figure 28, the parts were fit in the container, the salt was added, and the aluminum plates were placed on top to make weight and ensure a good compression. Salt is not a good conductor of heat, so it was difficult to achieve a uniform temperature distribution in the container [49]. The thermocouple was used to control the temperatures at the core of the recipient. This device, was used only once to adjust the process times according to the oven capabilities, the size of the stainless-steel container and the salt volume inside. Figure 29 shows the schematic of the specific annealing process, applied to both PEKK and CF-PEKK. The effectiveness of this treatment was

assessed based on the degree of crystallinity, determined by the color, and the dimensional and structural changes.

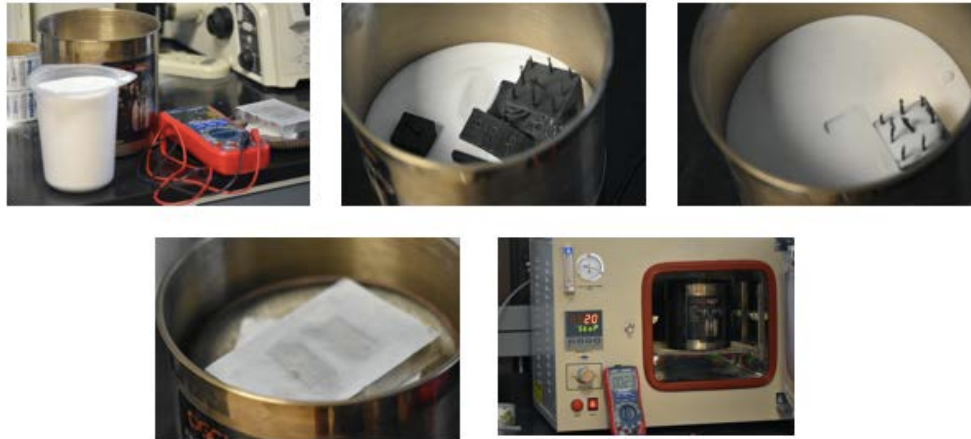


Figure 28. Step-by-step configuration of the annealing process

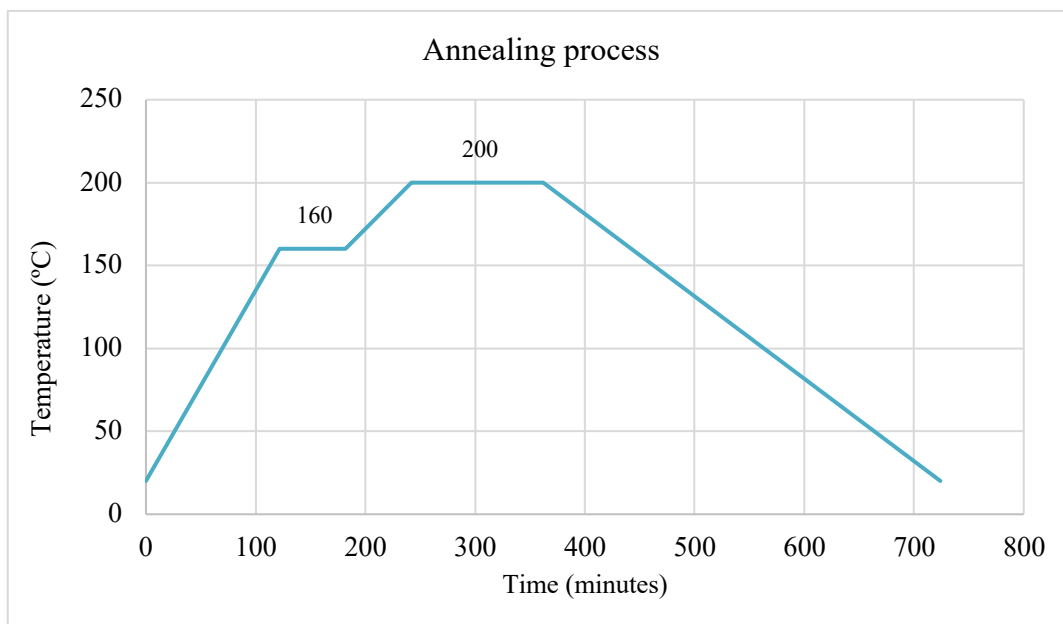


Figure 29. Schematic of the annealing process

The increase in the crystallization degree leads to a change in the material color. On the one hand, Figure 30 (a) shows the change in color experienced by PEKK during the annealing process. The right part, with a translucent gold color, corresponds to a PEKK coupon before annealing and the left part, with a light beige opaque color corresponds to an

annealed PEKK coupon. This change in color indicated that the applied post-treatment had successfully favored the crystallization of the thermoplastic. On the other hand, Figure 30 (b) shows the change in color experienced by CF-PEKK. The presence of the CF gives PEKK a grayish color that prevents visualizing the color of the matrix and thus, its degree of crystallization. Nevertheless, the annealed pieces showed a matte appearance, which allowed to verify the effectiveness of the treatment.

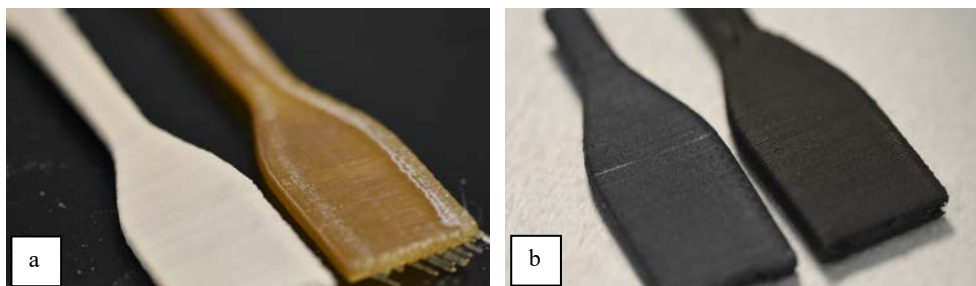


Figure 30. (a) PEKK color before (right) and after (left) annealing and (b) CF-PEKK color before(right) and after (left) annealing

As mentioned above, dimensions and features of interest of printed parts could be affected by annealing. Hence, the use of salt. In order to account for dimensional changes, measurements of both metrology parts were carried out before and after the post-treatment. As reported in Chapter 6, no changes in dimensions were detected. Furthermore, the key part that would allow to determine whether the treatment with salt was effective in preventing the collapse of the structure was the standard piece developed by Autodesk and Kickstarter. Fortunately, it kept its shape when raising the temperature above the crystallization temperature, which means that using salt for compacting complex parts during annealing is an effective approach.

Chapter 5. EFFECTS OF OVER-EXTRUSION ON POROSITY AND MECHANICAL PROPERTIES

5.1 OBJECTIVE

The objective of this chapter is to discuss the effects of over-extrusion on the internal structure as well as on the mechanical properties of PEKK and CF-PEKK parts manufactured via FFF based on the results obtained from the tensile tests and the void content analysis. It should be recalled that all the parts in the CAD file were printed at two EM, 1 and 1.05.

5.2 POROSITY ANALYSIS AND RESULTS

This section presents the void content analysis performed on the cross-section samples, shown in Figure 31. These parts were subjected to micro computed-tomography (micro-CT), a 3D imaging technique that uses X-rays to recreate cross-sections of real objects. The main advantage of this non-destructive technology is the high resolution that can be achieved. In particular, a resolution of 7 microns was used for this study. To put this number in context, medical CT scanners used for recreating physical body parts have 10 times greater resolutions (~70 microns) [50]. The optimal resolution is a function of the object size. According to standard guidelines, it should be 1,000 times smaller than the sample width.

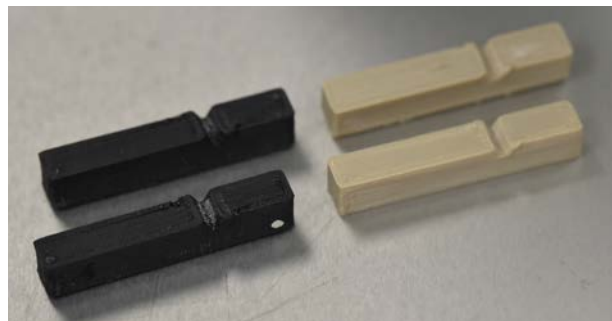


Figure 31. Cross-section samples of PEKK (right) and CF-PEKK (left) printed at the two EMs

Once the cross-section samples were loaded and the settings adjusted, the scanning was performed automatically by the device. Although the parts were regularly supervised, no user interaction was needed. As a result of the required magnification (image size relative to the physical part), more than 1,000 pictures per sample were collected. A commercial software called dragonfly was used for the 3D reconstruction of these images.

The procedure followed to visualize the voids in the samples was as follows. Firstly, all the images of each sample were loaded to the program. Dragonfly allows users to visualize the data as a single 2D slice or as a multi-view layout with three orthogonal views and one 3D view. Secondly, an image segmentation was performed in order to distinguish the material from the voids. Thanks to this partitioning, the software is able to determine the volume of the different types of segments in the reconstruction. Thus, the void fraction was determined as the volume of the segment corresponding to the pores. Finally, the brightness and intensities were adjusted until a good contrast was achieved, and photos from different perspectives were taken.

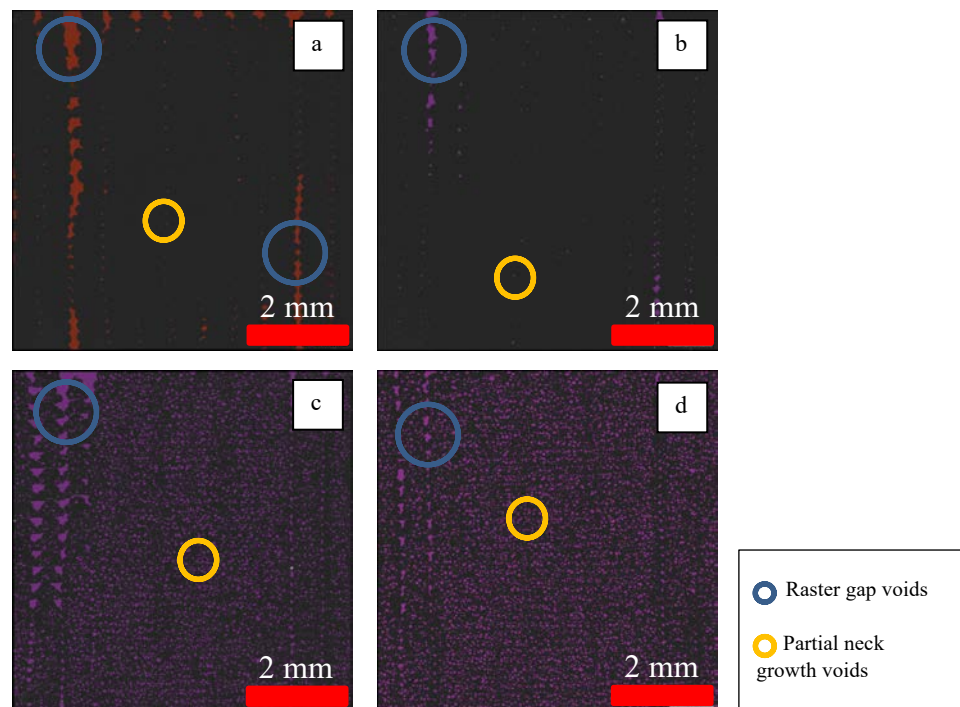


Figure 32. 2D views of the porosity of the whole section of: PEKK parts printed at an EM of (a) 1 and (b) 1.05; and CF-PEKK parts printed at an EM of (c) 1 and (d) 1.05

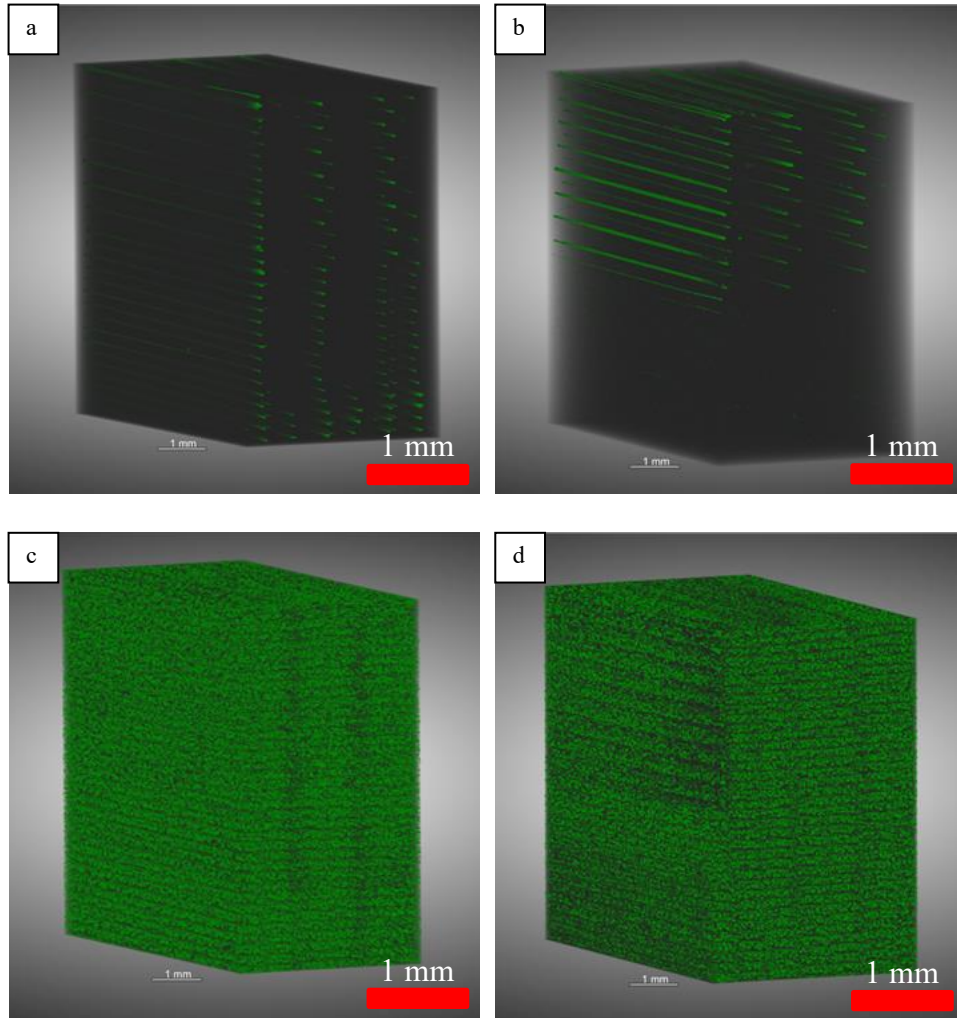


Figure 33. 3D views of the porosity of the whole section of: PEKK parts printed at an EM of (a) 1 and (b) 1.05; and CF-PEKK parts printed at an EM of (c) 1 and (d) 1.05

Two types of analysis were performed. Initially, the 2D slices and 3D views were analyzed as they came from the scanning, that is, the entire cross-section was examined. The results obtained for PEKK and CF-PEKK at the two EMs are shown in Figure 32 and Figure 33. The black part represents the material and the colored part the pores. For the two materials, the size and shape of the voids in the sides contrast with those in the interior. This is explained because they are two different types of voids. While the inner voids are partial neck growth voids, the outer pores are raster gap voids. Raster gap voids are separations between adjoining rasters and thus, they arise from the slicing of the CAD model [7]. To verify that indeed the large side pores were formed due to raster gaps, the sliced section of

the printed part was inspected with Simplify 3D. As shown in Figure 34, the infill pattern was not the optimal one and consequently, raster voids are present in the sides. On the contrary, partial neck growth voids emerge as a consequence of the imperfect coalescence between adjacent rasters. FFF printing conditions favor the solidification of layers before new material is deposited, which leads to the appearance of this pores. Partial neck growth voids are the major contributors to the porosity of 3D printed parts and they are very difficult to control. These pores and not raster voids, which depend on the specific CAD model and the way it is sliced, are the focus of interest of this study.

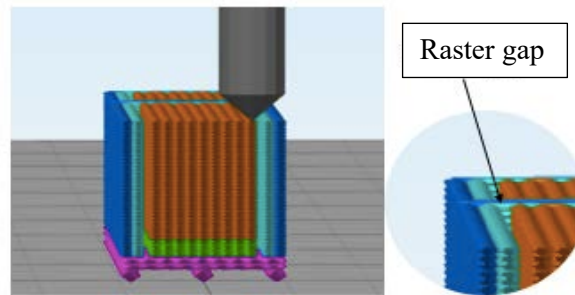


Figure 34. Raster gaps in the cross-sample

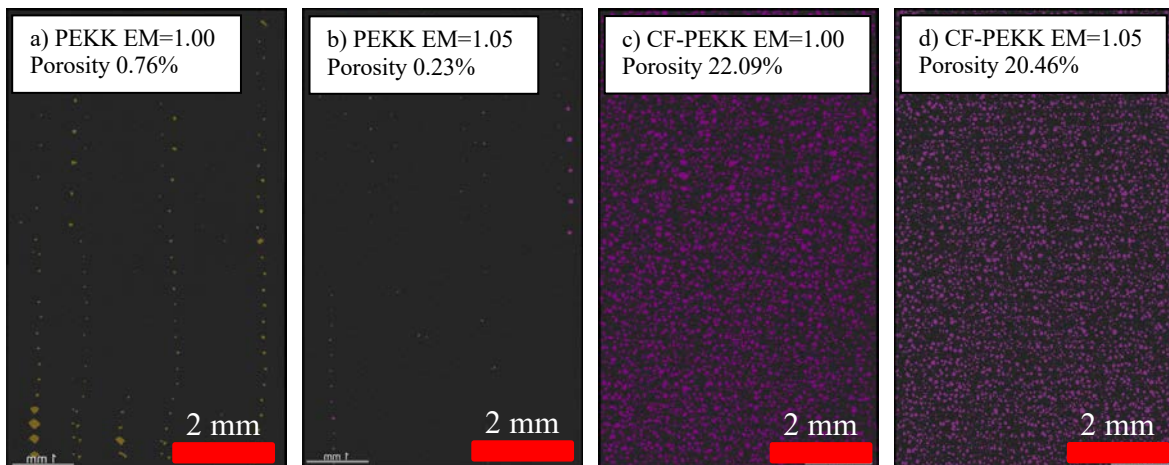


Figure 35. Internal porosity of PEKK printed at (a) $EM=1$ and (b) $EM=1.05$; and CF-PEKK at (c) $EM=1$ and (d) $EM=1.05$

In order to determine whether it is possible to reduce partial neck growth pores with an increase in the EM, it was necessary to crop the 2D slices and perform another analysis

to determine the internal porosity. Figure 35 shows the segmentation of the interior of the samples, without the raster voids. PEKK results indicate that 5% increase in the EM multiplier results in 0.53 pp decrease in porosity. Considering that the internal porosity of PEKK for a standard EM (1) is relatively low (0.76% as compared to 22.09% internal porosity for CF-PEKK), this approach is very effective to practically eliminate the internal void content. However, the improvement of the interlayer strength (if any) would be a function of the porosity variation and perhaps 0.53 pp is not enough to perceive changes. A linking of this analysis and the mechanical performance study is included in the last section of this chapter.

The porosity of CF-PEKK is much higher compared to that of PEKK. A fact that draws a lot of attention is that the degree of porosity of the whole section, including the raster voids, is lower than the degree of internal porosity. Given this result, CF-PEKK raw filaments were subjected to the same micro-CT analysis to verify if there were pores inside them. Images obtained from this analysis are shown in Figure 36. Indeed, it was found that CF-PEKK raw filaments contain a high percentage of voids, which explains the great porosity within the rasters. These voids are known as intra-bead voids [7] and they are not present in PEKK samples because they are unique to composite materials. Unlike inter-bead voids (like partial neck growth voids), intra-bead voids are not consistent in shape, orientation and distribution. The fact that they are contained within the filaments, makes it difficult to control them through printing parameters such as the EM.

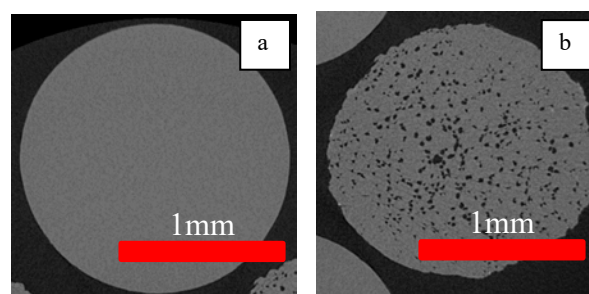


Figure 36. Porosity in (a) PEKK and (b) CF-PEKK raw filaments

Although it is not easy to visualize, a 5% increase in the EM resulted in a reduction of CF-PEKK internal porosity of 1.63 pp, from 22.09% to 20.46%. The degree of porosity

of the sample printed at the higher EM is still very high. However, as explained above, most of the voids are intra-bead voids and it is questionable whether over-extrusion can help to decrease this type of pores. Perhaps in this case, it would be more effective to look for alternative approaches to reduce the porosity of the bulk filaments, rather than further increasing the EM.

In conclusion, over-extrusion is an effective approach to reduce the void content in FFF printed parts. An increase in the EM decreases both the percentage and the size of internal voids. This reduction depends not only in the degree of over-extrusion, but also on the material. For the same increase in the EM, PEKK parts experienced a decrease in void content of 0.53 pp, whereas CF-PEKK samples experienced a reduction more than three times greater (1.63 pp). Finally, it is important to remark the high porosity of the composite material compared to the polymer alone, due to the presence of an additional type of voids contained in the raw filaments, intra-bead voids.

5.3 MECHANICAL PERFORMANCE ANALYSIS AND RESULTS

This section presents the tensile tests conducted in order to determine the ultimate tensile strength, Young's Modulus and strain to failure of the coupons printed in the z-direction. To carry out these tests, an MTS Criterion™ Model 43 universal test system with a 1 kN load cell was used. The testing speed was set to 0.5 mm/min, and the strain was measured using an MTS extensometer with a gauge length of 25.4 mm (1 inch). As shown in Figure 37, this extensometer has two metal pins that hook onto the tested specimen, preventing any slippage. Before conducting each test, the gage section of the coupon (width and thickness) was measured with a digital caliper, called Mitutoyo absolute digimatic, to achieve the highest accuracy in the results. Moreover, to ensure that the conclusions were reliable and following ASTM norm, at least five coupons of each material with a specific EM were tested. Before entering into general conclusions, the individual results of each material will be presented.



Figure 37. CF-PEKK coupon, held by the jaws of the tensile machine, with the extensometer placed in the gauge section

The first coupons to be tested were those made of PEKK. Figure 38 shows the appearance of these coupons once annealed. As explained in section 3.2, it was necessary to create a big skirt to ensure the adherence of the coupons to the printing bed. When ripping them from the raft, some extra material remained. In order to avoid any bending moment that could invalidate the tensile tests, this extra material had to be removed. For this purpose, the coupon's bases were sanded prior to the tests.



Figure 38. PEKK tensile coupons once annealed

The results obtained for PEKK are shown in Figure 39, Figure 40, and Figure 41. While Figure 39 and Figure 40 present the stress-strain curves of the coupons, Figure 41 makes a comparison between the mechanical properties derived from these curves at the two EMs. Firstly, it should be noted that only 5 specimens of each type could be tested. One of the coupons printed at an EM of 1 had a big crack (printing defect) in the gage section, which led to the invalidation of the test. In addition, the missing specimen printed at the higher EM,

broke when adjusting the jaws of the tensile machine. All the tested samples broken within the gage section.

For the standard extrusion multiplier (1.00), the following mechanical properties were obtained: 27.22 MPa for the ultimate tensile strength, 3.89 GPa for the Young's Modulus and 0.70% for the strain to failure (see Table 18 in ANNEX II for the mechanical properties of each test specimen). As shown in Figure 39, the stress-strain curves of all the tested specimens were similar in terms of stiffness, ductility and strength, except for the first one. This coupon had a little crack in the gage section, which probably caused the premature failure. Consequently, all the aforementioned mechanical properties were calculated without taking into account the results of this outlier. Secondly, the mechanical properties computed for PEKK specimens printed with an EM of 1.05 were: 28.03 MPa for the ultimate tensile strength, 3.82 GPa for the Young's Modulus and 0.73% for the strain to failure (see Table 18 in ANNEX II for the mechanical properties of each test specimen). As can be deduced from Figure 41, increasing the EM by 5% did not result in a significant improvement of the mechanical properties. In all cases the mean properties for the two EMs are very similar and the confidence intervals overlap, indicating that the change is not statistically significant.

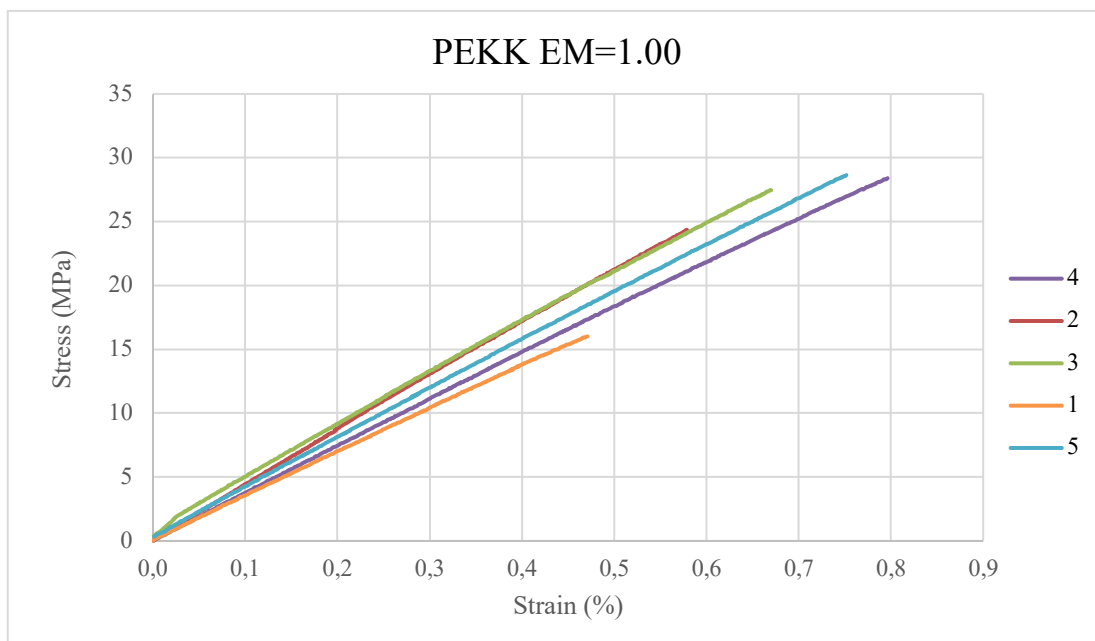


Figure 39. Stress-strain curve of PEKK tested specimens printed at an EM of 1.00

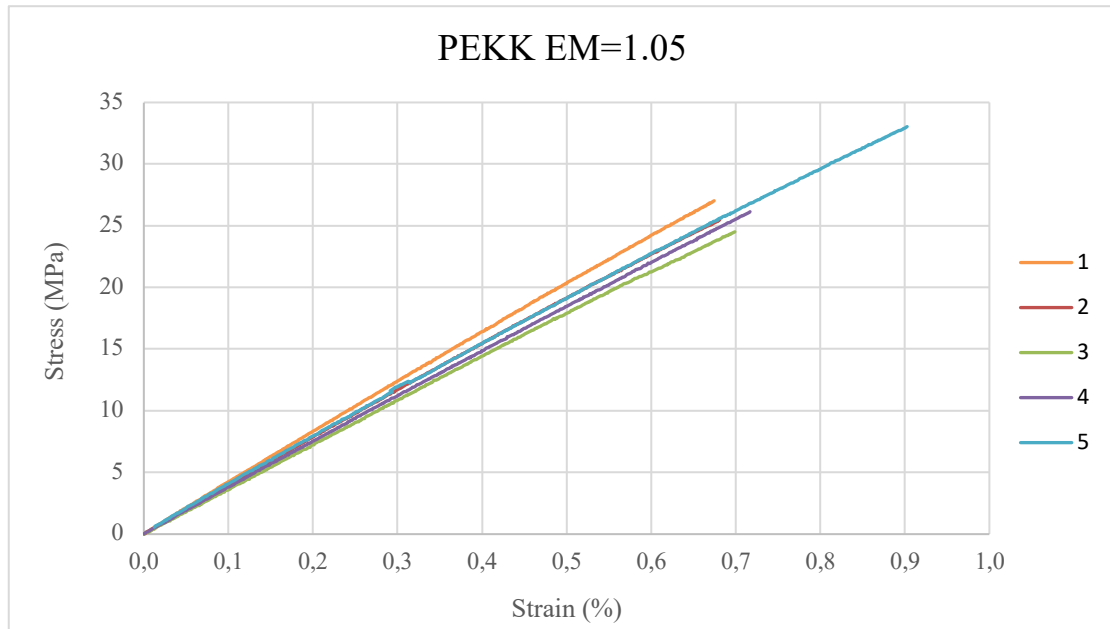


Figure 40. Stress-strain curve of PEKK tested specimens printed at an EM of 1.05

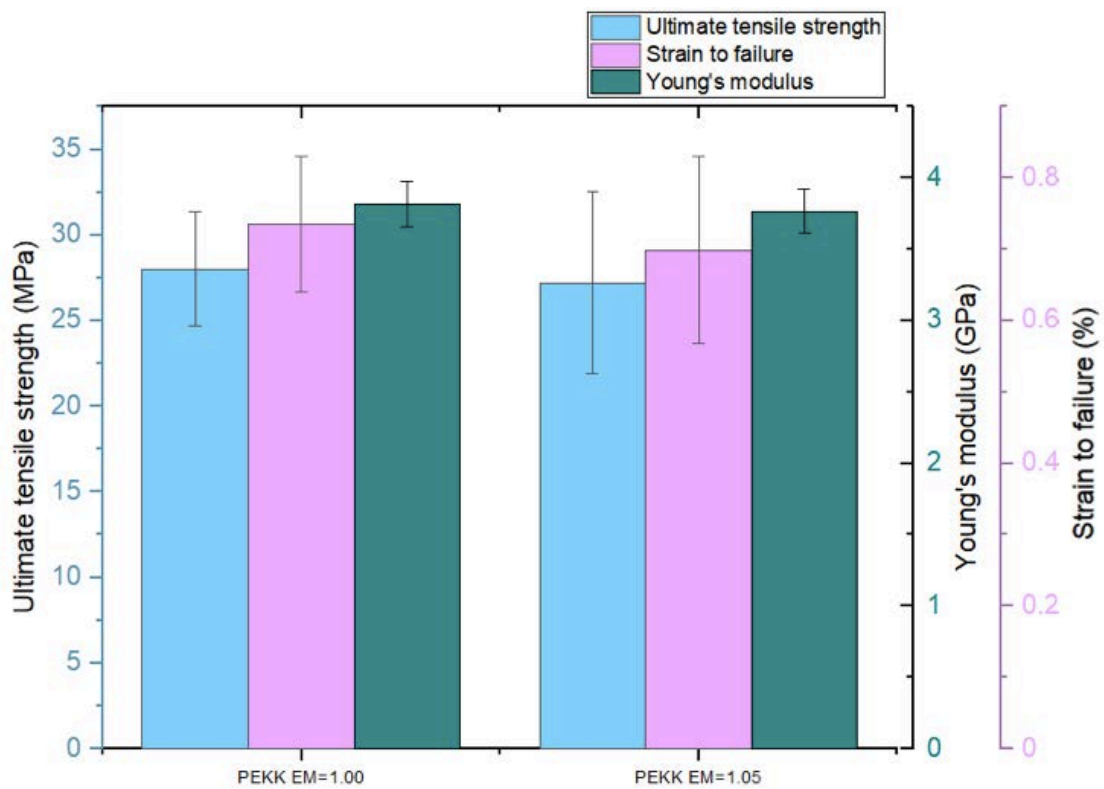


Figure 41. Comparison of the mechanical properties of PEKK printed at an EM of 1.00 and 1.05

The tests were then repeated with CF-PEKK coupons. As in the case of PEKK, these parts were sanded prior to testing in order to remove residual stresses and achieve completely flat samples. Figure 42 represents a CF-PEKK coupon as it came out from the annealing process and once the salt was removed and the surface was sanded.

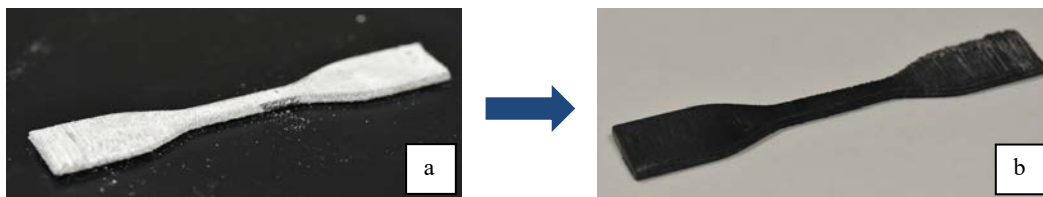


Figure 42. (a) CF-PEKK coupon as came from the annealing treatment (b) same coupons once the salt was removed and the surface was sanded down

The results from the tests are shown in Figure 43, Figure 44, and Figure 45. In this case, the six specimens were tested for the lower extrusion multiplier, but for an EM of 1.05, one of them broke during clamping before any force was applied. The mechanical properties of CF-PEKK parts printed with the standard EM (derived from the stress-strain curves shown in Figure 43) are as follows: 18.68 MPa for the tensile strength, 2.19 MPa for the Young's Modulus, and 0.95% for the strain to failure (see Table 19 in ANNEX II for the mechanical properties of each test specimen). In addition, the tensile strength, Young's Modulus and strain to failure of the samples printed at an EM of 1.05 were reported to be 24.77 MPa, 2.12 MPa and 1.26%, respectively (see Table 19 in ANNEX I for the mechanical properties of each test specimen). As can be deduced from these results, a 5% increase in the EM results in a 32.6% improvement of the tensile strength. By contrast, the Young's modulus and the strain to failure did not change significantly as will be explained below. This improvement of CF-PEKK mechanical performance contrast with the results obtained for PEKK. However, this outcome is consistent with the porosity reductions achieved for each material. The following section of this chapter (5.4), establishes a relationship between the tensile test results and the void content analysis.

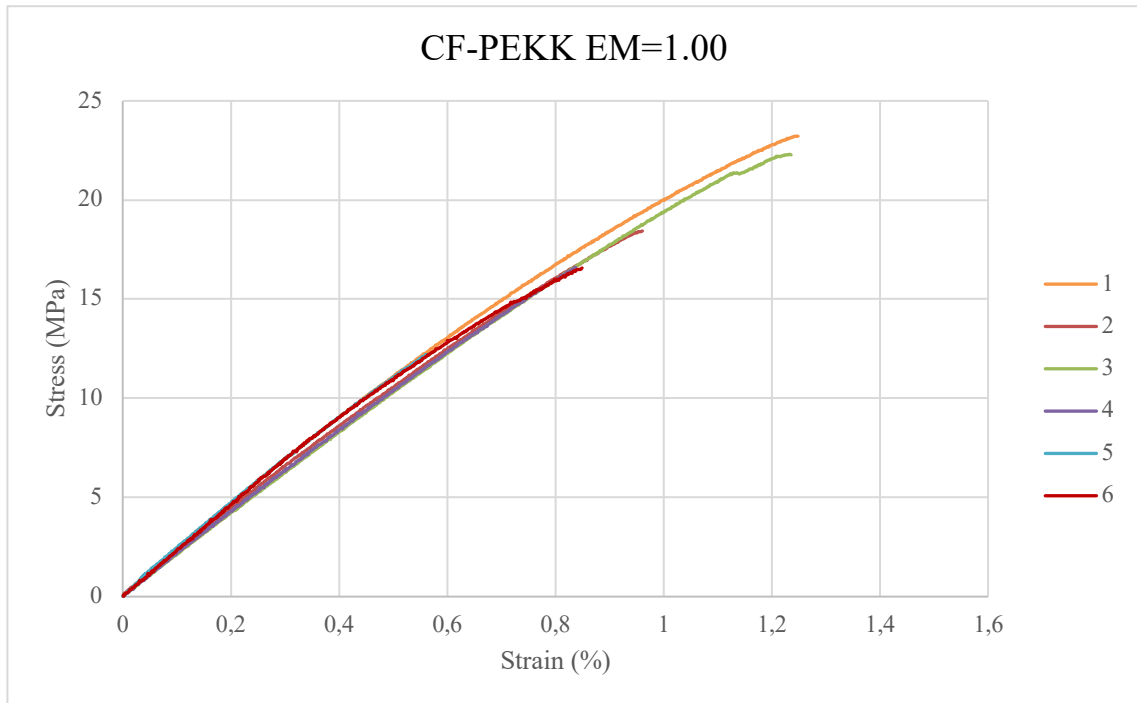


Figure 43. Stress-strain curve of CF-PEKK tested specimens printed at an EM of 1.00

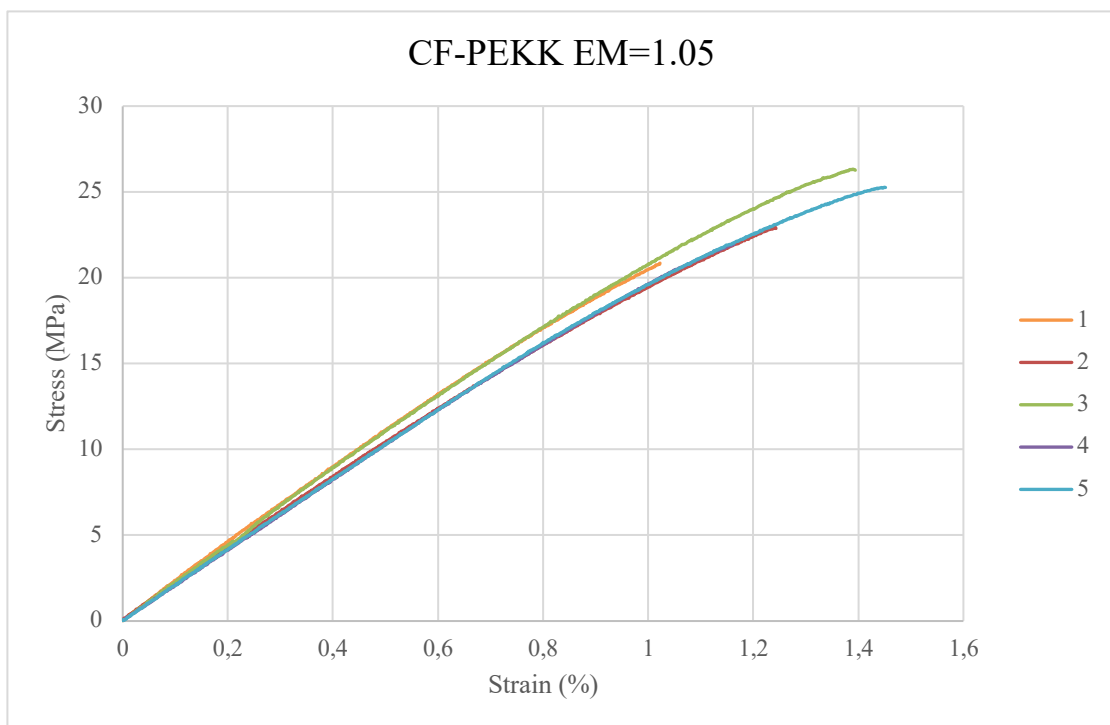


Figure 44 Stress-strain curve of CF-PEKK tested specimens printed at an EM of 1.05

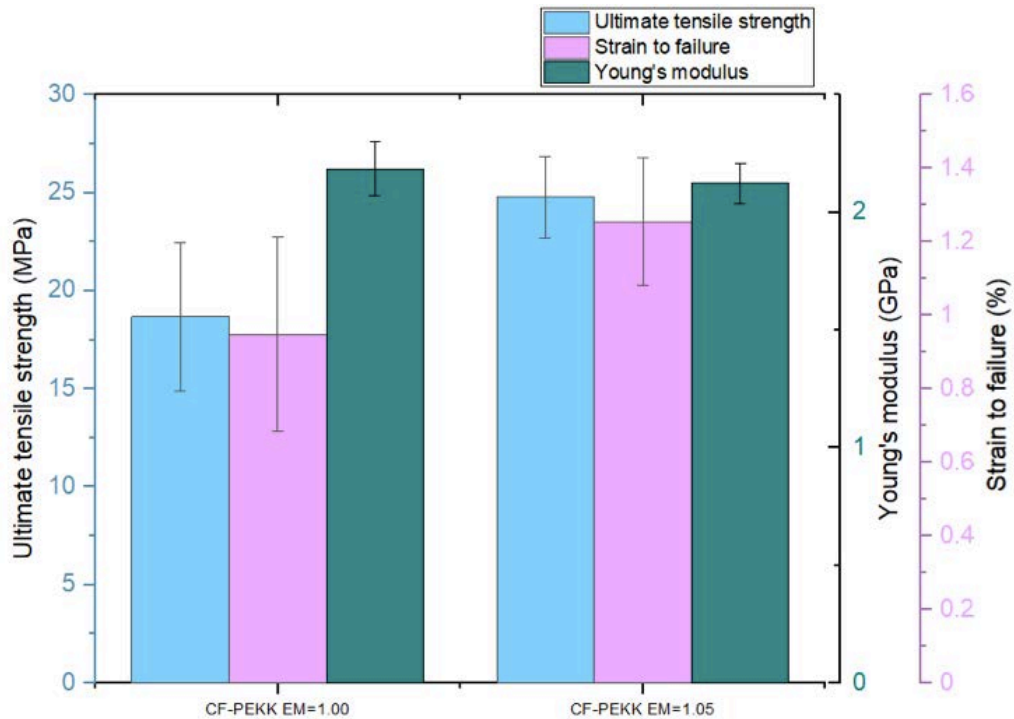


Figure 45. Comparison of the mechanical properties of CF-PEKK printed at an EM of 1.00 and 1.05

Before jumping to conclusions, it should be noted that the study carried out by T. Yap et al. [25] using the same printer and the same filaments, reported better mechanical properties for both materials. This discrepancy is especially noticeable in the strength of the tested specimens. The ultimate tensile strength of PEKK was determined to be around 72 MPa (2.64 times higher than that obtained in this study), and the ultimate strength of CF-PEKK was reported to be around 35 MPa (1.9 times greater than that identified in this paper). The cause of this wide variation may be due to the difference of the printing parameters used. However, there is another important factor to consider. In the cited study, the coupons were machined from blanks to the ASTM D638 Type IV size. In contrast, the tested specimens used for this research were directly printed using a CAD model with the shape and size required by the standard. By machining the coupons, it is possible to considerably reduce stress concentrations that arise from the layer-by-layer fashion process. As shown in Figure 46, stress concentrations come from the shape and remain even after the annealing process.

Likely, the microstructural pores and small cracks in between layers that emerged when printing were both responsible for premature failure.

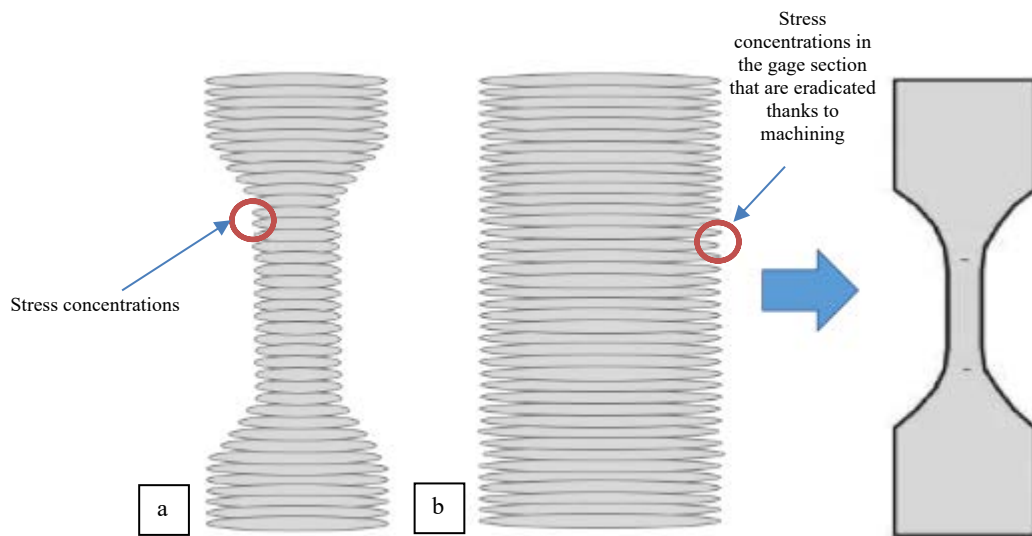


Figure 46. Stress concentrations in tensile coupons: (a) Coupon directly printed using a CAD model with the shape and size required by the standard (b) Coupon machined from a blank to the standard shape and size

Leaving aside the fact that the mechanical properties obtained in this study were probably affected by the way in which the coupons were printed, the results suggest that the improvement of mechanical performance via over-extrusion depends not only on the increase in the EM, but also on the material. Table 6 shows the anisotropy reduction achieved by both materials with a 5% increase in the EM. The anisotropy of each property for each material was calculated following Equation 1, and the theoretical properties were obtained from the technical data sheets provided by the manufacturers (3DXTech for PEKK [44] and Kimya for CF-PEKK [51]). As expected from the reported results, in the case of PEKK the anisotropy reduction is less than 5% for all the properties. This implies that over-extrusion is not able to improve the addressed limitation. Conversely, the slight increase in the EM results in a decrease of CF-PEKK strength and strain to failure anisotropy. Although the difference with respect to the theoretical properties is still very remarkable, it could be said that a 5% increase in the EM is an approximation to obtaining isotropic tensile properties.

$$\text{Anisotropy (\%)} = \left(1 - \frac{\text{experimental value}}{\text{expected value}}\right) \times 100$$

Equation 1. Formula to calculate anisotropy

		Expected properties	Properties EM=1.00	Properties EM=1.05	Anisotropy EM=1.00 (%)	Anisotropy EM=1.05 (%)	Anisotropy reduction (pp)
PEKK	S_{ut}	105.00 MPa	27.22 MPa	28.03 MPa	74.08	73.31	0.76
	E	3.20 GPa	3.77 GPa	3.82 GPa	17.81	19.38	-1.56
	ε	10.00%	0.70%	0.74%	99.30	99.26	0.04
CF-PEKK	S_{ut}	39.10 MPa	18.68 MPa	24.77 MPa	52.23	36.65	15.58
	E	2.90 GPa	2.19 GPa	2.12 GPa	24.48	26.90	-2.41
	ε	3.20 %	0.95%	1.26%	70.31	60.63	9.69

Table 6. Anisotropy of z-printed parts as a function of the EM for PEKK and CF-PEKK

Moreover, the study suggests that the only mechanical property affected by over-extrusion is the ultimate tensile strength. This conclusion cannot be proved with PEKK since the average properties obtained for both EMs are almost the same, with an anisotropy reduction of less than 5% in all the cases. By contrast, thanks to the 5% increase in the EM, CF-PEKK ultimate tensile strength and strain to failure improve by more than 30%. This is shown in Figure 47. In order to determine whether the difference between the mean properties calculated for the two EMs is statically significant, it is essential to compute the confidence intervals. Assuming the data collected (see Table 19 in ANNEX II) follows a Gaussian distribution, the confidence intervals were computed using Equation 2, at a confidence level of 95%. The results are reported in Table 7. In the case of the ultimate tensile strength, the confidence intervals do not overlap, which leads to the conclusion that the difference between the two strengths reported at the two EMs is statically significant at a 95% confidence level. For the strain to failure, the confidence intervals for both EMs overlap at a confidence level of 95%, which implies that the difference in the mean values

is not significant. In other words, while the ultimate tensile strength of CF-PEKK improves with an increase in the EM, the strain to failure does not experience a significant change. In addition, the Young's Modulus seems to be the property less affected by over-extrusion. This conclusion is in line with results obtained in similar studies [15, 39]. In one of the cited studies, it was necessary to increase the EM by 20% to perceive an increase of 11% in the Young' Modulus.

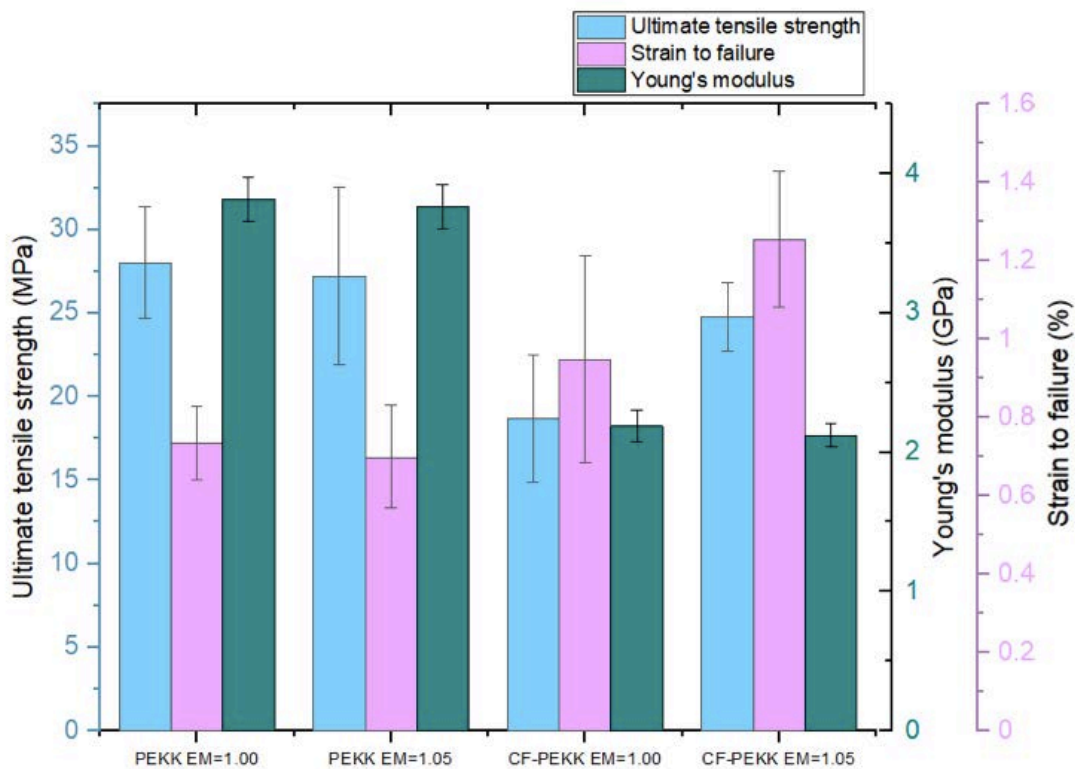


Figure 47. Comparison of the mechanical properties of PEKK and CF-PEKK printed at an EM of 1.00 and 1.05

$$CI = \bar{x} \pm z \times \frac{s}{\sqrt{n}}$$

Equation 2. Confidence interval formula assuming a Gaussian distribution, where \bar{x} is the mean of the sample, s the standard deviation, n the sample size; and z accounts for the confidence level

	Confidence interval for EM=1.00	Confidence interval for EM=1.05	Overlap
Ultimate tensile strength (MPa)	18.68 ± 3.03	24.77 ± 1.81	No
Strain to failure (%)	0.95 ± 0.21	1.26 ± 0.15	Yes

Table 7. Confidence intervals for the ultimate tensile strength and the strain to failure of CF-PEKK at the two EM

5.4 RELATIONSHIP BETWEEN POROSITY AND MECHANICAL PERFORMANCE

It is interesting to relate the two studies since internal voids act as stress concentrations, negatively affecting mechanical performance of FFF printed parts. The results obtained suggest that the improvement of the mechanical performance is a function of the porosity reduction. The greater the porosity reduction, the greater the improvement of the mechanical properties. As shown in Table 8, the decrease in PEKK void content is not enough to perceive an enhancement in the mechanical behavior. Furthermore, as discussed in the first section of the chapter, the maximum reduction in PEKK porosity is 0.76 pp, which corresponds with the internal porosity of the samples printed at the standard EM. This amount might not be enough to achieve a noticeable improvement of the mechanical out-of-plane performance. On the contrary, CF-PEKK samples experienced a 1.63 pp reduction in internal porosity and, as a consequence, the ultimate tensile strength improves by more than 30%. Therefore, there is a chance that a greater increase in the EM could result in a greater reduction of mechanical anisotropy. However, it should not be forgot that most of the internal pores of CF-PEKK come from the raw filaments and it is questionable whether intra-bead pores can be reduced via over-extrusion.

Variation of...	Porosity (pp)	Ultimate tensile strength (%)	Young's Modulus (%)	Strain to failure (%)
PEKK	↓0.53	↑2.96	↑1.37	↑5.08
CF-PEKK	↓1.63	↑32.58	↓2.86	↑32.29

Table 8. Relationship between the reduction of internal porosity and the % improvement of the mechanical properties

Chapter 6. EFFECTS OF OVER-EXTRUSION ON PRINTABILITY

6.1 OBJECTIVE

The objective of this chapter is to assess the effects of over-extrusion on the quality of additive manufactured parts made from PEKK and CF-PEKK. As mentioned in Chapter 2, there is no evidence that a greater than 1 extrusion multiplier results in a loss of printability of AM features of interest [15]. However, this conclusion was obtained for ABS, a low melting temperature polymer, and hence there is a need to determine whether it is applicable to PEKK and CF-PEKK. For this purpose, the calibration cube and the metrology part were printed at an EM of 1 and 1.05.

6.2 ASSESSMENT OF THE COMMON STANDARD PIECE DEVELOPED BY AUTODESK AND KICKSTARTER

6.2.1 PEKK

Table 9 shows the assessment score table for PEKK. As mentioned in section 4.4, to date, there are no studies on the annealing process using salt. Therefore, the printability assessment was carried out before and after the process to get a better understanding of its impact on the structure, dimensions and surface roughness of the parts. The scores remained unchanged and thus, it has been included only once. In addition, Figure 66 (see ANNEX I) and Figure 48 show the metrology part printed at the two EM before and after annealing, respectively.

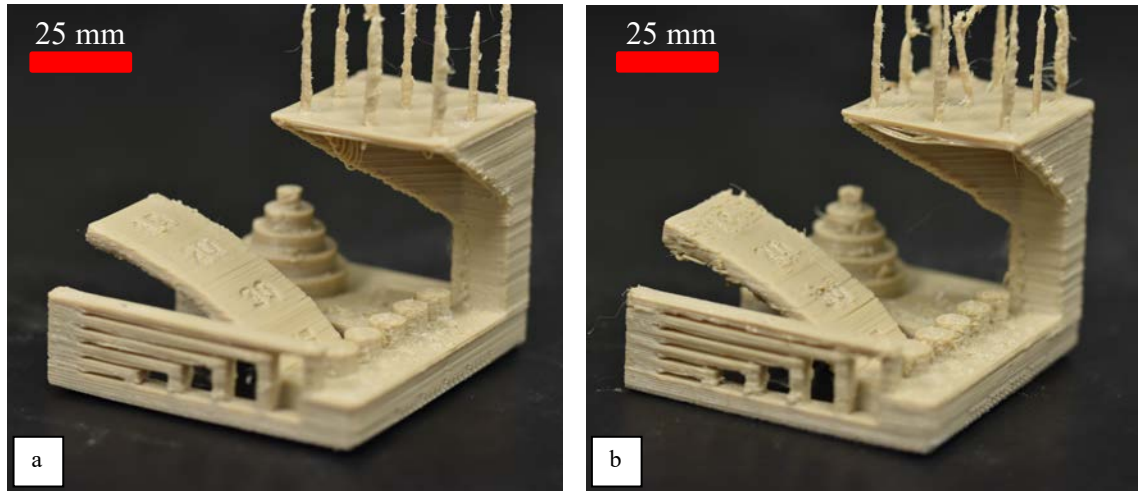


Figure 48. PEKK common standard piece developed by Autodesk and Kickstarter after annealing printed at an Extrusion multiplier of: (a) 1 and (b) 1.05

Extrusion multiplier	1.00	1.05	Score meaning
Dimension accuracy	3	2	The overall average error for EM=1 is 0.28 and 0.39 for EM=1.05
Fine flow control	0	2.5	For the lower EM, the spires were less than 30 mm long, whereas for EM=1.05 the spires were greater than 30 mm, but there was stringing between them
Fine negative features	0	0	No pins could be removed
Overhangs	3	2	For EM=1 the 45° and 30° overhangs were smooth, but the 15° and 20° differ from those ones. For EM=1.05, the printer complied the geometry, but there were some drops on the 15° overhang
Bridging	4	4	For both cases only one bridge was in contact with the surface beneath

Table 9. Assessment score for PEKK at the two different extrusion multipliers

Extrusion multiplier	1.00	Score meaning
Dimension accuracy	4	The overall average error is 0.118 mm
Fine flow control	2.5	The spires were greater than 30 mm long, but there was stringing between them
Fine negative features	5	All pins could be removed
Overhangs	4	Only the 15° overhang differ from the 45° overhang
Bridging	2	Three bridges were in contact with the surface beneath them

Table 10. Assessment score for PLA

From this analysis two main conclusions can be drawn. Firstly, for both EM the average score was below the mean (2.5), which means that overall PEKK does not offer a good printability. In order to get an idea of the scores obtained by other materials with a lower melting point, the same metrology part printed with PLA for the prototype was evaluated. The assessment score for this part is shown in Table 10. Moreover, other studies have computed that the mean score for ABS is around 3 out of 5 [15, 41]. The scores for both PLA and ABS contrast with those obtained for PEKK. Three major problems were detected for this material, fine flow control, negative features resolution and overhangs. The fact that the extrusion temperature was so high, almost twice that of the other cited polymers, is a problem when creating small diameters. Layers do not have enough time to cool down before new material is added and thus, they are unable to hold their shape. In this sense, it could be useful to reduce the temperature as much as possible (From the one used, 360°C, to the minimum one recommended by the filaments supplier, 345°) to check whether it is possible to improve these features. The problem with such temperature reduction, and the reason why the minimum temperature was not used for this research, is that a lower extrusion temperature results in a higher degree of porosity and poorer adhesion between layers.

Secondly, the comparison of the results obtained for the two EMs is in line with the conclusion obtained for ABS [15]. The assessment suggested that the higher EM improves fine flow control. Whereas with a standard EM the spires were less than 30 mm long, with an EM of 1.05 it was possible to achieve the minimum desired length. In contrast, the

dimension accuracy and the overhangs were slightly worse for a higher EM. The diameters were larger than expected due to small accumulations of material on the sides. Also, material drops could be detected for the 15° overhang (This is the most complex overhang as it is the furthest one from the base). Apart from these discrepancies, the rest of the features of interest were pretty similar. Overall, the mean score for an EM of 1 was 2 and 1.8 for an EM of 1.05.

6.2.2 CF-PEKK

It should be recalled that, as explained in section 4.3.3, serious clogging problems arose when printing with 3DXTech filaments and the study on CF-PEKK had to be repeated with other filaments provided by Kimya. The assessment scores for this material, as a function of the EM, are reported in Table 11. Figure 67 (see ANNEX II) and Figure 49 show the appearance of the parts printed at the different EM before and after the annealing process, respectively. As it was the case with PEKK, the scores obtained before and after the annealing treatment were the same, so only one table has been included.

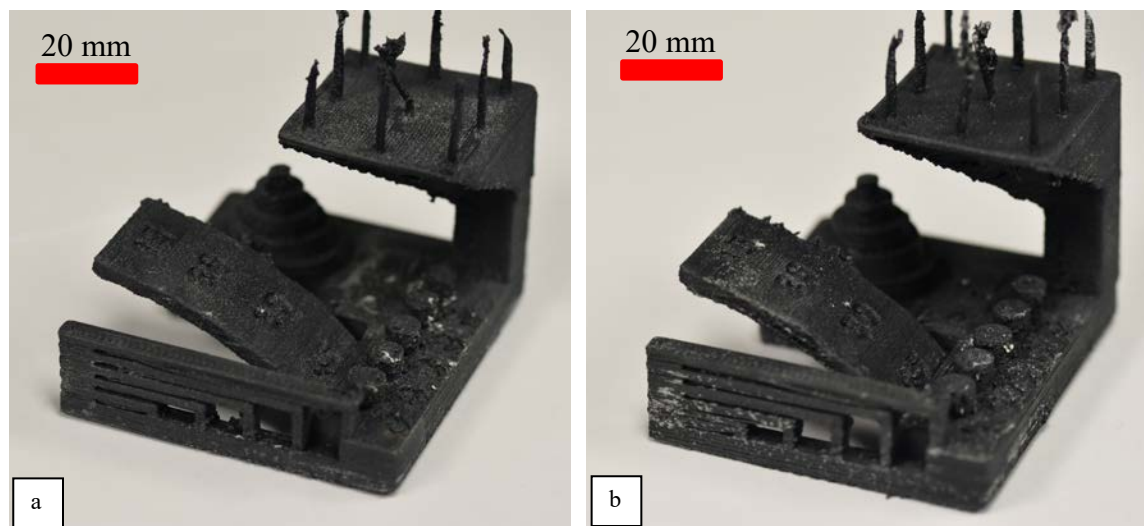


Figure 49. CF- PEKK common standard piece developed by Autodesk and Kickstarter after annealing printed at an Extrusion multiplier of: (a) 1 and (b) 1.05

Extrusion multiplier	1.00	1.05	Score meaning
Dimension accuracy	3	3	For both EM, the overall average error was between 0.21mm and 0.3 mm
Fine flow control	0	0	In both cases, the spires were less than 30 mm long
Fine negative features	0	0	No pins could be removed
Overhangs	3	3	The 15° and 20° overhangs were different from the 45° surface
Bridging	1	1	3 bridges were in contact with the surface beneath them

Table 11. Assessment score for CF-PEKK printed at different extrusion multipliers

This printability assessment has never been conducted on a high-performance composite. In fact, to date, there are no published papers aimed to characterize the quality of 3D prints made from CF-PEKK. This has its advantages and its inconveniences. Although this evaluation can be very useful for future improvements, it is very difficult to have a sense of whether the results are right or not.

The analysis suggests two main things: (1) CF-PEKK does not offer a good printability, and (2) the EM did not have any effect on the quality of the printed parts. Firstly, the results shown in Table 11 indicate that only the dimension accuracy and the overhangs scored above the mean. The error in the dimensions is due to small accumulations of material on the sides of the cylinders as shown in Figure 50 (a). This issue could be improved with an increase in the retraction parameters. However, as explained in section 4.3.3, using a higher retraction distance and a lower retraction speed results in a discontinuous flow with missing material, which is usually a more serious problem. This demonstrates that it is very difficult to find the optimal balanced retraction parameters for materials that require a high extrusion temperature. In addition, the printer was able to compile the overhangs geometry without material droops, but the farthest ones showed the staircase effect. This is illustrated in Figure 50 (b). The results for fine flow control, negative features resolution and bridging were very bad. Figure 50 (d) proves that the length of the spires did not reach 30 mm, Figure 50 (c) shows that none of the pins could be removed, and Figure 50 (e) evidences that almost all the bridges were in contact with the one beneath them. Most of these problems can be attributed to the high extrusion temperature required for this material.

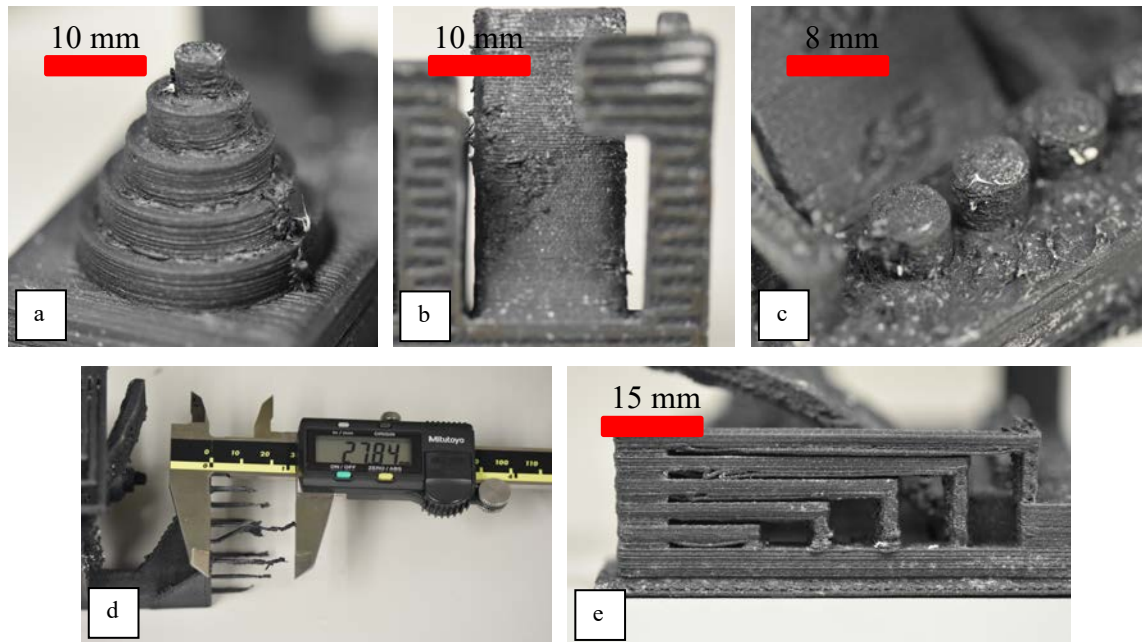


Figure 50. Geometry features of CF-PEKK metrology part: (a) material dimensions, (b) overhangs, (c) pins, (d) fine flow control; and (e) bridging

Secondly, the scores obtained for both EM are exactly the same, which suggests that a 5% increase in the quantity of filament per slice time that comes out from the nozzle does not have a negative impact on the print quality. This verifies the conclusion reached by several studies [25, 26] that as long as the increase in the EM is not very pronounced, the impact on surface roughness and printability is negligible.

6.3 ASSESSMENT OF THE CALIBRATION CUBE

The calibration cube was used to evaluate the impact of both the EM and the annealing process on the dimensions. For these purposes, measurements of the width, length and height of the cubes printed with the two EMs were taken before and after the post-treatment. Table 12 collects the measurements and errors.

		Expected dimension (mm)	Dimension before annealing (mm)	Error before annealing (%)	Dimension after annealing (mm)	Error after annealing (%)	Before vs. after annealing (mm)
PEKK EM=1.00	L	24	24.10	0.42	24.03	0.10	↓0.07
	W	24	24.13	0.54	24.12	0.48	↓0.01
	H	24	24.06	0.25	24.04	0.17	↓0.02
PEKK EM=1.05	L	24	24.22	0.92	24.27	1.10	↑0.05
	W	24	24.22	1.00	24.26	1.06	↑0.04
	H	24	24.10	0.42	24.06	0.25	↓0.04
CF-PEKK EM=1.00	L	24	24.22	0.92	24.37	1.52	↑0.15
	W	24	24.13	0.54	24.08	0.33	↓0.05
	H	24	24.06	0.25	24.11	0.46	↑0.05
CF-PEKK EM=1.05	L	24	24.55	2.30	24.60	2.48	↑0.05
	W	24	24.37	1.54	24.41	1.70	↑0.04
	H	24	24.98	4.08	25.36	5.67	↑0.38

Table 12. Calibration cube dimension accuracy assessment for both EMs before and after annealing

It is to be noted that only in one measurement, the height of CF-PEKK cube printed with an EM of 1.05, the dimensional error is greater than 5%. This case could be considered an outlier, since the part experienced some warping during the annealing process. Although the errors reported for a higher EM are slightly larger compared to the errors computed for a standard EM, they are still very small (generally less than 2.5%). Therefore, this indicates that a 5% increase in the filament feed rate is not enough to negatively affect the dimension accuracy of PEKK and CF-PEKK.

In addition, the results obtained indicate that there is hardly any different in dimensions between the measures taken before and after the post-processing treatment. Leaving aside the height of CF-PEKK cube, the biggest difference is 0.15 mm. Considering this value is more than 100 times smaller than the side of the cube, it could be concluded that the annealing process with salt was effective. Nevertheless, as mentioned above, the CF-PEKK cube printed at a higher EM experienced some warping in the upper face during the

annealing processes. This effect is shown in Figure 51. Neither the metrology parts analyzed in the previous section nor the rest of the cubes experienced any deformation. All of them were subjected to the same post-treatment, which suggests this is an exception. The main hypothesis is that either the cube was not well compressed in salt, or some salt clot exerted pressure on the top causing the deformation.



Figure 51. Warping experienced by the CF-PEKK calibration cube during annealing

Figure 52 and Figure 53 show PEKK and CF-PEKK calibration cubes, respectively. Although the dimensions were reasonably accurate; the quality of the surface was not good. As can be appreciated in all four cases, layer marks are distinctly visible on the surface, giving rise to the staircase effect, a very common quality issue in 3D printing. Poor surface quality is common to the cubes printed with the standard and higher EM, which is consistent with the conclusion drawn in the previous section that a 5% increase in the EM does not seem to negatively affect the quality of PEKK and CF-PEKK parts manufactured via FFF. Furthermore, the comparison of the cubes printed with both materials suggest that the layer height is a very important factor in the surface roughness, as advanced in the introduction of the report. For CF-PEKK, the layer height was reduced from 0.25 mm to 0.20 mm and the surface finish is clearly better than that of PEKK.

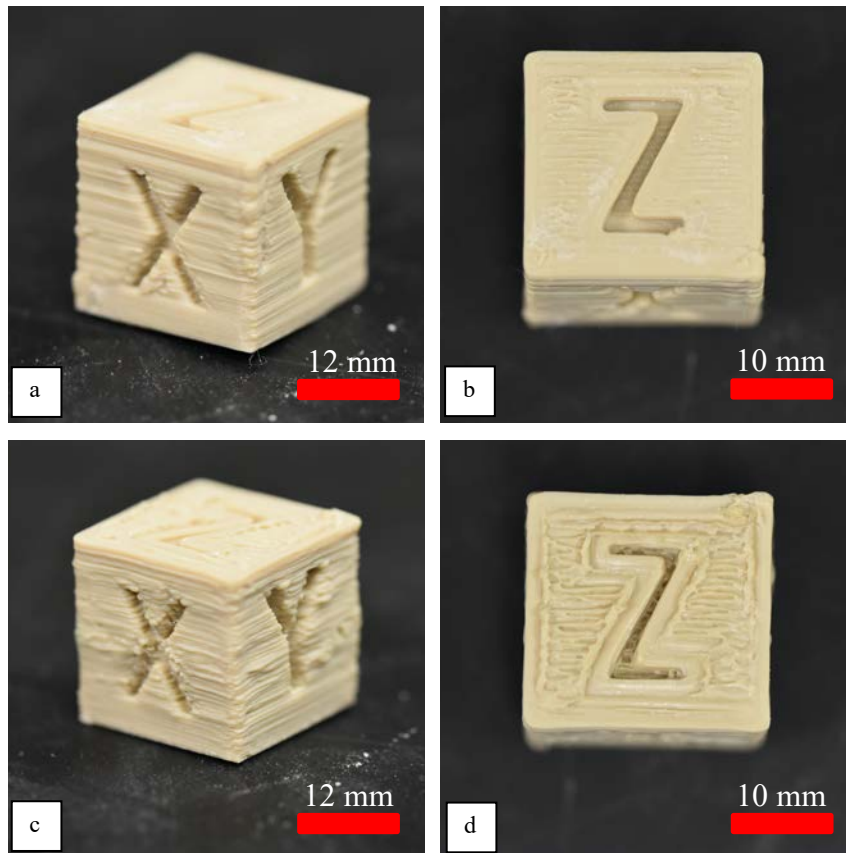


Figure 52. PEKK calibration cube printed at $EM=1.00$ (a) and (b); and at $EM=1.05$ (c) and (d)

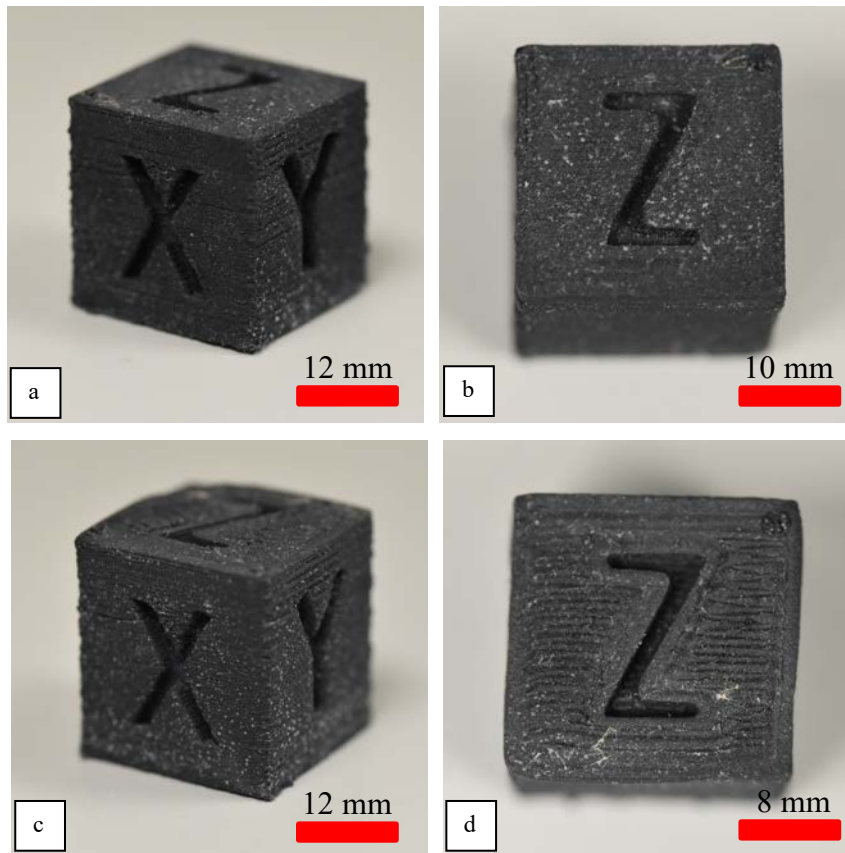


Figure 53. CF-PEKK calibration cube printed at EM=1.00 (a) and (b); and at EM=1.05 (c) and (d)

Chapter 7. FUTURE ORIENTATION OF FFF

This chapter provides an insight of future directions for FFF technology considering its benefits, limitations and expected growth. AM technologies are expanding very fast as they offer greater flexibility compared to other traditional manufacturing processes [52]. Among them, FFF is the most common technique. It stands out for its cost effectiveness in terms of materials and resources required, versatility, wide range of compatible materials; and fast processing. As shown in Figure 54, this technology is mainly present in the aerospace [53], automotive [54] and biomedical [55] industries. FFF enables users to choose the desired infill and thus, a reasonable number of aerospace and automotive parts designed by this technology are lighter compared to traditional designs. This advantage is directly related to sustainability. Growing environmental awareness has led to the goal of reducing greenhouse gas emissions, which can be achieved by manufacturing light-weight components that consume less fuel by using this technology. Moreover, FFF technology plays an important role in four-dimensional printing (4DP), a specific 3D printing technique increasingly common in the biomedical sector, where the fourth dimension refers to the smart behavior of the material over time. 4D printed objects can change their properties or structure under certain external stimuli such as temperature, water, light, heat and other environmental exposures [56]. 4DP is highly dependent on the material and considering that FFF has abundant feedstock compatible, more than 50% of 4D prints have been made using this technology.

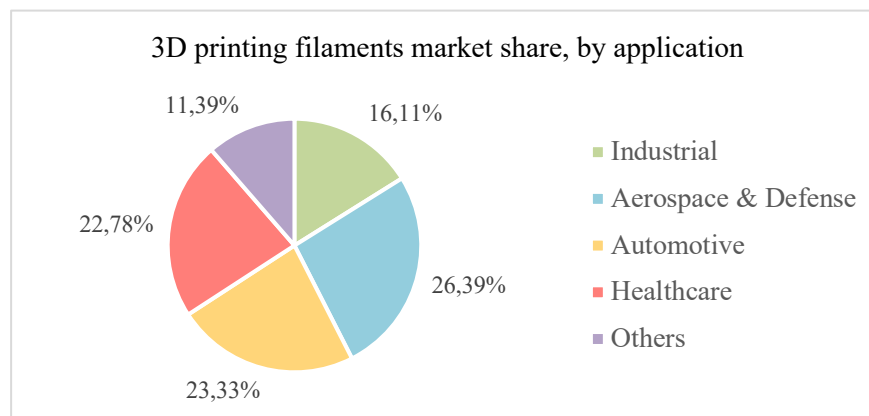


Figure 54. U.S. 3D printing filaments market share, by application, 2019 (%) [57]

Despite the advantages offered by FFF, there are some drawbacks that hinder the reliance on this technology for certain industrial applications beyond prototyping. As explained in detailed in Chapter 2, the most important shortcomings of FFF printed parts are poor interlayer bonding and high porosity leading to stress concentrations. These intrinsic deficiencies are the main causes of mechanical anisotropy and parts with worse than expected mechanical properties off the longitudinal direction. In addition, printability, which is evaluated in terms of surface roughness as well as dimensional accuracy and precision, is another unresolved challenge of FFF technology [4]. This study demonstrates the poor quality of parts printed with a high-performance thermoplastic (PEKK) and its CF composite. Surface roughness is a key aspect in the fabrication of assembly parts and other engineering components since it can affect the mechanical performance, tolerances and fits. There is a formula aimed to predict the surface roughness of FFF printed parts [58] based on the nozzle profile and considering the effects of printing parameters, slicing settings and filament properties. Dimensional accuracy and resolution also play a key role in the final usability of the printed part. Significant variations in size, warping or shrinkage can result in the invalidation of the part's functionality. These quality factors are highly dependent on the printing parameters but, to date, there is no model providing a comprehensive optimization of the input settings. As a consequence of these limitations, many of the aforementioned industrial applications are focused exclusively on prototyping. This is shown in Figure 55, where prototyping represents almost 50% of the global 3D printing market share.

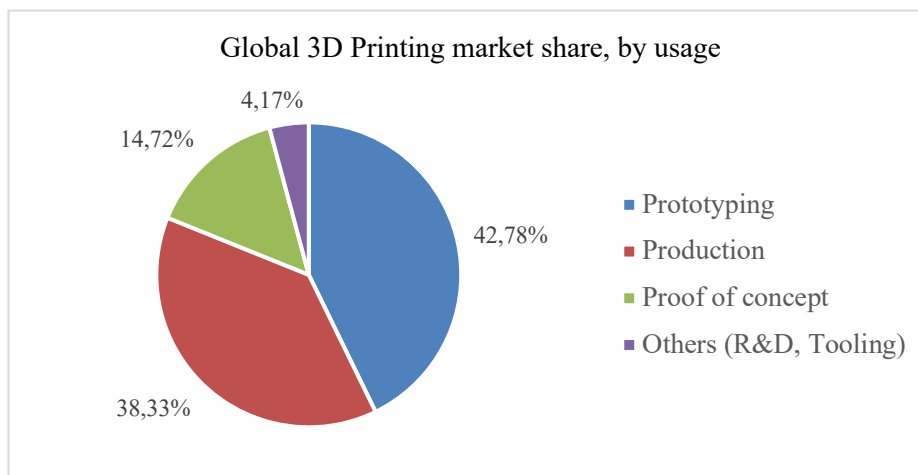


Figure 55. Global 3D Printing market share, by usage in 2021[59]

As shown in Figure 56, the global 3D printing filament market grew substantially from 2016 to 2019 and experienced a significant drop in 2020 due to the COVID-19 pandemic. However, the market is recovering at a good pace and is expected to surpass pre-crisis year (2019) revenues this year (2022). In addition, the market is anticipated to expand at a compound annual growth rate (CAGR) of 18.76% over the next 5 years. This growth is expected to be centered in North America, where the estimated CAGR exceeds the global CAGR [57]. The main forces that are driving the development of FFF technology are the interest of governments in less time consuming and low-cost industrial processes; the increasing demand for 3D printed parts made of materials with improved mechanical properties such as high-performance thermoplastics and composites; and the struggle to establish production energy efficient systems that support sustainability (ANNEX III presents the alignment of the project with the sustainable development goals - SDGs - established by the United Nations).

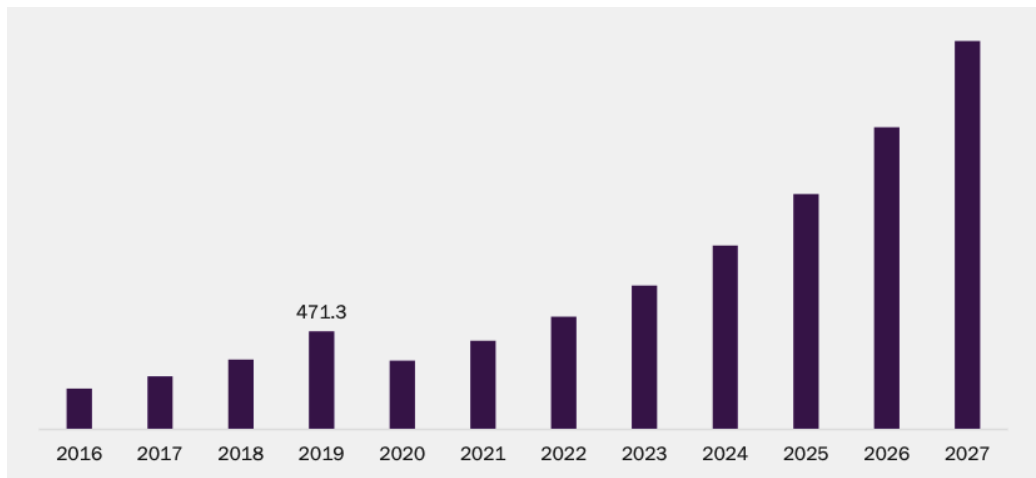


Figure 56. Global 3D printing filament market size 2016-2027 (USD Million) [57]

To encourage continued advancement of this technology, the future directions could fall into several categories: materials, printers, research and development (R&D) of design guidelines, and talent. Figure 57 outlines the most important points of each of these categories, explained as follows. Although FFF is compatible with many materials, some of them can be harmful to human health (high exposure to styrene can be cancerogenic [57]) and others are incompatible with the SDGs (some composite materials are very difficult to recycle due to their heterogeneous structure [60]). Given the growing concern and regulation

of pollution from manufacturing processes, the development of environmentally sustainable materials, namely biobased and biodegradable plastics, could be essential to encourage the interest in this AM technique [61]. The use of these materials, which emit less greenhouse gases than other thermoplastics and decompose naturally by living microorganisms, could have a strong untapped potential in the field of 3D printing.

Moreover, as has been demonstrated in this and other studies [25], composite materials made of a thermoplastic matrix reinforced with CF such as CF-PEEK and CF-PEKK have a high porosity that worsen the mechanical behavior of printed parts. In order to establish FFF as a mass production technology, it is crucial that composite filaments are of high quality. The increased demand for parts printed with high-performance materials is also directly linked to the development of 3D FFF printers. Currently, most 3D FFF printers available on the market are desktop printers designed for materials with a low melting temperature (up to 250°C) such as ABS and PLA. Nevertheless, the growing demand of materials with high melting temperatures (350°C - 400°C) for the aerospace and automotive industries requires the development of high-performance printers to guarantee printing stability and the achievement of professional results. In other words, there is a need for the 3D printer market to adapt to the new generation of materials.

In the field of research, it should be noted that governments of U.S.A, China, India, Korea and U.K, among others, as well as the tech giants are investing more and more money in 3D printing technologies [59]. In order to convert FFF from batch to mass production, research efforts should focus on developing qualitative and quantitative methods to quickly determine the optimal printing parameters. The settings that provide the best quality depend on both the material and the printer used. This paper demonstrates that the search for the optimal parameters is a complex process that requires the use of a large amount of material. It is not feasible to spend that much time and material on a manufacturing process every time a new machine, material or product is to be incorporated, and hence the need to establish comprehensive design guidelines. In addition, tests should be carried out to check the effectiveness (depending on the material) and standardize the use of different pre- and post-processes to improve part quality and properties [4]. Another key point in FFF's transition from batch to mass production is finding solutions to mechanical anisotropy of printed parts.

There is an urgent need to search for methods that can reduce porosity as well as improve interlayer bonding. For instance, the aim of this paper is to study over-extrusion as a new approach for improving the mechanical performance of PEKK and CF-PEKK parts. The results obtained from this and other studies [15] indicate that over-extrusion is not a general method, but rather a material-dependent technique. Also, there are two other limitations associated with over-extrusion: (1) it is difficult to find the right balance between increasing the EM to improve mechanical properties and worsening the quality of the part, and (2) a slight increase in the EM only affects the tensile strength. It may be more efficient to focus efforts on improving the printing process with the application of external pressures other than gravity, and reducing intra-bead pores of composite filaments.

Manpower is the fifth factor to consider in order to drive the development of FFF technology. According to the cited study [62], the number of publications relating FFF technology to talent is expected to increase from 121 (in 2020) to 325 over the next 5 years. The skills required for the usage of FFF technology could be divided in design skills and technical skills. On the one hand, the future use of FFF for industrial applications demands people who are able to design complex parts suitable for the process and to slice the parts correctly. As mentioned in the Chapter 1. it is desirable to avoid the use of supports that can damage the surface in contact. In addition, it is very important to pay attention to the slicing since a bad slicing can lead to undesirable pores (raster gap pores) or printing failures (e.g. it is very important to evaluate whether it is necessary to use a raft for the print or not). On the other hand, manual skills are required for the printing stage. Desktop printers are straightforward to use, but high-performance FFF printers need to be manually calibrated every time a new print is carried out. Moreover, the higher the extrusion temperature, the more serious the problems are likely to be (e.g. nozzle clogging in the case of CF-PEKK using 3DXTech filaments). The growing interest in high-performance materials and composites calls for experts in the usage and repair of high-temperature 3D printers.

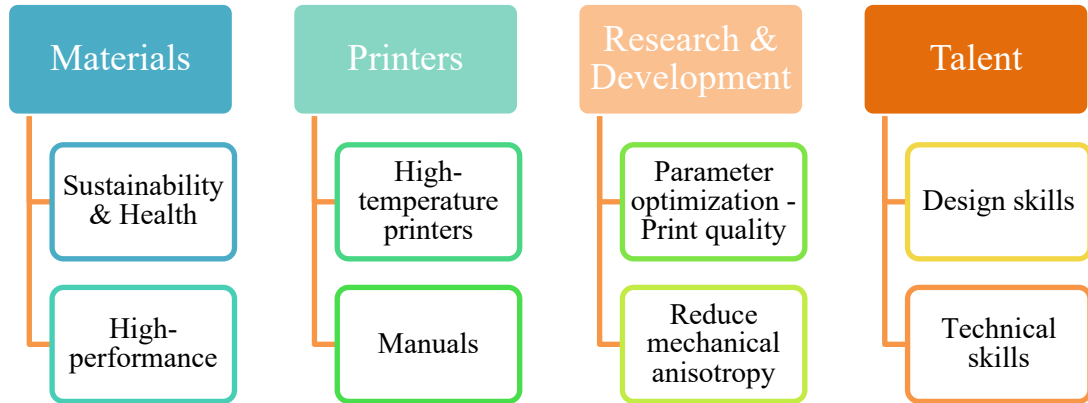


Figure 57. Future directions to drive the development of FFF technology

Chapter 8. CONCLUSIONS

This study investigates over-extrusion as a potential solution to decrease the large degree of anisotropy of PEKK and CF-PEKK parts manufactured via FFF. The results suggest that the improvement of the mechanical performance is a function of the porosity reduction which, in turn, a function of the material. For PEKK, a 5% increase in the EM results in a 0.53 pp porosity reduction and no improvement in mechanical properties is detected. Going further, the maximum porosity reduction that could be achieved with a further increase in EM would be 0.72 pp, which corresponds to the porosity obtained for a standard EM. However, it is questionable whether this porosity reduction is sufficient to appreciate an improvement in the mechanical behavior. For CF-PEKK, a 1.63 pp reduction in internal porosity is achievable. The final porosity with the higher EM (20.46%) is still very high due to the presence of intra-bead voids in the raw filaments, but it results in an improvement of the mechanical properties, especially noticeable in the ultimate tensile strength that increases by 32.6%. The 5% increase in the EM is not enough to appreciably enhance the Young's modulus and the strain to failure.

This study also demonstrates that a slight over-extrusion does not have a negative impact on the printability of PEKK and CF-PEKK. In both cases, printed parts do not offer a good quality due to the high processing temperatures. This is especially noticeable in the fine flow control, negative features resolution and, in the case of CF-PEKK, in bridging. In addition, it should be highlighted that annealing PEKK and CF-PEKK parts packed in salt is an effective approach for increasing the degree of crystallization, while preventing structural and dimensional changes.

Lastly, this study includes a vision of the future of FFF. The analysis of the advantages and limitation of this technology, as well as the factors driving its growth (interest of large companies and governments, economic framework, sustainable regulation, etc.), suggest focusing efforts on two key points: (1) developing sustainable high-performance materials, and (2) the elimination of intrinsic deficiencies of the process. The development of materials with excellent mechanical properties involves the development of quality filaments, the development of compatible high-temperature printers, and the

development of manpower. Secondly, eliminating intrinsic deficiencies of the process requires finding solutions to mechanical anisotropy and poor quality of printed parts. As demonstrated in this study, the effectiveness of over-extrusion in improving anisotropy depends on the material as well as on the mechanical property. This leads to the already existing need to look for alternative methods with a better capacity for mechanical performance improvement. What is more, the transition of FFF technology from batch to mass production demands the development of comprehensive design guidelines.

Chapter 9. REFERENCES

- [1] S.A. Kumar, R.V.S. Prasad, Chapter 2 - Basic principles of additive manufacturing: different additive manufacturing technologies, in: M. Manjiaiah, K. Raghavendra, N. Balashanmugam, J.P. Davim (Eds.), *Additive Manufacturing*, Woodhead Publishing 2021, pp. 17-35.
- [2] M. Leary, Chapter 1 - Introduction to AM, in: M. Leary (Ed.), *Design for Additive Manufacturing*, Elsevier 2020, pp. 1-6.
- [3] X. Zhang, F. Liou, *Introduction to additive manufacturing*, 2021, pp. 1-31.
- [4] S. Singh, G. Singh, C. Prakash, S. Ramakrishna, Current status and future directions of fused filament fabrication, *Journal of Manufacturing Processes* 55 (2020) 288-306.
- [5] H. Bikas, P. Stavropoulos, G. Chryssolouris, Additive manufacturing methods and modelling approaches: a critical review, *The International Journal of Advanced Manufacturing Technology* 83(1) (2016) 389-405.
- [6] A.B. Varotsis, I. Simon, What is FDM (Fused Deposition Modeling) 3D printing? Explained by Hubs, 2013. <https://www.hubs.com/knowledge-base/what-is-fdm-3d-printing/>.
- [7] Y. Tao, F. Kong, Z. Li, J. Zhang, X. Zhao, Q. Yin, D. Xing, P. Li, A review on voids of 3D printed parts by fused filament fabrication, *Journal of Materials Research and Technology* 15 (2021) 4860-4879.
- [8] X. Gao, S. Qi, X. Kuang, Y. Su, J. Li, D. Wang, Fused filament fabrication of polymer materials: A review of interlayer bond, *Additive Manufacturing* 37 (2021) 101658.
- [9] J. Allum, A. Moetazedian, A. Gleadall, V.V. Silberschmidt, Interlayer bonding has bulk-material strength in extrusion additive manufacturing: New understanding of anisotropy, *Additive Manufacturing* 34 (2020) 101297.
- [10] N.P. Levenhagen, M.D. Dadmun, Improving Interlayer Adhesion in 3D Printing with Surface Segregating Additives: Improving the Isotropy of Acrylonitrile–Butadiene–Styrene Parts, *ACS Applied Polymer Materials* 1(4) (2019) 876-884.
- [11] H. Gonabadi, A. Yadav, S.J. Bull, The effect of processing parameters on the mechanical characteristics of PLA produced by a 3D FFF printer, *The International Journal of Advanced Manufacturing Technology* 111(3) (2020) 695-709.
- [12] V. Kishore, C. Ajiñjeru, A. Nycz, B. Post, J. Lindahl, V. Kunc, C. Duty, Infrared preheating to improve interlayer strength of big area additive manufacturing (BAAM) components, *Additive Manufacturing* 14 (2017) 7-12.
- [13] V. Kishore, A. Nycz, J. Lindahl, C. Duty, C. Carnal, V. Kunc, Effect of Infrared Preheating on the Mechanical Properties of Large Format 3D Printed Parts, United States, 2019.
- [14] A.R. Torrado, C.M. Shemelya, J.D. English, Y. Lin, R.B. Wicker, D.A. Roberson, Characterizing the effect of additives to ABS on the mechanical property anisotropy of specimens fabricated by material extrusion 3D printing, *Additive Manufacturing* 6 (2015) 16-29.
- [15] P.K. J. Ghorbani, Y. Shen, M. Tehrani, Reducing Mechanical Anisotropy in Fused Filament Fabrication Additive Manufacturing via Over-Extrusion, (under review).
- [16] I. Ferreira, M. Machado, F. Alves, A. Torres Marques, A review on fibre reinforced composite printing via FFF, *Rapid Prototyping Journal* 25(6) (2019) 972-988.
- [17] S.H. Ahn, M. Montero, D. Odell, S. Roundy, P.K. Wright, Anisotropic material properties of fused deposition modeling ABS, *Rapid Prototyping Journal* 8(4) (2002) 248-257.
- [18] M. Spoerk, F. Arbeiter, H. Cajner, J. Sapkota, C. Holzer, Parametric optimization of intra- and inter-layer strengths in parts produced by extrusion-based additive manufacturing of poly(lactic acid), *Journal of Applied Polymer Science* 134(41) (2017) 45401.
- [19] P. Wang, B. Zou, H. Xiao, S. Ding, C. Huang, Effects of printing parameters of fused deposition modeling on mechanical properties, surface quality, and microstructure of PEEK, *Journal of Materials Processing Technology* 271 (2019) 62-74.
- [20] L. Wang, W.M. Gramlich, D.J. Gardner, Improving the impact strength of Poly(lactic acid) (PLA) in fused layer modeling (FLM), *Polymer* 114 (2017) 242-248.
- [21] N. Aliheidari, J. Christ, R. Tripuraneni, S. Nadimpalli, A. Ameli, Interlayer adhesion and fracture resistance of polymers printed through melt extrusion additive manufacturing process, *Materials & Design* 156 (2018) 351-361.

- [22] A.C. Abbott, G.P. Tandon, R.L. Bradford, H. Koerner, J.W. Baur, Process-structure-property effects on ABS bond strength in fused filament fabrication, *Additive Manufacturing* 19 (2018) 29-38.
- [23] J.F. Rodriguez, J.P. Thomas, J.E. Renaud, Maximizing the Strength of Fused-Deposition ABS Plastic Parts, 1999.
- [24] X. Gao, D. Zhang, S. Qi, X. Wen, Y. Su, Mechanical properties of 3D parts fabricated by fused deposition modeling: Effect of various fillers in polylactide, *Journal of Applied Polymer Science* 136(31) (2019) 47824.
- [25] T. Yap, N. Heathman, T. Phillips, J. Beaman, M. Tehrani, Fused Filament Fabrication and Selective Laser Sintering of PAEK Polymers and their Composites, (under review).
- [26] E. Gordeev, A. Galushko, V. Ananikov, Improvement of quality of 3D printed objects by elimination of microscopic structural defects in fused deposition modeling, *PLOS ONE* 13 (2018) e0198370.
- [27] W. contributors, Polyactic acid, 2022. https://en.wikipedia.org/w/index.php?title=Polylactic_acid&oldid=1083137089. (Accessed 3 May 2022).
- [28] O. Martin, L. Avérous, Poly(lactic acid): plasticization and properties of biodegradable multiphase systems, *Polymer* 42(14) (2001) 6209-6219.
- [29] R. Hagen, 10.12 - Polylactic Acid, in: K. Matyjaszewski, M. Möller (Eds.), *Polymer Science: A Comprehensive Reference*, Elsevier, Amsterdam, 2012, pp. 231-236.
- [30] M. Jamshidian, E.A. Tehrany, M. Imran, M. Jacquot, S. Desobry, Poly-Lactic Acid: Production, Applications, Nanocomposites, and Release Studies, *Comprehensive Reviews in Food Science and Food Safety* 9(5) (2010) 552-571.
- [31] B. Yin, Q. He, L. Ye, Effects of deposition speed and extrusion temperature on fusion between filaments in single-layer polymer films printed with FFF, *Advanced Industrial and Engineering Polymer Research* 4(4) (2021) 270-276.
- [32] S. Bardiya, J. Jerald, V. Satheeshkumar, Effect of process parameters on the impact strength of fused filament fabricated (FFF) polylactic acid (PLA) parts, *Materials Today: Proceedings* 41 (2021) 1103-1106.
- [33] G. Bräuer, K. Sachsenhofer, R.W. Lang, Material and process engineering aspects to improve the quality of the bonding layer in a laser-assisted fused filament fabrication process, *Additive Manufacturing* 46 (2021) 102105.
- [34] M. P., PEEK vs PEKK: Which High Performance Material Should You Choose?, June 24, 2021. <https://www.3dnatives.com/en/peek-vs-pekk-240620214/#!>
- [35] L. Quiroga Cortés, N. Caussé, E. Dantras, A. Lonjon, C. Lacabanne, Morphology and dynamical mechanical properties of poly ether ketone ketone (PEKK) with meta phenyl links, *Journal of Applied Polymer Science* 133(19) (2016).
- [36] V. Miner. <https://visionminer.com/products/thermax-pekk>.
- [37] P. Cheremisinoff, *Handbook of Engineering Polymeric Materials*, Boca Raton, 1997.
- [38] H. Pérez-Martín, P. Mackenzie, A. Baidak, C.M. Ó Brádaigh, D. Ray, Crystallinity studies of PEKK and carbon fibre/PEKK composites: A review, *Composites Part B: Engineering* 223 (2021) 109127.
- [39] B.W. Kaplun, R. Zhou, K.W. Jones, M.L. Dunn, C.M. Yakacki, Influence of orientation on mechanical properties for high-performance fused filament fabricated ultem 9085 and electro-statically dissipative polyetherketoneketone, *Additive Manufacturing* 36 (2020) 101527.
- [40] <https://www.3dbenchy.com/>.
- [41] <https://github.com/kickstarter/kickstarter-autodesk-3d/tree/master/FDM-protocol>.
- [42] <https://www.thingiverse.com/thing:1278865>.
- [43] C. McCowan, T. Siewert, D. Vigliotti, The NIST Charpy V-notch Verification Program: Overview and Operating Procedures, (2022).
- [44] THERMAX PEKK-C, Technical Data Sheet. https://www.3dxtech.com/product/thermax-pekk-c/?attribute_pa_diameter=1-75mm&attribute_pa_weight=100g&attribute_pa_color=natural.
- [45] Filament2Print, What is retraction in 3D printing? Definition and adjustments, 2018.
- [46] R. Rane, A. Kulkarni, H. Prajapati, R. Taylor, A. Jain, V. Chen, Post-Process Effects of Isothermal Annealing and Initially Applied Static Uniaxial Loading on the Ultimate Tensile Strength of Fused Filament Fabrication Parts, *Materials* 13(2) (2020).
- [47] C. Basgul, T. Yu, D.W. MacDonald, R. Siskey, M. Marcolongo, S.M. Kurtz, Does annealing improve the interlayer adhesion and structural integrity of FFF 3D printed PEEK lumbar spinal cages?, *Journal of the Mechanical Behavior of Biomedical Materials* 102 (2020) 103455.

- [48] C. Kitchen, TESTING THE STRENGTH OF 3D PRINTS RE-MELTED IN SALT, 2020. <https://www.cnckitchen.com/blog/testing-the-strength-of-3d-prints-re-melted-in-salt>.
- [49] A.G. Tantillo, Annealing of Fused Filament Fabricated Nylon 6 with Elevated Isostatic Pressure, Rochester Institute of Technology, 2019.
- [50] A. du Plessis, C. Broeckhoven, A. Guelpa, S.G. le Roux, Laboratory x-ray micro-computed tomography: a user guideline for biological samples, GigaScience 6(6) (2017) 1-11.
- [51] Kimya PEKK Carbon 3D Filament. <https://www.kimya.fr/en/product/pekk-carbon-3d-filament/>.
- [52] S. Rahmati, 10.12 - Direct Rapid Tooling, in: S. Hashmi, G.F. Batalha, C.J. Van Tyne, B. Yilbas (Eds.), Comprehensive Materials Processing, Elsevier, Oxford, 2014, pp. 303-344.
- [53] J.C. Najmon, S. Raeisi, A. Tovar, 2 - Review of additive manufacturing technologies and applications in the aerospace industry, in: F. Froes, R. Boyer (Eds.), Additive Manufacturing for the Aerospace Industry, Elsevier 2019, pp. 7-31.
- [54] D.K. Yadav, R. Srivastava, S. Dev, Design & fabrication of ABS part by FDM for automobile application, Materials Today: Proceedings 26 (2020) 2089-2093.
- [55] N.A.S. Mohd Pu'ad, R.H. Abdul Haq, H. Mohd Noh, H.Z. Abdullah, M.I. Idris, T.C. Lee, Review on the fabrication of fused deposition modelling (FDM) composite filament for biomedical applications, Materials Today: Proceedings 29 (2020) 228-232.
- [56] C. Yuan, T. Lu, T.J. Wang, Mechanics-based design strategies for 4D printing: A review, Forces in Mechanics 7 (2022) 100081.
- [57] 3D Printing Filament Market Size, Share & Trends Analysis Report By Type (Plastics, Metal, Ceramics), By Plastic Type (Polylactic Acid, ABS), By Application (Industrial, Aerospace & Defense), By Region, And Segment Forecasts, 2020 - 2027, Grand view research website, 2020, p. 100.
- [58] D.-K. Ahn, S.-m. Kwon, S.-H. Lee, Expression for Surface Roughness Distribution of FDM Processed Parts, 2008.
- [59] e global 3D printing market is projected to grow from \$18.33 billion in 2022 to \$83.90 billion by 2029, at a CAGR of 24.3% in forecast period, 2022-2029, Fortune Business insights website, 2022, p. 130.
- [60] Y. Yang, R. Boom, B. Irion, D.-J. van Heerden, P. Kuiper, H. de Wit, Recycling of composite materials, Chemical Engineering and Processing: Process Intensification 51 (2012) 53-68.
- [61] A. Dey, I.N. Roan Eagle, N. Yodo, A Review on Filament Materials for Fused Filament Fabrication, Journal of Manufacturing and Materials Processing 5(3) (2021) 69.
- [62] M. Ahmadifar, K. Benfriha, M. Shirinbayan, A. Tcharkhtchi, Additive Manufacturing of Polymer-Based Composites Using Fused Filament Fabrication (FFF): a Review, Applied Composite Materials 28 (2021) 1-46.
- [63] <https://www.3dnatives.com/3D-compare/es/impresoras-3d/aon-m2/>.
- [64] R. Stewart, Thermoplastic composites — recyclable and fast to process, Reinforced Plastics 55(3) (2011) 22-28.
- [65] A. Wijk, I. van Wijk, 3D printing with biomaterials: Towards a sustainable and circular economy, 2015.

ANNEX I

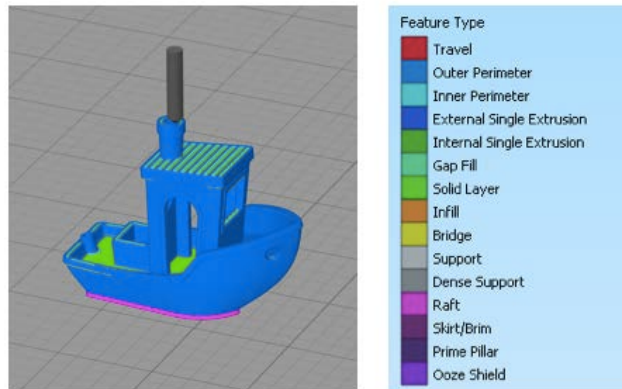


Figure 58. Pre-print simulation of the 3dBenchy made with Simplify3D

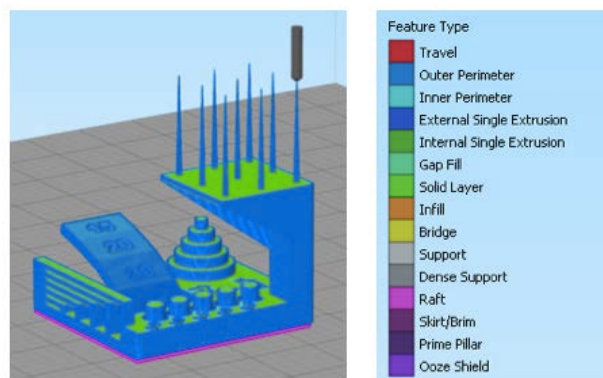


Figure 59. Pre-print simulation of the metrology part made with Simplify3D

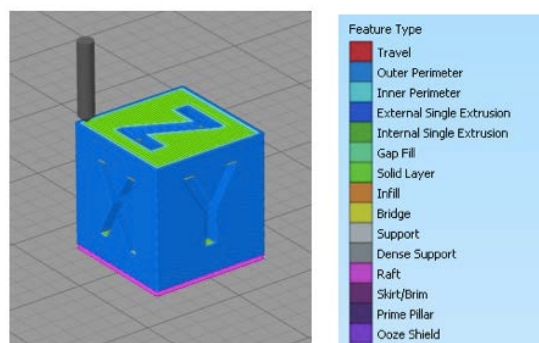


Figure 60. Pre-print simulation of the calibration cube made with Simplify3D

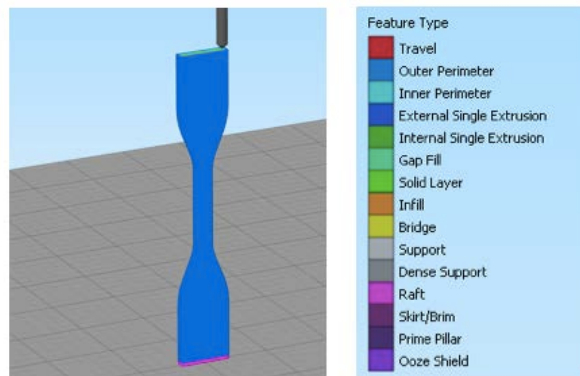


Figure 61. Pre-print simulation of ASTM D638-14 type IV specimen made with Simplify3D

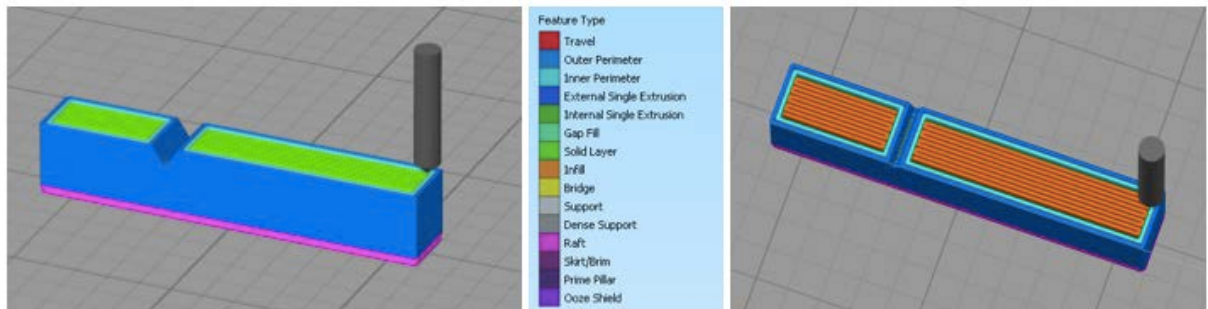


Figure 62. Pre-print simulation and raster pattern of the cross-section sample made with Simplify3D



Figure 63. Original Prusa i3 MK3

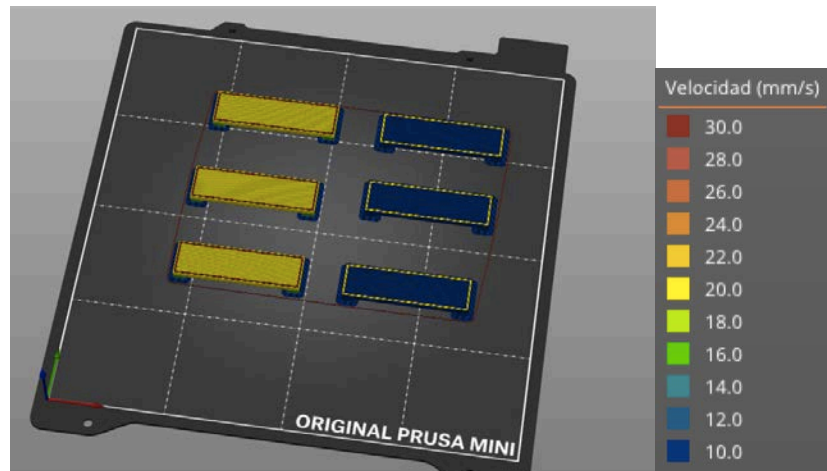


Figure 64. CAD FILE created for the PLA bridging study



Figure 65. AON3D m2 printer [63]

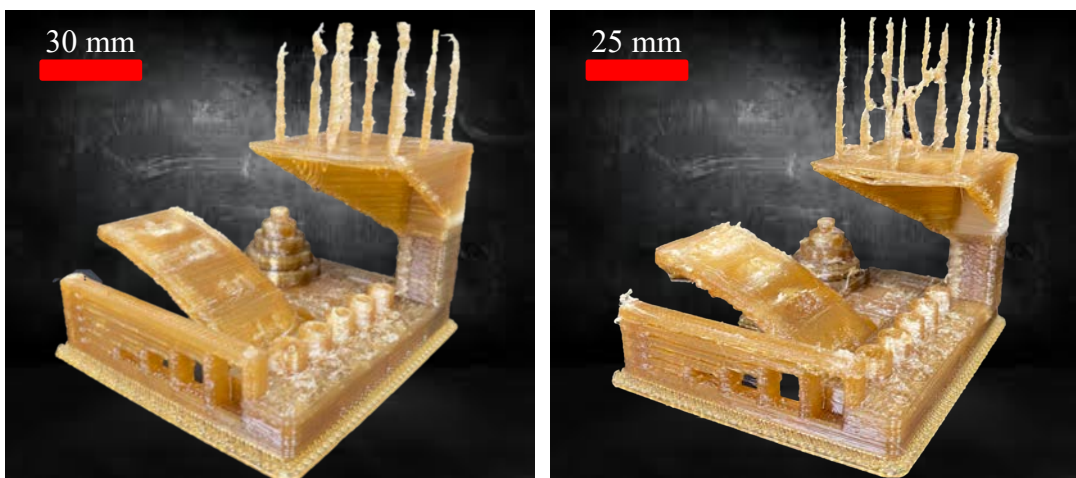


Figure 66. PEKK common standard piece developed by Autodesk and Kickstarter before annealing printed at an Extrusion multiplier of: (a) 1 and (b) 1.05

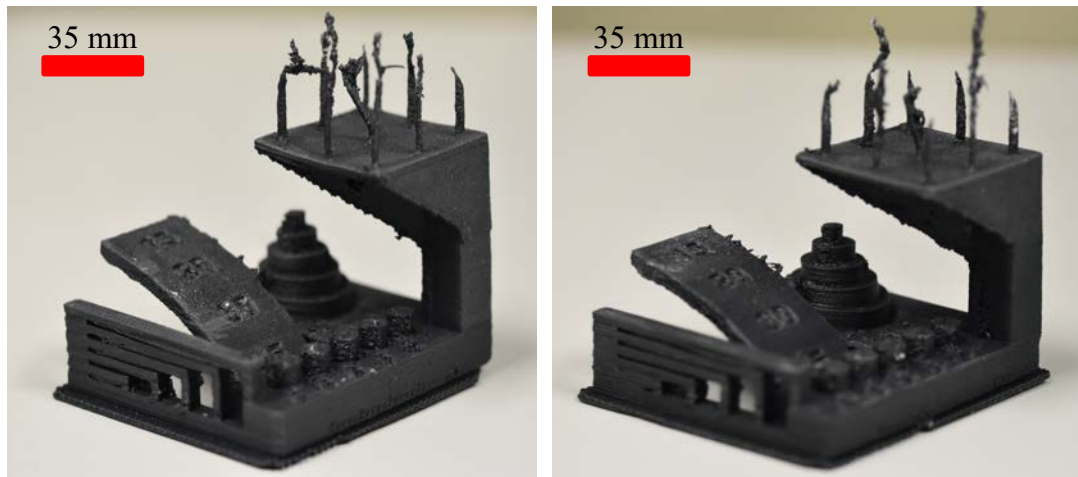


Figure 67. CF- PEKK common standard piece developed by Autodesk and Kickstarter before annealing printed at an Extrusion multiplier of: (a) 1 and (b) 1.05

ANNEX II

DIMENSIONS (see Figure 13)	Specimen dimensions for Type IV, mm (in.)
W - Width of narrow section	6 (0.25)
L - Length of narrow section	33 (1.30)
WO - Width overall	19 (0.75)
LO – Length overall	115 (4.5)
G – Gage length	25 (1.00)
D – Distance between grips	65 (2.5)
R – Radius of fillet	14 (0.56)
RO – Outer radius	25 (1.00)

Table 13. Dimension of type IV ASTM D638-14 tensile coupons

PRINTING PARAMETERS	DEFAULT VALUES
Nozzle Temperature for the first layer (°C)	210
Nozzle Temperature (°C)	215
Bed Temperature (°C)	60
Layer Height (mm)	0.05
Speed for printing movements (mm/s)	20 – 30
Infill (%)	15
Bridging flow rate	1

Table 14. Initial printing parameters for PLA

PROPERTIES	VALUES
Density (g/cc)	1.29
Glass transition temperature (°C)	165
Melt temperature (°C)	335
Tensile modulus (MPa)	3,200
Tensile strength (MPa)	105
Tensile elongation (%)	10

Table 15. Physical, mechanical and thermal properties of PEKK provided by 3DXTech [44]

PRINTING PARAMETERS	DEFAULT VALUES
Nozzle diameter (mm)	0.60
Extruder	1.00
Retraction distance (mm)	0.60
Retraction speed (mm/s)	30
Nozzle Temperature (°C)	375
Bed Temperature (°C)	140
Heated chamber (°C)	120
Layer Height (mm)	0.25
Printing speed (mm/s)	20

Table 16. Initial printing parameters for PEKK

PROPERTIES	VALUES
Density (g/cc)	1.27
Glass transition temperature (°C)	160
Melt temperature (°C)	350
Tensile modulus (MPa)	2,900
Tensile strength (MPa)	39.1
Tensile elongation (%)	3.2

Table 17. Physical, mechanical and thermal properties of CF-PEKK provided by Kimya [51]

		Ultimate tensile strength (MPa)	Young's Modulus (GPa)	Strain to failure (%)
EM=1.00	Coupon nº 1*	16.02	3.41	0.47
	Coupon nº 2	24.36	4.04	0.58
	Coupon nº 3	27.48	3.98	0.67
	Coupon nº 4	28.40	3.64	0.80
	Coupon nº 5	28.65	3.87	0.75
	Mean	27.22	3.89	0.70
	Standard deviation	1.97	0.18	0.10
EM=1.05	Coupon nº 1	27.03	4.02	0.67
	Coupon nº 2	27.35	3.91	0.68
	Coupon nº 3	25.78	3.64	0.70
	Coupon nº 4	26.14	3.70	0.72
	Coupon nº 5	33.84	3.83	0.90
	Mean	28.03	3.82	0.73
	Standard deviation	3.31	0.16	0.10

Table 18. Reported mechanical properties for each of the PEKK coupons, sample mean and standard deviation.

* This test specimen had a little crack in the gage section, which probably caused the premature failure. Consequently, the mechanical properties were computed without considering the results of this outlier.

		Ultimate tensile strength (MPa)	Young's Modulus (GPa)	Strain to failure (%)
EM=1.00	Coupon nº 1	23.64	2.15	1.25
	Coupon nº 2	18.44	2.21	0.96
	Coupon nº 3	22.27	2.06	1.24
	Coupon nº 4	17.36	2.08	0.84
	Coupon nº 5	13.19	2.25	0.56
	Coupon nº 6	17.21	2.37	0.85
	Mean	18.68	2.19	0.95
	Standard deviation	3.78	0.11	0.26
EM=1.05	Coupon nº 1	23.86	2.15	1.02
	Coupon nº 2	24.59	2.10	1.24
	Coupon nº 3	26.27	2.26	1.39
	Coupon nº 4	21.94	2.07	1.16
	Coupon nº 5	27.21	2.04	1.45
	Mean	24.77	2.12	1.26
	Standard deviation	2.07	0.09	0.17

Table 19. Reported mechanical properties for each of the CF- PEKK coupons, sample mean and standard deviation.

ANNEX III

The Sustainable Development Goals are, as its name suggests, 17 goals adopted by the United Nations in 2015 with the aim of fighting for a more sustainable world. This research addresses various SDGs. The primary goal aligned with this study is **goal number 12**: “Ensure sustainable consumption and production pattern”. More specifically, one of the targets of this goal is the following: “By 2030, substantially reduce waste generation through prevention, reduction, recycling and reuse”. This paper is focused on PEKK and CF-PEKK as promising materials for high-demanding industrial applications. Since PEKK is a thermoplastic it can easily be reheated above the melting temperature and reuse for other purposes. Moreover, thermoplastics composites such as CF-PEKK are in the spotlight due to the ease with which they can be proceed and recycled [64]. According to recent market researches, fibers reinforced with a thermoplastic matrix are becoming the optimal choice to replace traditional materials. Considering that CF-PEKK has a density that is 60% lesser than the density of aluminum, this composite could be a good alternative to save weight and avoid wasting material. Going further, the weight reduction in airplanes and cars that could be achieved by replacing certain parts made of traditional materials with PEKK or CF-PEKK parts would lead to a reduction in fuel consumption and greenhouse gas emissions. This effect is directly related to **goal 13**, which advocates the fight against climate change. From a process perspective, FFF offers many advantages over traditional manufacturing processes. The amount of material used for a print is practically if not exactly the amount of material needed to manufacture the part. This contrasts with traditional processes, where the total amount of material to make a part is greater than the amount of final material that makes up the part (net form). From a material savings perspective, this technology is also useful to manufacture parts that need to be replaced without having to change all the machinery. Lastly, it is worth noting that FFF is compatible with a wide range of materials, including biomaterials. Expanded use of these materials could be key to achieving a more circular and sustainable economy [65].

This study is also aligned with **goals 9 and 3**. On the one hand, goal 9 promotes sustainable industrialization and foster innovation. Target 9.5 calls on scientific

development, emphasizing the need for technological innovation and increasing people dedicated to research. This project, focused on one of the most promising AM processes, tries to offer a simple but effective approach to reduce the limitations of this technology. On the other hand, the research could indirectly contribute to target 3.b from the third SGDs. PEEK has properties that resemble those of human bones and thus, it is currently used for medical implants as a substitute for titanium. The development of processes to manufacture these implants is essential and FFF is one of the best candidates for this application.